

Impacts of fringing oyster reefs on wave attenuation and marsh erosion rates

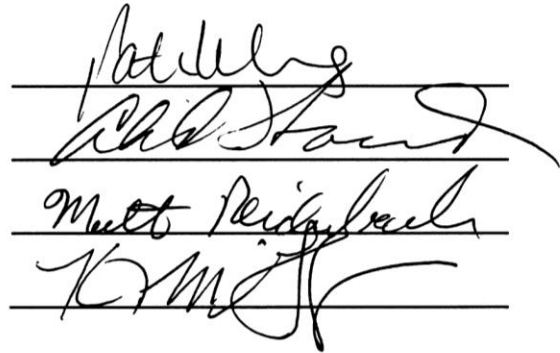
Sara Reid Taube
Austin, Texas

Bachelor of Arts, Vanderbilt University, 2010

A Thesis presented to the Graduate Faculty
of the University of Virginia in Candidacy for the Degree of
Master of Science

Department of Environmental Sciences

University of Virginia
May, 2013


The image shows four handwritten signatures, each written on a horizontal line. From top to bottom, the signatures are: 1. A cursive signature that appears to be 'Sara Reid Taube'. 2. A cursive signature that appears to be 'Matt Reidgabel'. 3. A cursive signature that appears to be 'K. M. J.'. 4. A cursive signature that appears to be 'K. M. J.'. The signatures are written in black ink on a white background.

Abstract

Mainland marshes in the Virginia Coast Reserve have been eroding at rates that vary both spatially and temporally. Data from these study sites showed statistically significant upward trends in the rate of shoreline retreat over the course of the last 52 years. This increase in erosion rates corresponds to an increase in the frequency of hurricanes and tropical storms passing within 100 km of the study sites. The correlation between hurricane frequency and erosion rates suggest that these high-energy storms could have been the main cause of rapid marsh-edge erosion. Average erosion rates from this study were similar to those measured by McLoughlin et al. (2011) on other mainland marshes in the Virginia Coast Reserve, as was the spatial variability. Erosion at the study sites was less than the regional erosion rate calculated in Hog Island Bay to be $1.2 \text{ m}\cdot\text{yr}^{-1}$. Oyster reefs were shown to have successfully dissipated wind-wave energy, the primary driver of erosion in the Virginia Coast Reserve, and have the potential to work as an erosion control method. For significant waves, the mean dissipation of wave power was 49%. Attenuation of wave energy was determined by multiple factors, primarily water depth above the reef and significant wave height. An ideal range of depths at which reefs were most effective was identified, above which, additional increases in water depth diminished the interaction. This occurred because although waves continued to grow with greater water depth, the decay in orbital motion with depth was sufficient that the waves were no longer strongly modified by the underlying reef surface. Strategic installment of reefs based on prominent wind direction and fetch in relationship to marsh shorelines is likely key to greater erosion mitigation.

Acknowledgments

There are many people who deserve immeasurable thanks for their assistance with my work, without which it would not have happened. I would like to thank my adviser, Patricia Wiberg, for her guidance, thoughtful feedback, and analytical expertise, as well as my committee members, Karen McGlathery, Matt Reidenbach, and Alan Howard for their help and insight. I am incredibly grateful for Sean McLoughlin- his patience with all of my hundreds of questions, teaching me every machine, program, and process, and for sharing all of his own work, which blazed a path for me to follow. I truly would not have finished this undertaking without him. I would like to thank Barry Truitt, John Porter, Dave Carr, Stephanie Phelps, Jennie Rheuban, Meg Miller, Jill Greiner, Cat Wolner, Jessica Gephart, Jon Walter, Jenny Hansen, Chris Gist, Kelly Johnson, and David Furbish for their wealth of knowledge, and again, patience with my many questions.

A great deal of thanks is in order for the entire ABCRC staff, especially David Boyd for handling my boat trips, sampling help, and companionship for the last two years. I am grateful for the field assistance from Gavin Bruno, Pat Luckenbach, Jennie Rheuban, and Nancy Peters. I would also like to thank my office mates, Dirk Koopmans, Dana Gulbransen, Talia Dibble, Melissa Duvall, and Sean McLoughlin, for their company during those long hours in the office and providing feedback on many ideas. Thank you to Jared Pienkos, Amanda Benson, Kelly Dennen, and Marne Zahner, for keeping me sane. Lastly, I need to thank my parents, Judy and Eric, and my brother and sister-in-law, Alex and Adair, for their encouragement, constancy, interest in my work, and love.

Funding for this project was provided by the Virginia Coast Reserve Long Term Ecological Research project funded through National Science Foundation grants Division of Environmental Biology (DEB) 123773. Additional support came from the University of Virginia Presidential Fellowship through the Department of Environmental Sciences.

Table of contents

Abstract.....	i
Acknowledgments.....	ii
Table of contents.....	iv
List of figures.....	vi
List of tables.....	viii
Introduction.....	1
Coastal erosion.....	1
Marsh erosion.....	2
Waves in shallow bays.....	4
Marsh-edge characteristics.....	6
Oyster reefs as erosion control.....	7
Objectives.....	15
Study sites.....	15
Box Tree sites.....	18
Northern sites.....	22
Methods.....	25
Digital shoreline analysis.....	25
Site characteristics.....	30
Sediment sampling.....	31
Ecology.....	34
Hydrodynamic measurements.....	34
Wave environment.....	37
Results.....	40
Digital shoreline analysis.....	40
Physical properties.....	49
Ecology.....	54
Tides and currents.....	57
Wind conditions.....	61
Fetch.....	64
Wave environment.....	66

Wave events	81
Wave power	87
Reef dissipation of wave energy	93
Discussion	97
Rates and variability of erosion	97
Marsh and reef attributes	99
VCR erosion rate comparison	102
Erosion rates and storm events	106
Wave environment	109
Reef dissipation of wave energy	114
Wave power	110
Conclusion	119
References	123
Appendix I – additional methods	131
Appendix II – additional data	133

List of figures

Figure 1: Wind and wave power in the VCR modeled by Mariotti et al. (2010).	5
Figure 2: Site locations for studies of oyster reef erosion control.	8
Figure 3: From NOAA Living Shorelines - "Coastal Shoreline Continuum & Typical ‘Living Shorelines’ Treatments.”.....	14
Figure 4: The Virginia Coast Reserve study and comparison site locations	17
Figure 5: Southern study and comparison	20
Figure 6: BT5 reef profile and cross-sections.....	21
Figure 7: BT6 reef profile and cross-sections.....	21
Figure 8: Northern study and comparison sites	23
Figure 9: SEB3 reef profile.....	24
Figure 10: Digital Shoreline Analysis Software components c.....	28
Figure 11: PVC marker poles and survey transects 2011-2012.....	31
Figure 12: Hydrodynamic instrument configuration.	36
Figure 13: Diagram of wave gauge placement around BT5 reef.....	37
Figure 14: Average erosion rates between 1957 and 2009.	41
Figure 15: Box plots of erosion rates from 1957-2009.....	42
Figure 16: Northern study sites average erosion rates.....	44
Figure 17: Box Tree study sites average erosion rates	45
Figure 18: Average erosion rates for tested intervals	47
Figure 19: Interval erosion rate statistics.....	48
Figure 20: Fit plot of study sites average erosion rates for time intervals.....	49
Figure 21: Grain size distribution and median grain size	52
Figure 22: Sediment organic matter as a function of median grains size	53
Figure 23: Biomass measurements.	55
Figure 24: Crab burrow area estimates	56
Figure 25: Sampling period water depths relative to MSL at SEB3 and CRM4.....	58
Figure 26: Sampling period water depths relative to MSL at BT5 and BT6.....	59
Figure 27: WAHV2 wind rose September 2011 - September 2012..	61
Figure 28: Wind roses for sampling periods.....	63
Figure 29: Wind direction frequencies	64
Figure 30: Fetches at study sites.	65
Figure 31: Example of H_s and wind speed time series from BT5.....	67
Figure 32: Significant wave height statistics for full data sets and Records of Interest ...	68
Figure 33: Fetch, winds, and significant wave height by wind direction for SEB3.	71
Figure 34: Fetch, winds, and significant wave height by wind direction for CRM4.....	72
Figure 35: Fetch, winds, and significant wave height by wind direction for BT5.	73
Figure 36: Fetch, winds, and significant wave height by wind direction for BT6.	74
Figure 37: Water depth, significant wave height, and wind time series for sites BT5 and BT6.	76
Figure 38: Water depth, significant wave height, and wind time series for sites SEB3 and CRM4.....	77

Figure 39: BT5 and BT6 significant wave heights correlation plots	78
Figure 40: SEB3 and CRM4 significant wave height correlation plots.....	80
Figure 41: BT5 <i>Bsig</i> and <i>Msig</i> response to wind speed and reef water depth.....	85
Figure 42: BT6 <i>Bsig</i> and <i>Msig</i> response to wind speed and reef water depth.....	86
Figure 43: CRM4 <i>Bsig</i> and <i>Msig</i> response to wind speed and reef water depth.....	87
Figure 44: CRM4 wave power density statistics.	90
Figure 45: BT5 wave power density statistics.	91
Figure 46: BT6 wave power density statistics.	92
Figure 47: Change in significant wave height as a function of various factors.....	94
Figure 48: Wave bases for BT5.....	95
Figure 49: BT5 wave dissipation as a function of water depth to the reef..	96
Figure 50: Variation in mainland marsh erosion rates in the south-central VCR.....	98
Figure 51: Fit plots for average erosion rates at study sites and storm frequency and impact.....	108
Figure 52: Conceptual diagram of decoupling between waves and reef surface.....	117
Figure 53: Linear and power law fits of wave power density to edge erosion rates.....	113
Figure 54: Power spectral density plot with rectangles	132
Figure 55: Elkins Island shorelines and rate of erosion.....	136
Figure 56: Inter-island shorelines and rates of erosion.....	137
Figure 57: northern Fowling Point shorelines and rates of erosion.....	138
Figure 58: Upshur Neck shorelines and rates of erosion.....	139
Figure 59: SEB3 and CRM4 fit plots for increasing erosion rates over time.....	140
Figure 60: BT5 and BT6 fit plots for increasing erosion rates over time.....	141
Figure 61: A series of box plots from BT5 used for analysis in the relationship of significant wave height to other measured variables.....	146

List of tables

Table 1: Marsh erosion rates in the United States and Europe.	4
Table 2: Hydrodynamic sampling schedule of deployments at study sites.	35
Table 3: Kruskal-Wallis results testing for significant differences in average erosion rates from 1957-2009.	43
Table 4: Statistics for interval erosion rate differences within a site.	46
Table 5: Average erosion rates in meters per year for all time intervals	47
Table 6: Linear regression results of erosion rate increase with time.	49
Table 7: Physical characteristics of study and comparison sites.	50
Table 8: Mean tidal range, and average water speed, velocity, and direction of flow for study sites.	60
Table 9: Significant wave height statistics.	68
Table 10: Statistics for wave data sets before and after selecting records of interest.	83
Table 11: Wave power density averages for sites CRM4, BT5, and BT6 records of interest.	89
Table 12: Mean rates of change along marsh edges	97
Table 13: Comparison of average erosion rates from oyster reef studies, observation methods, and relevant statistics.	105
Table 14: Frequency of storm events within 100 km of study sites during each interval.	109
Table 15: Linear regression results testing the relationship of hurricane frequency and intensity with erosion rates.	109
Table 16: ANOVA results of tidal speeds.	133
Table 17: Statistical results testing for differences in wind speed and wind direction during the sampling periods and one year.	133
Table 18: Statistical results for ANOVA tests of physical properties.	133
Table 19: Grain size and organic attributes of sediment samples.	134
Table 20: Aerial image georectification error and ground resolution.	134
Table 21: Fetch area estimates.	134
Table 22: Linear regression results for erosion rates and physical properties.	142
Table 23: Hurricanes and tropical storms within 100 km of the VCR during erosion rate study periods.	143
Table 24: Statistical analysis of major hurricane events with respect to average erosion rate.	144
Table 25: Linear regression results for the relationship between significant wave height and hydrodynamic variables.	145
Table 26: ANOVA results for change in significant wave height.	151
Table 27: Grain size distributions.	152
Table 28: Carbon and nitrogen content in sediment samples.	155

Introduction

Coastal erosion

Coastal shoreline erosion has been a growing issue for many decades because of the human propensity to build along the coast. Thirty- eight percent of the world population lives within 100 km of a coast and 53% of the US population is within 80 km (NOAA 2003, Cossett et al. 2008). Greater concern has arisen in recent years due to the threat of coastal inundation from sea-level rise. In their fourth report released in 2007, the Intergovernmental Panel on Climate Change (IPCC) projected that average sea-level will rise 0.18-0.59 m by 2090-2099 relative to 1980-1999, based on model data (IPCC 2007). Wetland preservation, in particular, has garnered attention because of the significant contribution to the environment and economy that these areas provide. For wetlands, the greatest concern related to increased sea-level rise is a loss of land area due to erosion, both vertically and horizontally.

The current practice to slow erosion in mid-Atlantic marshlands on the US East Coast is to build bulkheads or rock walls which prevent landward migration (Titus et al. 2009, Chesapeake Bay Foundation 2007). This can be detrimental because land that might otherwise keep pace with sea-level rise by vertically accreting and moving landward will be inundated due to the stationary retention methods that block migration (Titus et al. 2009). The concept of Living Shorelines has been popularized in recent years, promoted as a creative, low-impact, and sustainable shoreline management technique that incorporate natural plants and materials. Fringing oyster reefs, a recommended Living Shorelines structure, are becoming a more common erosion

mitigation method. Studies conducted in Alabama, Louisiana, Mississippi, and North Carolina have shown that these reefs help reduce the impact of waves on the shoreline, increase sediment size, and enhance the growth of seagrass (Stricklin et al. 2009; Piazza et al. 2005; Meyer et al. 1997, Scyphers et al. 2011), all of which are major variables in stabilizing marsh shorelines. The majority of these studies suggested that oyster reefs are most effective in low energy environments, such as lagoons and shallow bays, and have little to no effect in higher energy areas. Successful results from these studies and the popularized implementation of oyster reefs as shoreline protection, despite the minimal information on the mechanisms of this process, prompted this investigation into the possibility of oyster reefs as an alternative means of shoreline management on Virginia's Eastern Shore.

Marsh erosion

Salt marshes are found in the intertidal zone, acting as a bridge between land and water. They are unique environments in that there is a semi-diurnal cycling of flooding and exposure that is crucial to the maintenance of the system. Salt marshes rely on tides to bring in sediment and nutrients in order to build the marsh platform and nourish plants that live there. Marsh ecosystems are home to numerous flora and fauna, including fish, birds, invertebrates, insects, crustaceans, and a number of endemic species. Marshes are also breeding and hunting grounds that play an important role in the life cycle of some fauna. In keeping with the idea of marshes as bridges, they also function as buffer zones against storms (Pethick 1992), dampening the effect wind and water would otherwise have on the land.

In the 20th century alone, over 18,000 hectares of coastal land have eroded in the Chesapeake Bay, likely with an increasing rate of loss with time (Wray et al. 1995). Already at least thirteen marsh islands that were present in colonial times have vanished completely (Downs et al. 1994). A Maryland study showed that marsh islands are eroding at a faster rate than upland islands, and are prone to submergence because of a deficient source of new sediment (Wray et al. 1995), placing marsh islands at even greater danger. On the Eastern shore of Virginia, marsh sediment accumulation rates are only 36-57% of the local sea-level rise (Hobbs et al. in press). On Bloodsworth Island, Maryland in the Chesapeake Bay, erosion along the perimeter of the marsh accounted for an average 61% of total land loss, indicating that the shoreline is more vulnerable to wave attack than the interior is to subsidence, interior-pond formation, and channel enlargement (Downs et al. 1994). In the Nanticoke Estuary, another Chesapeake Bay location, marsh loss rates were calculated to be near or greater than 1% per year of total land area, which is comparable to rates seen along the Gulf Coast, and greater than other rates along the US Atlantic Coast (Kearney et al. 1988). Studies in Europe and the rest of the United States show that lateral erosion rates on the Virginia Eastern Shore fall in the middle of the observed range of shoreline erosion (McLoughlin 2010, Table 1). As of 2009, the rate of sea-level rise in the Virginia Coast Range (VCR) ranged between 3.8-4.0 mm·yr⁻¹, one of the higher rates seen along the East Coast (Mariotti et al. 2010).

Table 1: Marsh erosion rates in the United States and Europe. Table recreated from in McLoughlin 2010.

Location	Erosion Rate (m yr ⁻¹)	Duration of Study (yrs)	Study
<i>United States</i>			
Delaware Bay, NJ	3.21	38	<i>Phillips (1986a)</i>
Rehoboth Bay, DE	0.14 – 0.43	3	<i>Schwimmer (2001)</i>
Chesapeake Bay, MD	1.2	139	<i>Wray et al. (1995)</i>
Hog Island Bay, VA	~ 1.2	41	<i>Kastler and Wiberg (1996)</i>
York River Estuary, VA	0.21	95	<i>Byrne and Anderson (1978)</i>
Pamlico Sound, NC	0.79 – 0.91	25 – 32	<i>Phillips (1986a)</i>
Mississippi Delta, LA	~ 1	67	<i>Wilson and Allison (2008)</i>
<i>Europe</i>			
Dengie Peninsula, UK	1.1	9	<i>van der Wal and Pye (2004)</i>
Blackwater Estuary, UK	0.5 - 1	8	<i>van der Wal and Pye (2004)</i>
Foulness Point, UK	4 - 16	19	<i>Stoodley (1998)</i>
The Oosterschelde, Netherlands	~ 1	N/A	<i>van Eerd (1985a)</i>
Sado Estuary, Portugal	0.17	11	<i>Moreira (1992)</i>
Venice Lagoon, Italy	1.2 – 2.2	2	<i>Day et al. (1998)</i>

Sea-level rise is a two-fold variable in that it is expected to increase wave heights in shallow bays, accelerating lateral erosion along the fringing marshes (Mariotti et al. 2010), and increase inundation of low-lying areas (Phillips 1968, Finkelstein and Hardaway 1988, Kearney and Stevenson 1991). Projected increases in the rate of sea-level rise are predicted to result in increasingly unfavorable conditions for marsh accretion (Phillips 1986). Serious alterations to the environment, likely by human intervention, will be needed in order to maintain the health of marshes in the coming years (Cox et al. 2003, Kearney et al. 1988).

Waves in shallow bays

Wind-generated wave attack is the predominant agent of marsh retreat through the process of scarp erosion (Möller et al. 1999). Wind speed, wind direction, fetch, and water depth are the critical factors influencing wave formation (Fagherazzi and Wiberg 2009). Fetch (the distance over which wind can blow across the water surface without obstruction) is restricted in many of these lagoons, but in those with greater fetch, waves

are not as high as they would be in deeper water owing to effects of water depth on wave height. Wind direction is an important factor because it dictates the direction in which waves will travel, which affect the intensity of wave attack on any given shoreline (Marani et al. 2011). Analysis of winds in the Virginia Coast Reserve showed that winds blew most frequently from 180°-210° and 330°-60°, which followed the general orientation of the coastline (Figure 1A). Therefore, marshes facing north-northeast or south-southwest with large fetches tended to have greater wave power striking those shores (Figure 1B).

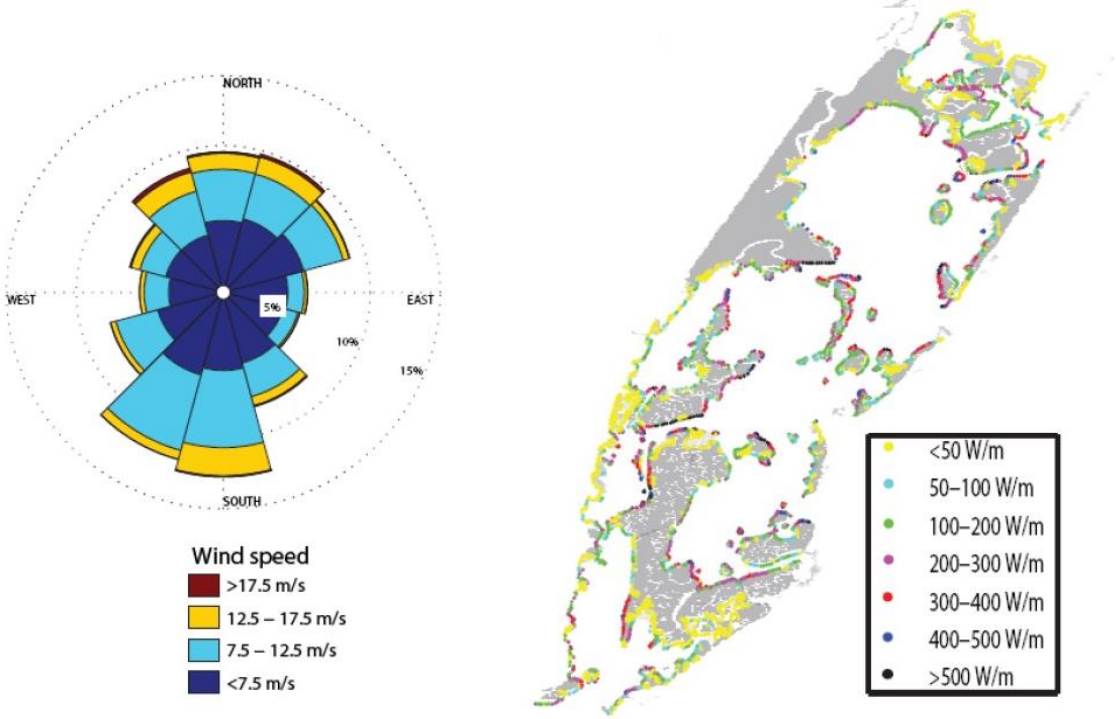


Figure 1: Wind and wave power in the VCR modeled by Mariotti et al. (2010). Wind statistics on the oceanside of the Chesapeake Bay from 1996-1999 (left). Wave powers along marsh boundaries weighted with wind statistics (right). Figures presented in Mariotti et al. (2010).

Marsh-edge characteristics

Work by McLoughlin (2010) explored erosional processes at four salt marsh locations in the VCR, characterizing methods of erosion and physical properties of the sites. The different processes and rates of erosion were attributed to physical attributes of the marsh, wave patterns, bathymetry, and effects of plants and animals living there (McLoughlin 2010, Feagin et al. 2009). The primary cause of erosion in this area is from waves impacting the shoreline (Wray et al. 1995, Day et al. 1998, Schwimmer 2001, Mariotti et al. 2010), but statistical analysis of erosion as a function of wave energy was not able to explain all of the variation (McLoughlin 2010). Vegetation morphology and density have been shown to be indicative of marsh edge stability (McLoughlin 2010, van Eerd 1985, Knutson et al. 1982). Trends on Bloodworth Island showed that a decrease in vegetation was correlated with an increased erosion rate, particularly along the perimeter of the marsh island (Downs et al. 1994). Aboveground, grass canopies dissipate wave energy, the extent of which is affected by both canopy height and stem density. Belowground, the trussing capability of the vegetation roots stabilizes sediment, armoring it against wave attack (van Eerd 1985).

There are many factors that contribute to bank destabilization, among them is the presence of crab burrows. Salt marshes on the Virginia Eastern Shore have three species of fiddler crabs, *Uca minax*, *U. pugilator*, and *U. pugnax* (Teal 1958). The fiddler crab is a major reworker of sediment, whose burrows weaken the structure of the marsh groundwork. Previous work has suggested that high densities of burrows formed by *Sesarma reticulatum* and *Panopeus herbstii*, the purple marsh crab and the Atlantic mud

crab, along the marsh edge are associated with higher erosion rates (McLoughlin 2010). These burrows tend to be larger with multiple chambers and greater complexity compared to *U. spp* burrows, due to the communal habitation of these species (Allen and Curran 1974). Despite this, it is likely that the fiddler crab burrows also contribute to destabilization along the marsh edges, though possibly to a lesser degree.

The sediment that comprises the marsh also influences its susceptibility to erosion and can account for some of the variability at sites within the same region (Rosen 1980). In the Virginia portion of the Chesapeake Bay, four levels of shoreline vulnerability have been identified based on their sedimentary properties: permeable sand beaches (mean erosion rate of $0.85 \text{ m}\cdot\text{yr}^{-1}$); beaches with a layer of sand on top of impermeable pre-Holocene sediment ($1.14 \text{ m}\cdot\text{yr}^{-1}$); marsh barrier beaches of sand overlying peat ($0.66 \text{ m}\cdot\text{yr}^{-1}$); and marsh margins ($0.54 \text{ m}\cdot\text{yr}^{-1}$) (Rosen 1980). The Feagin et al. (2009) study did not find a relationship between sediment size and erosion. McLoughlin (2010) found that marshes with greater proportions of medium to coarse sand showed lower rates of erosion compared to locations with higher proportions of silts and clays in Hog Island Bay.

Oyster reefs as erosion control

Oyster reefs are known to stabilize intertidal sediment and influence hydrodynamic patterns within estuarine environments (Meyer et al. 1997, Piazza et al. 2005, Coen et al. 2007, Dame and Patten 1981). Because of their potential stabilizing effects, building oyster reefs close to eroding intertidal marshes has been considered as a means of slowing or reversing shoreline erosion (Scyphers et al. 2011). Modeling of

energy flows through oyster reefs shows that reefs change water current patterns (Dame and Patten 1981) and can increase the coefficient of drag up to five times over that for a bare mud bed (Whitman and Reidenbach 2012). Four previous studies, summarized below, have investigated the efficacy of oyster reefs as a form of erosion control. These studies concluded that reefs are successful in this capacity though only in low energy environments (Piazza et al. 2005, Stricklin et al. 2009). Each study approached oyster reef erosion control with different objectives in various locations (Figure 2).

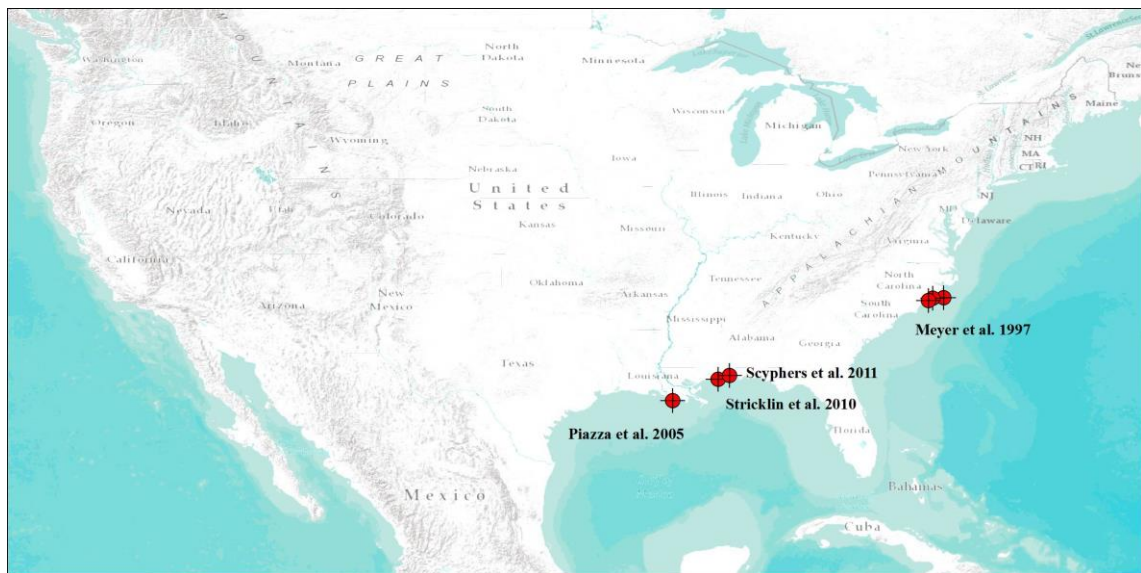


Figure 2: Site locations for studies of oyster reef erosion control.

At two locations in Mobile Bay, AL, three 5 x 25 m rectangular-trapezoid oyster reefs were created from local oyster shell over geo-textile fabric and covered by plastic mesh which was anchored in place by rebar (Scyphers et al. 2011). The reef height was slightly below mean low-low water (MLLW) to maximize potential wave attenuation, oyster settlement, and habitat for local fish. However the reef heights declined over time to as low as 0.3 m due to reef footprint spreading, which undermined the study.

Vegetation line retreat on adjacent marshes was measured periodically throughout the

two-year study by distance from rebar stakes placed at 25 m intervals along each 100 m shoreline (one control and one study at each of the two locations). At the first location, where the reef footprint expanded by almost 300% due to wave-driven spreading, significance testing showed there was no difference in the retreat rate at the reef site ($2.55 \text{ m}\cdot\text{yr}^{-1}$) compared to the control ($2.7 \text{ m}\cdot\text{yr}^{-1}$). The reef at the second location decreased shoreline retreat by 45% over the course of the study, having eroded slightly more than 3 m compared to ~ 4.5 m at the control site. This study suggests that oyster reefs do affect erosion but require more solid structures for this mid-level energy environment (Scyphers et al. 2011).

In Louisiana, small, created fringe reefs were useful in slowing shoreline erosion and were found to have high rates of spat recruitment, which increase reef size and add sustainability to the existing structure (Piazza et al. 2005). The initial dimensions of the reefs, created from shucked oyster shell, were 25 x 1 x 0.7 m, and were built as close to the marsh as possible (< 5 m). This was deemed an ideal method to help control the Gulf of Mexico shoreline in Louisiana because the material is native to the region, and relatively inexpensive, assuming a constant source of oyster shell. Data from the twelve-month study showed that mean shoreline retreat was significantly lower at low-energy sites with created reefs. High-energy locations did not exhibit differences in erosion whether there was a reef present or not. It was suggested that this outcome was either because the small, created reefs were insufficient protection in this particular study, or that fringing shell reefs in general are not enough to fully protect shorelines. There were two major storm events (extremely high energy) during the study period (September and

October 2002), neither of which significantly changed the erosion rates at the sites with their passage, regardless of the presence of oyster reefs. However, the month following each storm did have greater loss rates at all sites, which were attributed to the storm loosening sediment. Scour from the edges of the reefs affected the shorelines behind them, suggesting that longer reefs may be more protective than shorter ones. The study concluded that created fringing oyster reefs did slow shoreline retreat, but were effective only in low-energy settings (Piazza et al. 2005).

Other studies have examined whether different sorts of oyster reefs, such as natural versus man-made, or cultched versus non-cultched, exhibit differing erosion rates. In Jackson County, Mississippi, man-made reefs were built alongside long-standing natural reefs in a marsh area in order to determine whether one was more effective than the other. These marshes are similar to those found on the Virginia coast, composed mostly of sands and clays, and covered by meadows of *S. alterniflora* (Stricklin et al. 2010). The created reefs were built in front of the marsh, 30.5 m by 1.8 m, and set 92 m or more laterally from the natural reef with which it was paired. These reefs were created by placing shell bags filled with 0.03 m³ of oyster cultch and trays containing shell bags of cultch on top of a mud flat such that they were roughly 15 cm above the flat. A cultched reef is one that has had fossilized shell, coral, or other material of similar properties that has been made by living aquatic organisms, placed on or near the reef (Merriam-Webster). The purpose of cultch is to provide a hard substrate on which oyster spat can settle, enhancing the growth rate of the reef (The Oyster Restoration Project 2012). In order to mimic the patchiness of natural reefs, shell bags and trays were placed

so they covered 30-35% of the designated reef area. During the 21-month study (November 2006-June 2008), constructed reefs resulted in equivalent or better erosion reduction compared to natural reefs at all sites. There were significant differences between both energy at the site and reef treatments. At the high energy location, the cultched site eroded 1.68 m ($0.12 \text{ m}\cdot\text{yr}^{-1}$) and the non-cultched site 1.96 m ($0.14 \text{ m}\cdot\text{yr}^{-1}$). At the low energy location the cultched site eroded 0.34 m ($0.02 \text{ m}\cdot\text{yr}^{-1}$) and the non-cultched site eroded 1.40 m ($0.10 \text{ m}\cdot\text{yr}^{-1}$). Retreat periods differed between the three bayous as well as reef types, and some sites initially advanced for 7 months before retreating for the remainder of the study (14 months). A second site accreted for all but the last month of the study, and the third had a steady rate of retreat for the duration of the 21 months. There is no mention of change in wave environment during these periods of erosion and accretion but these bayous are low-energy by nature, microtidal ($\sim 0.5 \text{ m}$), and can be wind-driven (Stricklin et al. 2010).

Similar to the experiment in Mississippi, the aforementioned study in North Carolina (Meyer et al. 1997) examined the difference in the effects of cultched and noncultched reefs on erosive dampening at three nearby locations. Marshes in this study were originally dredged material disposal sites, which were altered by the U.S. Army Corps of Engineers and planted with *S. alterniflora* and *Spartina patens* (a high marsh grass) in 1987, the former of which dominated the lower intertidal zone by the time of the study. The design involved twelve constructed reefs, each 5 m wide by 20 m long, built perpendicular to the shoreline by depositing 1.5 m wide by 0.25 m deep bands of cultch (crushed oyster shell, in this study) at the fringe of the marsh, leaving a 3 m buffer of

non-cultched marsh between plots. The stability of each site was measured by the sediment surface change along the midline of each plot. Overall, there was no significant difference in shoreline movement between the treatments, but a number of measurement periods did vary significantly between cultched and noncultched plots within the same study site. Two sites did show a notable difference in shoreline change between cultched and noncultched plots over the course of the whole study period (20 months). At the first site, the cultched plot accreted +0.52 m (+0.31 m·yr⁻¹) and the non-cultched plot eroded -1.11 m (rate of -0.67 m·yr⁻¹). The second site's cultched plot accreted +0.77 m (+0.46 m·yr⁻¹) and the non-cultched site eroded -1.05 m (-0.63 m·yr⁻¹) (Meyer et al. 1997).

Results from these studies showed that oyster reefs were useful wave-dampening agents, which performed best in low energy environments, and in some cases, promoted accretion. Based on the low-energy lagoon-type environments in three of these studies, the similarities suggest that oyster reefs may work as erosion control in the Virginia Coast Reserve.

As an alternative to conventional shoreline management techniques, the National Oceanic and Atmospheric Administration (NOAA) recommends installing native reef-building oysters whose structures can perform a number of ecosystem services (NOAA 2013a) (Figure 3). These natural submerged breakwaters absorb wave energy, protect the shoreline, and enhance critical habitats, in addition to filtering impurities from the water benefits seagrass, fish, and invertebrates (NOAA 2013b). Oyster reefs are an example of an ideal breakwater substrate advocated by the Living Shoreline movement, which strives to incorporate greater amounts of native substances over man-made material. In response

to the Deepwater Horizon oil spill, Living Shoreline projects, including the installation of oyster reefs, have been started in Alabama, Florida, Louisiana, Mississippi, and Texas as a remediation method (TNC 2011).

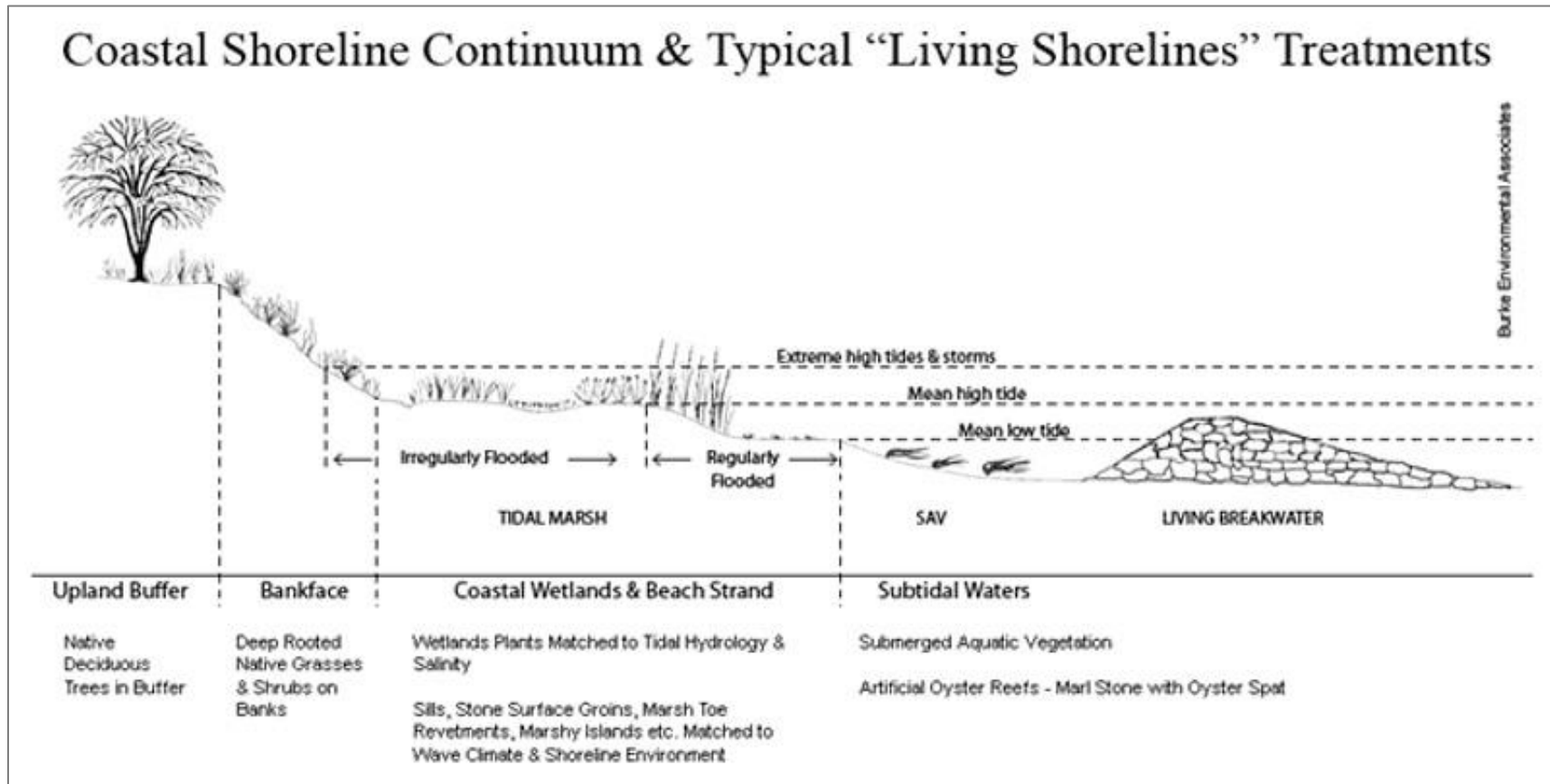


Figure 3: From NOAA Living Shorelines - "Coastal Shoreline Continuum & Typical ‘Living Shorelines’ Treatments." Illustration of suggested materials to use in each coastal shoreline zone. Reef-building oysters were recommended for the living breakwater because they would protect the shoreline.

Objectives

The purpose of this study was to determine whether or not oyster reefs are effective at dissipating wave energy and reducing marsh edge retreat in the shallow bays of the Virginia Coast Reserve on the Eastern Shore of Virginia. There were three primary objectives that helped address this question:

- Are any of these marshes predisposed to higher rates of erosion based on physical characteristics and overall wave environment?
- What are the rates of shoreline change over the past fifty years and how have they varied in space and time? Are the rates different for marsh edges protected by oyster reefs compared to nearby unprotected marshes?
- Does wave energy dissipate as it passes over oyster reefs towards the marsh? If so, how do the reefs change the waves and to what degree?

Study sites

This study was conducted on salt marshes found on the ocean side of the southern end of the Delmarva Peninsula (Figure 4), which encompasses the Virginia Coast Reserve and serves as a Long Term Ecological Research (LTER) site. The selected study sites are all protected by The Nature Conservancy (TNC) of Virginia, as are the oyster reefs in the vicinity. Four marsh sites were selected for study due to partial blocking of on-coming waves by oyster reefs, located in two different areas along the mainland edge of the VCR (Figure 4). Current research shows that oyster reefs were most successful at

diminishing erosion in low energy environments, which influenced the selection of these particular sites. The sites were also chosen so as to have two different basic environments: a closed shallow bay with small defined reefs vs. a more open lagoon with larger, dispersed reef. Two sites were selected within each region for comparison and replication. Tides in both regions were semi-diurnal, with mean tidal range of 1.2 m (Fagherazzi and Wiberg 2009). In both regions, two comparison sites were identified that were not associated with any oyster reefs and were in close proximity to the study sites with reasonably similar apparent physical and hydrologic attributes.

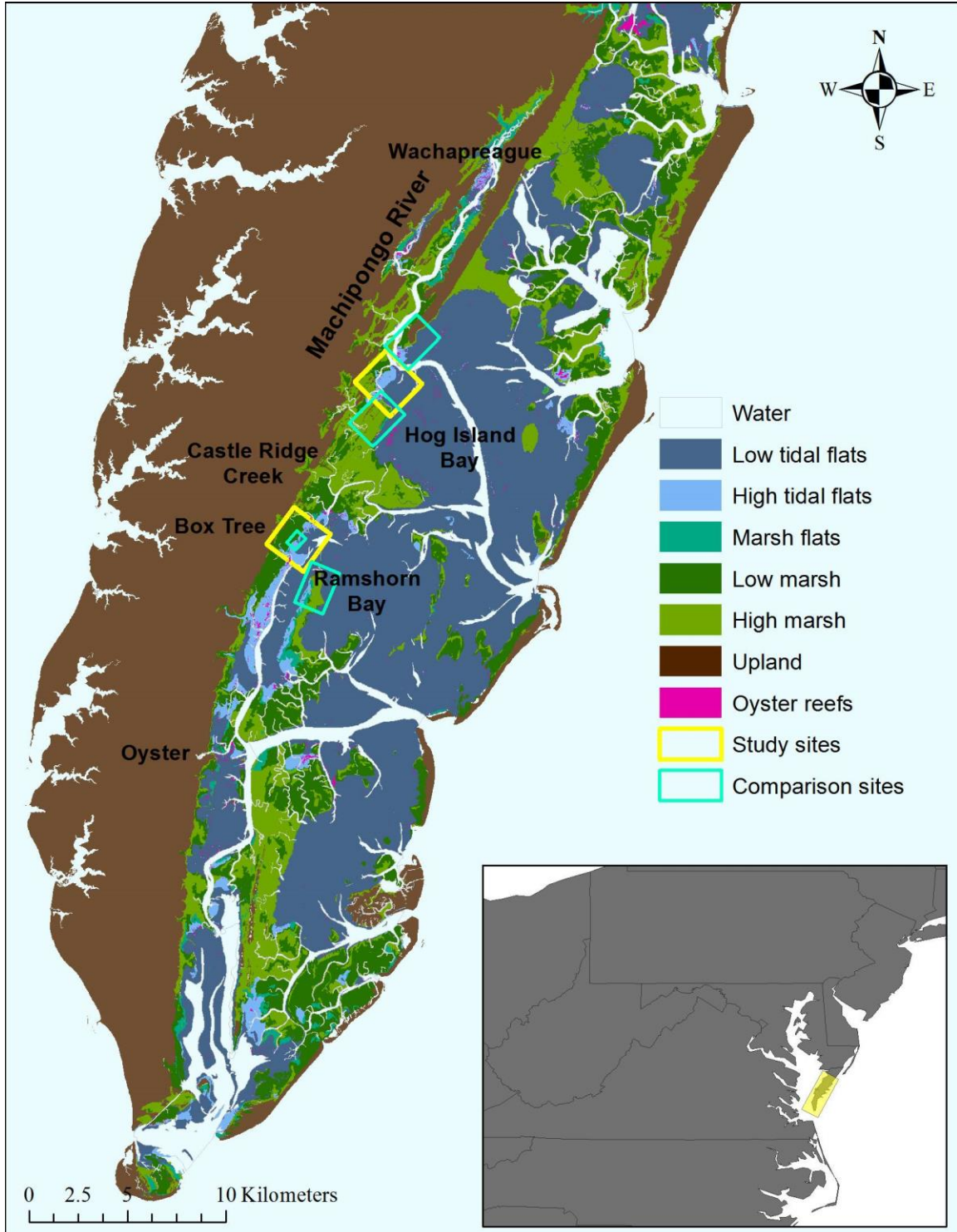


Figure 4: The Virginia Coast Reserve study and comparison site locations with land types illustrated. There are two study sites within each yellow box – SEB3 and CRM4 to the north, and BT5 and BT6 to the south. Oyster reefs as measured by The Nature Conservancy are visible in pink.

Box Tree sites

The two southern sites were found near Ramshorn Bay, in an area known as Box Tree (Figure 4). They were both marsh islands close to the mainland and were remnants of an old sand dune (Barry Truitt, personal communication, 2012, hereafter as Truitt 2012), which had been taken over by the cordgrass, *Spartina alterniflora*, and fiddler crabs (*Uca* spp.), interspersed with the succulents, *Salicornia virginica* and *Salicornia bigelovii* (Silberhorn 1976). They were situated on top of a discontinuous sheet of sand and pebbly sand ridges and swales 1-2 m in height and 2-4 km apart (Swift et al. 2003). Both islands had oyster reefs built off the seaward side by waterman, Jack Johnson, for harvesting and transplanting oyster seed, which were created in the 1950's or 60's (Truitt 2012). The oysters that settled on these reefs and others in the VCR were American eastern oysters, *Crassostrea virginica*, which were considered native transplants and are found along the length of the Atlantic seaboard (USGS 2004). The base of the reef near Box Tree site 5 (BT5) was made of crushed whelk shells, and the Box Tree site 6 (BT6) reef was comprised of oyster castles on the shoreward side and old oyster shells on the seaward half. The BT6 reef was nearly perpendicular to the middle of the marsh island and the BT5 reef was about 30 degrees from perpendicular. The BT5 reef was a fairly loose shape with gently sloping sides that gradually descended into the mud at the edge of the reef (Figure 6). The BT6 reef had more topography than the BT5 reef because of the combination of base materials. The section made of oyster castles had a relatively uniform elevation and was approximately 0.5 m wide. The old shell section resembled the BT5 reef – gently sloping sides and looser shape that gradually sunk to the mud as the

reef expanded outward (Figure 7). Both marsh islands had exposed mainland to either side that was open to Ramshorn Bay and both were scattered with large populations of periwinkle snails (*Littoraria irrorata*), which are the most prominent grazers on coastal Atlantic salt marshes (Silliman and Bertness 2002).

The comparison sites for this region included the mainland marsh that run between BT5 and BT6 (inter-island – I-I), as well as Elkins Marsh (Elk), which was a peninsula on the eastern edge of Ramshorn Bay (Figure 5). The Elkins shoreline did experience greater wave energy than any other site as predicted by the Mariotti et al. 2010 model (Figure 1), and was more typical of a barrier island environment than a low-energy lagoon like the study sites. The inter-island hydrodynamics and other physical properties were indistinguishable from those of the study islands.

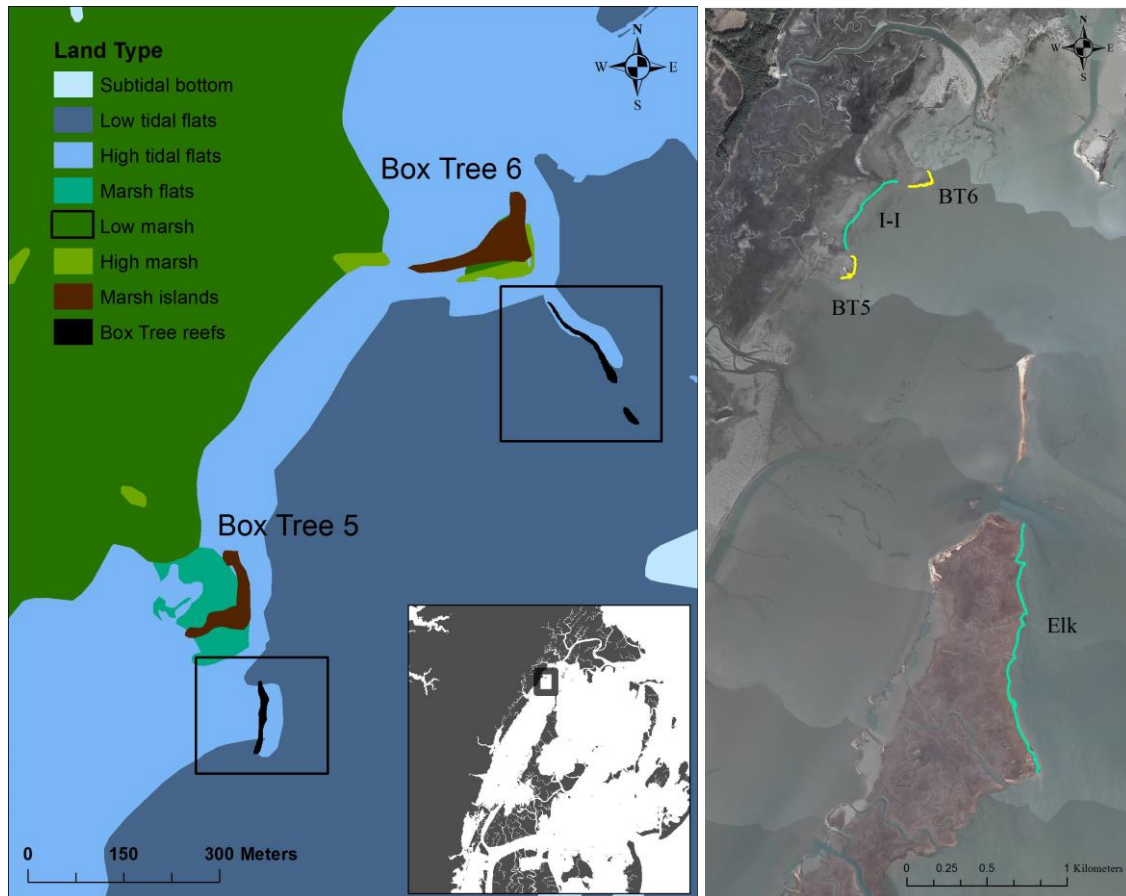


Figure 5: Left panel: southern study sites, Box Tree 5 and Box Tree 6 – marsh islands fronted by small, linear reefs. Right panel: comparison sites (Inter-Island and Elkins Island) in relation to study sites.

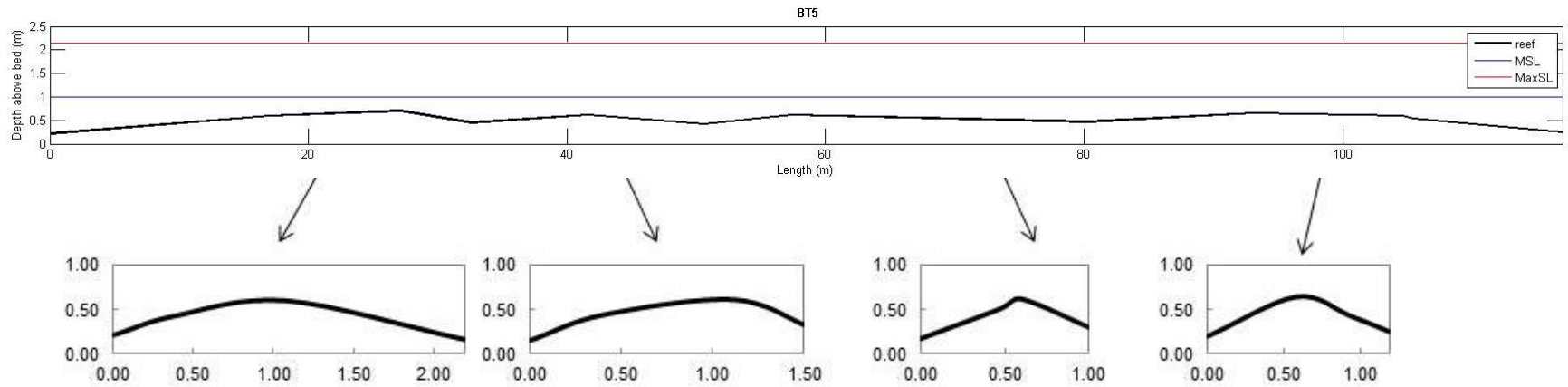


Figure 6: BT5 reef profile and cross-sections. Average width of discrete reef structure was 3-5 m and sides of reef gradually taper off into muddy bottom. Blue line on upper plot indicates MSL and red line is maximum recorded depth.

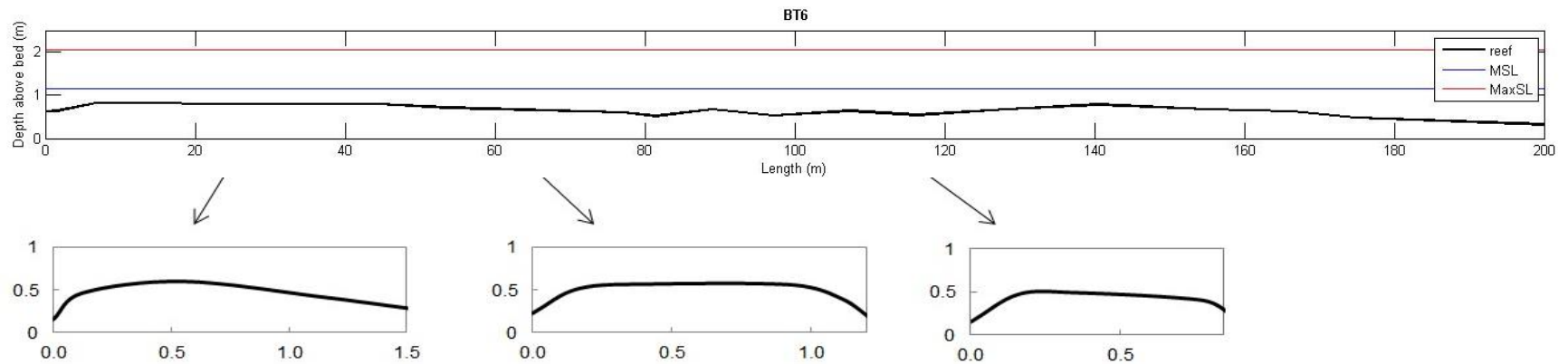


Figure 7: BT6 reef profile and cross-sections. Average width of discrete reef structure was 0.5-2 m. The section closer to the marsh (left on panel) was made of oyster castles and had steep sides, farther out was based on old shells and gradually sloped toward the bottom. Blue line on upper plot indicates MSL and red line is maximum recorded depth.

Northern sites

The Northern sites (Figure 8), Southeast Bend 3 (SEB3) and the convergence of Castle Ridge Creek and the Machipongo River (CRM4), were mainland marshes. SEB3 was fronted by an old, natural reef (Truitt 2012) that extended out in front of Castle Ridge Creek to shield the southwestern portion of the shoreline, with a smaller, more seaward section open to the ocean. The reef was more wide-spread and muddier than the Box Tree reefs, with small channels, and large patches with high piles of oysters (Figure 9). The CRM4 reef was also an old, natural reef (Truitt 2012), but had a more defined shape than the SEB3 reef, though it was also large, muddy, and channel-ridden. This reef fronted the southwestern shoreline of the marsh, leaving the eastern, seaward section open to the edge of Hog Island Bay. There were two comparison sites for this region – northern Fowling Point (nFP) and Upshur Neck (UN) (Figure 4). The Northern comparison sites were predicted to have similar wave powers at the shoreline as the study sites. However, Upshur Neck, a highly developed area, was likely influenced by the structures built there such as houses and boardwalks, both of which affect hydrodynamics.

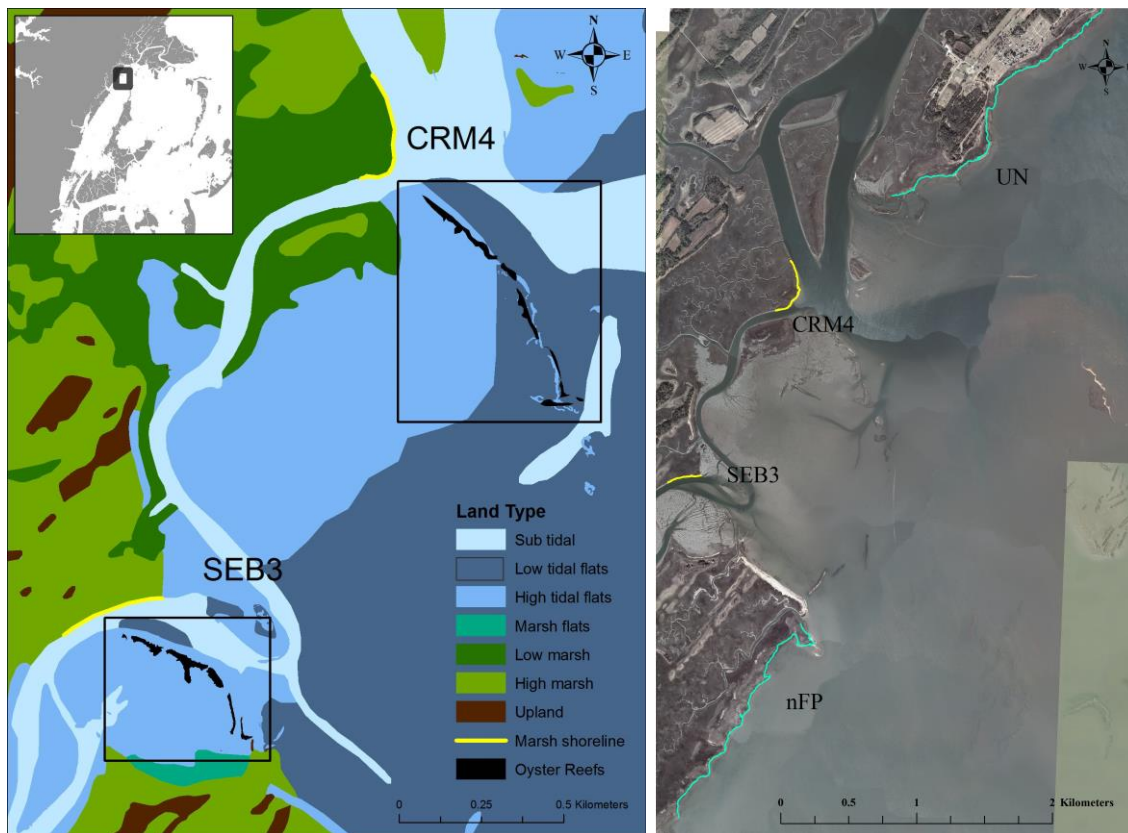


Figure 8: Left panel: Northern study sites, Southeast Bend 3 and Castle Ridge/Machipongo 4 with their respective oyster reefs. Right panel: comparison sites (Upshur Neck and northern Fowling Point) in relation to the Northern study sites.

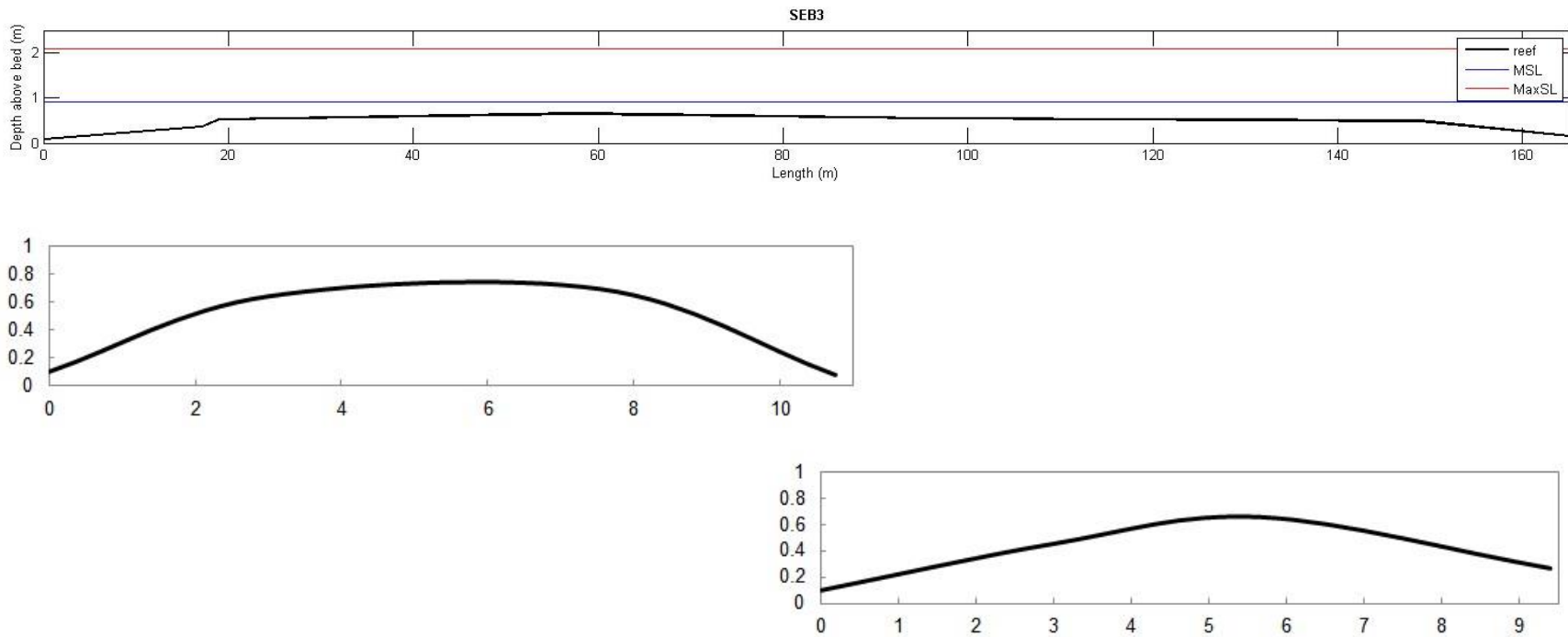


Figure 9: SEB3 reef profile for section closest to marsh. Reef extended another 450 m and varied in width from 1-10 m interspersed with patches of mud and small channels. Blue line on upper plot indicates MSL and red line is maximum recorded depth. No CRM4 profile available due to poor survey data quality.

Methods

Digital shoreline analysis

Geographical Information Systems (GIS) 10 software (ESRI, Redlands, CA) was used to perform marsh shoreline analysis, both short-term and long-term (Fletcher et al. 2003). Short-term analysis used repeat GPS surveys of the vegetation line of each marsh, taken roughly six months apart, to determine shoreline change rates. The raw survey data were corrected using NOAA's Online Positioning User Service (OPUS) and processed in Trimble Geomatics Office before being imported into ArcMap, a GIS interface. The GPS points were digitized into a single shoreline and analyzed by Digital Shoreline Analysis System (DSAS), a GIS extension specifically for calculating shoreline change (Thieler et al. 2009, McLoughlin 2010). The surveyed shorelines were not analyzed in conjunction with the shorelines extracted from aerial photography because they did not use the same datum, thereby greatly increasing the probability of error in accurately positioning the shorelines in relation to each other. Distances between the PVC pole markers and the shoreline as of June 2012 were measured to obtain a rough gauge of how much the site had changed in about a year. These measurements were compared to the GPS surveys with the understanding that this data set was not as accurate as the GPS surveys because some of the poles had been uprooted and washed away or were embedded in a slump block that had detached from the marsh edge all together.

Long-term analysis used five aerial images of Northampton County, VA, spanning a sixty-year period. Images were provided by the USDA Farm Services Agency

(years 1957, 1966, and 1994) and the Virginia Base Mapping Program (VBMP) (2002, 2007). These images were selected based on time interval, image quality, and availability. Images from 2002-2007 were previously orthorectified by VBMP, but earlier images were not. These images were given spatial context with the georectification tool in ArcMap using stable structures such as buildings and roads as ground control points, though some creek intersections were used when there were no other viable options (Higginbotham et al. 2004, Kastler 2003). The images were rectified over the 2009 VBMP orthographs with polynomial transformations, using second or third order when possible for greatest accuracy. Shorelines were digitized by creating a new feature class within ArcMap and digitally tracing the vegetation line on-screen for each image.

The DSAS program requires a compiled layer of digitized shorelines for each site, a baseline off of which to cast transects, and the transect layer itself (Figure 10) to calculate rates of change over time and associated statistics, such as the change between the oldest and youngest shorelines, and linear regression rate. Shoreline change analysis was performed for the entire 52-year period as well as at quasi-decadal intervals to determine any change in erosion rate over time. A standard method for comparing this type of data is an ANOVA (ANalysis Of VAriance), however all four of the data sets were non-normal and had unequal variances, which violated assumptions for an ANOVA. Because the data did not deviate too much from normal but did have high variance, a Kruskal-Wallis (McDonald 2009) test was used - the non-parametric analog of ANOVA. The main concern with non-parametric tests is the potential for loss of power in analysis. However this was not an issue for this data set because there was such

a large difference between sites. All of these comparisons were made using the Bonferroni Correction with $\alpha = 0.05/6 = 0.0083$, necessarily increasing the confidence level for each test because there were six total. With each test the probability of a Type I error was 0.05 and each subsequent test increased this probability by 0.05, (i.e. the second comparison had a 0.075 chance of committing a Type 1 error, et cetera). Therefore, by using $\alpha = 0.0083$ for each individual comparison the overall confidence in the six tests was 95%.

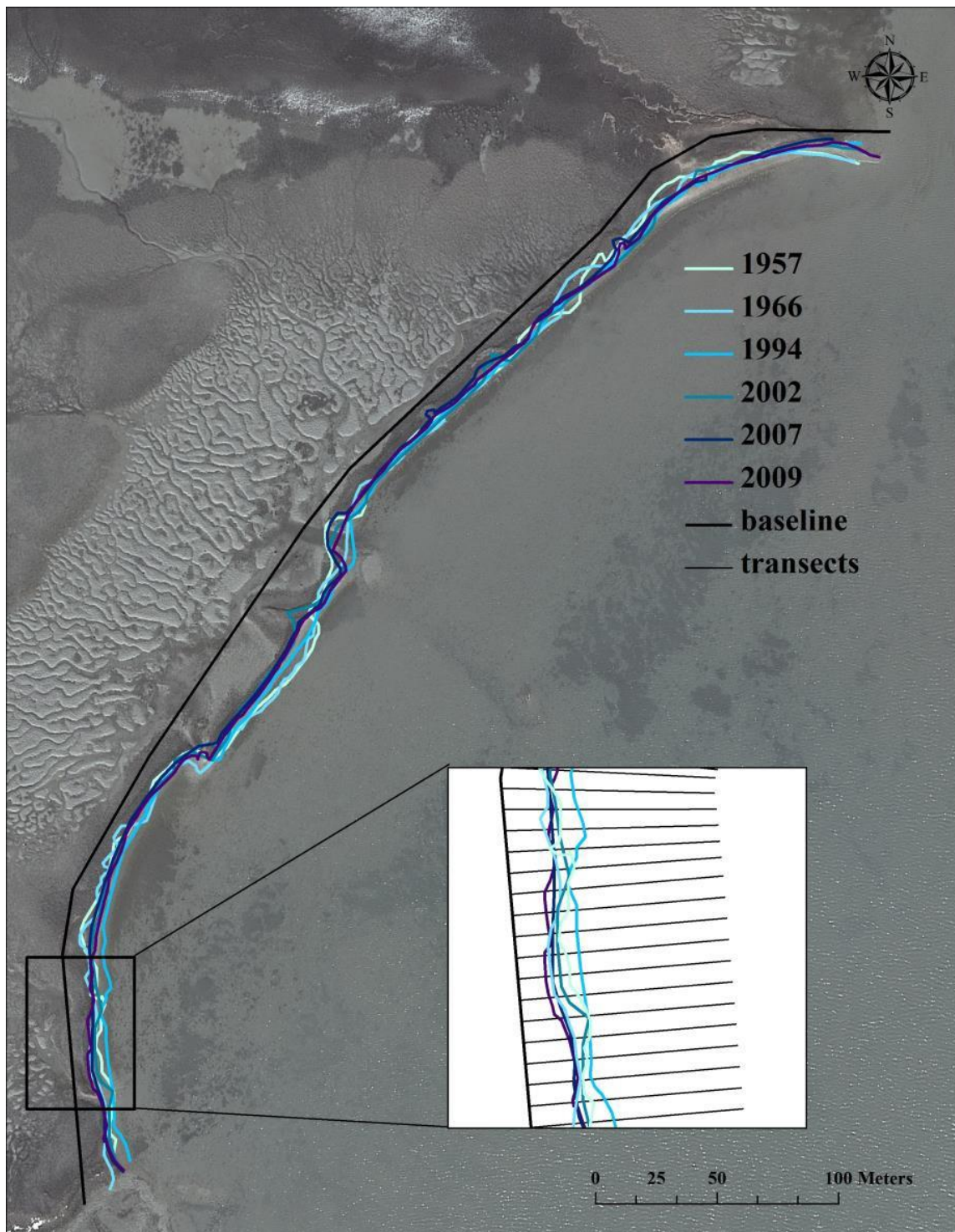


Figure 10: Digital Shoreline Analysis Software components consisting of a baseline (black line), transects (parallel lines in inset), and digitized shorelines with the dates images were taken. Shorelines were hand-mapped on screen after georectification with minimal associated error (RMS values less than 2). Transects were drawn by the program at 5 m intervals along the baseline, which was drawn in as a generalization of the shoreline for transect casting purposes.

There were a number of potential sources of error in the digital assessment of shoreline change beginning with error in the initial photographs due to distortion from the angle of the camera, lens quality, image resolution, condition of print negatives, and scanning the image (Moore 2000). The georectification process undoubtedly introduced some error. Potential ground control points (GCPs) were limited because the majority of each image depicted the lagoon and marsh which inherently had a restricted number of stable features. In addition, the VCR is in a rural area that has few unchanging structures like buildings and roads close to the shoreline. There was also possible warping of the georectified images because quality GCPs were not always available in the southeast corner, mostly showing open water. However, RMS errors were all less than 2, which was below the acceptable limit of 5 for lateral shoreline analysis (Hughes et al. 2006), and high order polynomial transformations were used, both of which decreased the probability of error (Table 20). Error could also have been introduced during the shoreline digitization process, particularly if the image had low resolution or an indistinct delineation between marsh and water. The vegetation line was the most distinguished feature in the majority of images and was used as the shoreline indicator for its visibility and independence of tidal level which varied from image to image. Complex shorelines with low-grade edges are more difficult to correctly identify and ultimately decrease accuracy of the digitization process (Cox et al. 2003). Additionally, historical maps of the study area were located from the mid to late 19th century that were primarily used for navigation and surveying. They were intriguing visual comparisons but had insufficient resolution or coverage to be included in the analysis of the sites.

Site characteristics

Each marsh was characterized in order to determine if there was a particular set of variables that influenced rates of marsh accretion or erosion. All sites were surveyed by taking global positioning system (GPS) surveys using the Trimble© R8 GNSS system (Trimble, Sunnyvale, CA), once during the summer and winter of 2011, and the summer and fall in 2012. These surveys followed the vegetation line as a reference point for the marsh edge regardless of tide level, with resolution less than 0.5 m. During the last survey in the fall of 2012, measurements were taken perpendicular to the shoreline across five transects in order to determine marsh elevation (Figure 11). During the first survey in the summer of 2011, 2 cm diameter PVC pipes were inserted into the marsh at 15 m intervals along the shoreline as a visual key for any short-term change (Figure 11) which was measured the following summer. Both types of surveys tracked the vegetation line, as it was the most consistent measure of the marsh extent. Shape files provided by TNC from 2008 were used for the oyster reef physical analysis. Data in the shape files included area, density, type, and location of each reef.

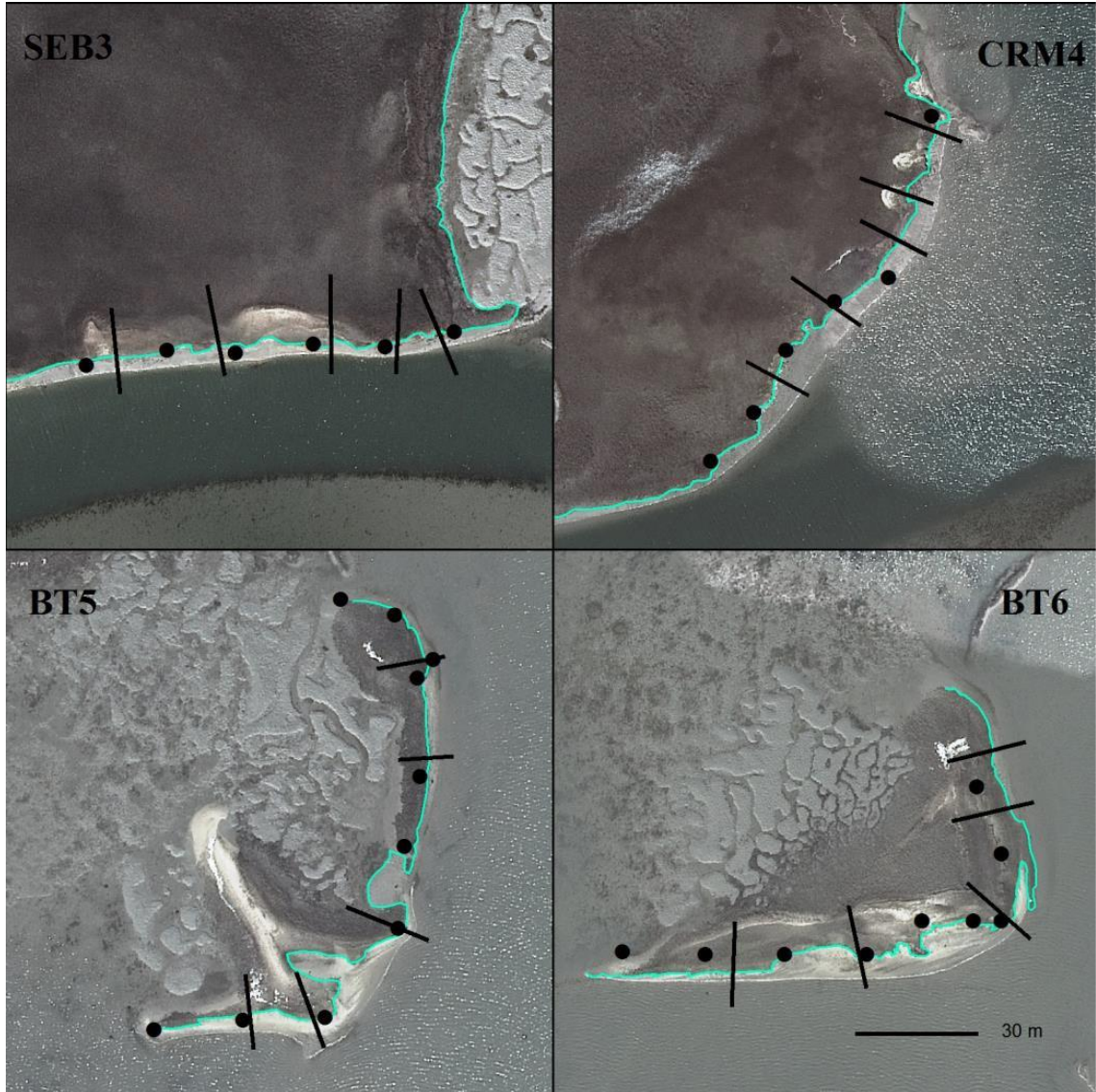


Figure 11: PVC marker poles and survey transects 2011-2012. Marker poles (dots) were used to track short-term change and transects (lines) were used for marsh elevation profiles.

Sediment sampling

Sediment grain size and organic content were quantified for each marsh as grain size is an important factor in sediment resuspension. Using a modified plastic syringe, 30 mL sediment samples were taken adjacent to PVC poles that have been placed along the

vegetation line of the marsh site at regular intervals (Figure 6). Two samples were taken at each marker pole, one for grain size, and one for bulk density and loss on ignition. There were 10-13 sample sites on each of the four protected marshes and a total of 10 each on the comparison sites (northern Fowling Point, Elkins Marsh, and the inter-island marsh); no samples were taken at Upshur Neck due to private land ownership. This was the only on-site analysis done for the control sites. For grain size analysis, samples were wet sieved with a 2 mm sieve and placed in a glass jar with salt water to settle. Excess water was siphoned off after all particles had settled and 50-200 mL of bleach was added to remove any organic material, replacing the spent bleach once a week. Samples were then flushed with salt water over a period of two or three days to remove the bleach, the purpose of the salt water being to encourage faster particle settling. A number of samples still exhibited bubbling after bleach treatment for up to five months so another method of organic content removal was employed. After rinsing the samples clean of bleach with water, 50 mL of 30% hydrogen peroxide solution was added to the samples. This procedure was continued, adding 50 mL once more, and then 25 mL, until the effervescence ceased (Wheatcroft et al. 2012, Law 2012).

The organic-free sample was placed in a 50 mL centrifuge tube to settle again before siphoning off excess water. If the sample was mostly clay or mud, a 5% sodium hexametaphosphate solution was added as a dispersant to keep particles from flocculating and resulting in false values from the particle size analyzer (PSA). Three sub-samples were taken from the 50 mL centrifuge tube and placed in 15 mL tubes to be processed by the PSA, an LS 13 320 Laser Diffraction Particle Size Analyzer (Beckman Coulter, Brea,

CA), to give percent of the sediment in each size class ranging from 0.375 μm to 2 mm. The three replicates were averaged by the PSA software and the average was used for further data analysis.

To obtain the percent organic matter, approximately 20 g of sediment were taken from the second sample and dried at 50° C for 48 hours to remove all water, using the difference between wet and dry weight to determine bulk density. The dried samples were placed in a muffle furnace for six hours at 500° C to burn off all organic material. Organic content was determined as the weight of the sample lost on ignition. The remainder of the sample was dried and finely ground for tinning in preparation for carbon and nitrogen analysis. Five cores, 2.5 cm in diameter to a depth of 40 cm, were taken for ^{210}Pb dating to establish an estimated deposition rate within the last century at the study sites. A single core was taken on each of the four protected marsh sites, as well as one sample from an unprotected area between each of the Northern and Southern sites. The cores were sliced in 1 cm increments from 0-20 cm depth, and then in 2 cm increments to the bottom of the core. Cindy Palinkas at UCMES processed and interpreted these samples by the standard method described in Nittrouer et al. (1979). These results were considered poor due to multiple failures of acid digestion which resulted in incomplete profiles for all but one core. Because of the sparse and inconsistent results these data were not considered further. Dried and ground sediments were analyzed for carbon and nitrogen content which was not utilized in this study but can be found tabulated in Appendix II (Table 28).

Ecology

Marsh ecology plays a role in shaping the shoreline and influences erosion rate (McLoughlin 2010). Crab burrows were counted using a 625 cm² quadrat and measured with calipers to determine surface density. Above and belowground biomass was sampled in the high season of productivity (June-August 2011) at the marker poles along each marsh edge (Figure 6) using a 15 cm diameter PVC tube to core 20 cm below the surface. Shoots that fell within the tube were counted then trimmed at the marsh surface and placed in paper bags for drying and weighing. The core was sliced into four sections of 5 cm each and processed as described by Castillo et al. (2008) and Gross et al. (2001). All dried material was summed for each site to determine total biomass above and belowground. A linear regression was used to test all physical attributes against erosion rates.

Hydrodynamic measurements

Hydrodynamic measurements included tides, waves, and water velocity in the region surrounding the oyster reefs at of the each study sites. At each reef, an AquaDopp Pro© (Nortek AS, Rud, Norway) was placed just behind the interior tip of the reef and an RBR Submersible Tide and Wave Recorder TWR-2050P (RBR Ltd., Ontario, Canada), referred to here as a wave gauge, was placed roughly 10 m out on either side of the reef (Figure 12). The wave gauges recorded tide elevation and wave conditions every 30 minutes, with tides recorded at 1 Hz and averaged over a ten-minute period, and waves sampled at 4 Hz and averaged over 5 minutes. The AquaDopp Profiler (ADP) recorded tidal velocity and water level. Velocity was recorded every 30 minutes at 1 Hz, averaging

over a period of 10 minutes at 0.5 m increments of elevation within the water column, the minimum for the ADP used in this study, and a blanking distance of 0.2 m above the bottom. The instruments were left at each site for a minimum of two weeks (Table 2).

Meteorological data for the period of each deployment was obtained from the NOAA buoy at Wachapreague, VA (WAHV2) located 20 km to the north of CRM4. Following Mariotti et al. (2010), we assumed that there was sufficient uniformity of winds within the VCR to apply this data to our study locations. Atmospheric pressure recorded by WAHV2 was used to correct pressure measured by the ADP and TWR for atmospheric forcing after which the pressure values were converted to water depth. Water levels from the TWR gauges, the ADP, and Wachapreague tide gauge were checked for agreement. Wind conditions at WAHV2 were divided into eight 45° bins by direction (N: 337.5°-22.5°, NE: 22.5°-67.5°, etc.) and used to gather statistics such as average wind speed and variance in order to better understand wind patterns during the sampling period.

Table 2: Hydrodynamic sampling schedule of deployments at study sites. Water velocity was measured by a Nortek AquaDopp Profiler and waves were sampled by RBR TWR-2050P wave gauges.

Location	Measuring	Start date	End date
SEB3	water velocity	12/17/2011	1/7/2012
	waves	12/17/2011	1/7/2012
CRM4	water velocity	7/25/2011	8/8/2011
	waves	12/17/2011	1/7/2012
BT5	water velocity	7/7/2011	7/21/2011
	waves	2/15/2012	3/7/2012
BT6	water velocity	9/22/2011	9/24/2011
	waves	2/15/2012	3/7/2012

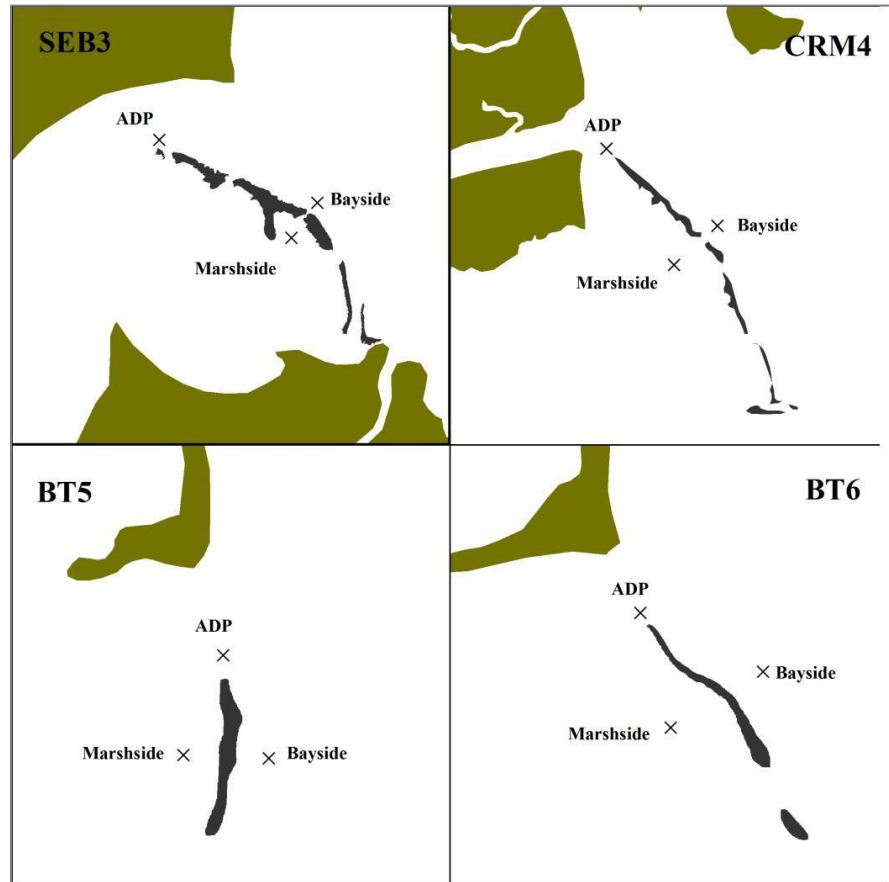


Figure 12: Hydrodynamic instrument configuration around oyster reefs at study sites. RBR wave gauges were placed approximately 10 m to either side of the oyster reefs, and the ADP at the end of the reef nearest the marsh.

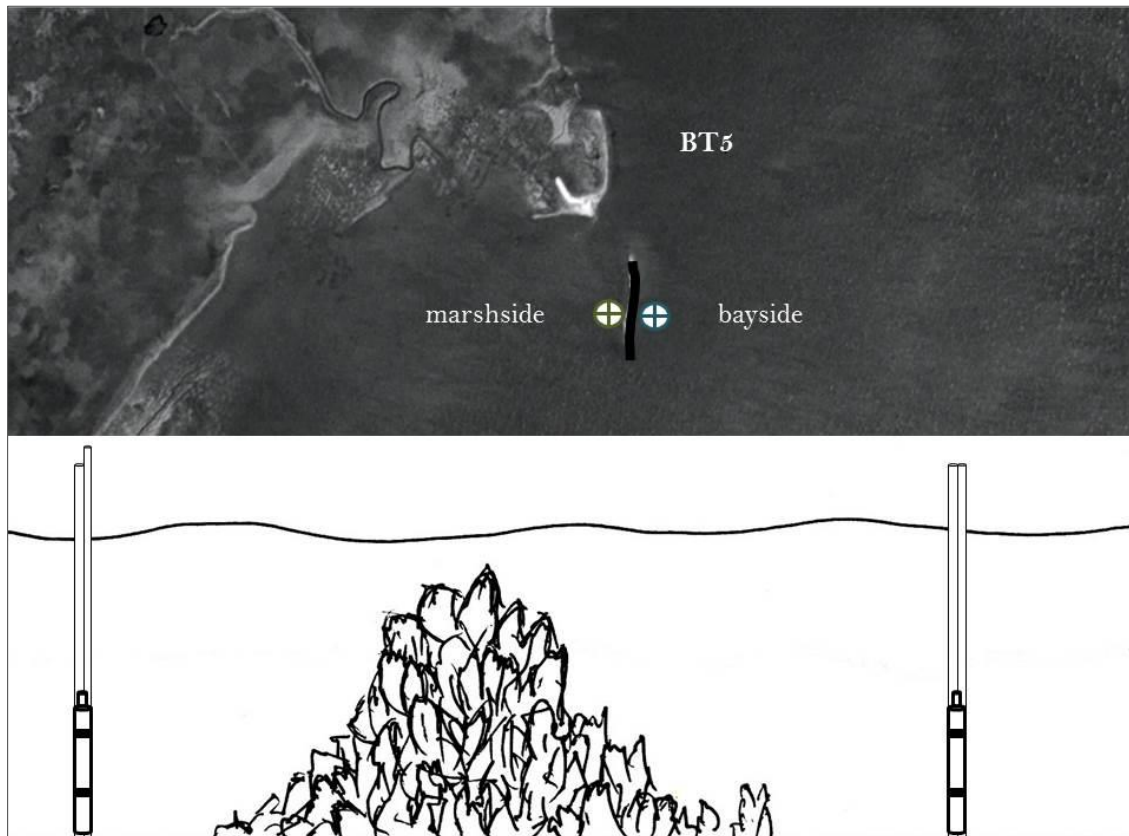


Figure 13: Diagram of wave gauge placement around BT5 reef (lower panel not to scale). Gauges were placed roughly 10 m to either side of the middle of the reef. NB: sketch is not to scale.

Wave environment

Collected wave data was used to characterize the wave environment and determine dissipation in wave energy over the oyster reefs. Significant wave height (H_s) was initially graphed over the simultaneous wind speed and wind direction data during the course of the deployment as a qualitative visualization of wave height in response to wind. During each deployment there were relatively brief wave events (lasting a few hours) separated by periods of low wave heights ($H_s < 0.03$ m). Because high waves are known to be the main driver of marsh edge erosion (e.g., Marani et al. 2012), only

records with $H_s > 0.03$ m for each pair of wave gauges were analyzed. Huang et al. (2012) used a minimum significant wave height of 0.05 m in their study of wave attenuation in a shallow coral reef lagoon which had significant wave heights considerably larger than in this study (0.7-1.2 m).

Pairs of wave records were identified based on the magnitude of difference in significant wave height and were categorized as either “similar” or “different” where “different” meant a change in wave height. A minimum threshold for change in significant wave height (ΔH_s) was applied in order to locate records that would be most useful in determining influential factors of dissipation. The threshold was set to 0.02 m on the basis that it was the average difference between the pair of wave gauges when $H_s > 0.03$ m at the Box Tree sites; the same threshold was applied to all sites for consistency. The focus of this analysis was on these cases with notable changes in wave height to better understand when and why those differences occurred. These records of interest (ROI) were classified as to whether waves were higher on the bayside or the marshside of the reefs. Wind direction data was compared to the side with the higher waves to determine whether the larger waves were on the upwind side of the reef. The ΔH_s in the ROI were analyzed based on many factors, including wind speed, wind direction, water column depth, and water depth above the reef in order to determine conditions contributing to the greatest wave heights at each site. Linear regression models were run in SAS (Statistical Analysis System, Cary, NC) to determine the variables of greatest influence.

The comparison of wave spectra is a standard method for determining energy dissipation in coral reef studies and was applied here for oyster reefs. In order to quantify change in energy, spectra for the same wave record were plotted together for visual comparison. These spectra were further analyzed in MATLAB (MathWorks, Natick, MA) to identify major contributing factors to the mechanism of wave dissipation, such as the impact of change in dominant frequency of the wave and energy associated with each frequency. To simplify the analysis a rectangle having the same area as the integral of the spectrum, a height equal to the maximum power spectral density, and a central frequency equal to the median spectral frequency was created to represent the salient aspects of each wave spectrum. The rectangle was used to determine attributes such as shift in frequency (rectangle width, w , and central frequency f_{50}), and peak energy (rectangle height, h). Other variables were calculated for statistical testing of correlation with energy dissipation such as bottom orbital velocity, power, and wave length. These factors plus measurements of wave height, wind, and water depth were tested for potential relationships with wave attenuation. Due to the consistent clarity of relationships between variables at BT5, this data set was the focus of further analysis. Each pair of variables was plotted as a box plot wherein the independent variable was divided into three subgroups (low, medium, and high values) in order to observe general trends. For more detailed methods, see Appendix 1.

Wave power is a common metric for characterizing waves in relation to marsh-edge erosion. We calculated wave power following the approach set by Mariotti et al.

$$(2010), P = c_g E \text{ where } c_g \text{ is group velocity given by } c_g = \frac{\omega}{k} \left(1 + \frac{2kd}{\sinh(2kd)} \right), E = \frac{\rho g H^2}{8}$$

is wave energy and d is water depth. The wave number, k , is calculated from an iterative solution given by Sherwood and Wiberg (2008) and the angular frequency, ω , is 2π divided by the significant wave period, T_s . We averaged wave power time series at each site over the whole wave record (similar to Marani et al, 2011) and for those cases when $H_s > 0.03$ m. These estimates of wave power used were compared to values from Mariotti et al. (2010) for the VCR, Schwimmer (2001) in Rehoboth Bay, DE, and Marani et al. (2011) with estimates for the Venice Lagoon. In the latter two studies the authors present arguments for the predictive value of wave power in regard to marsh edge retreat. Their findings were compared to erosion measurements and wave power estimates from this study for context.

Wave base is the depth at which water motion is less than 4% of the value at the surface, the equation for which in deep water is $WB = \lambda/2$. In this study, we were interested in the depth at which the underlying oyster reef ceased to significantly affect surface waves. This was characterized as $WB_{d_{reef}} = \lambda/x$, where x was determined based on the wave measurements at BT5. The depth at which change in dissipation over the reef began to decline was considered the cutoff.

Results

Digital shoreline analysis

Analysis of erosion rates during the 52-year period analyzed with aerial photos indicated that all four study sites were eroding at significantly different rates from each other and that those rates varied through time (Figure 14, Figure 15). These rates were

well within the range of rates determined for the comparison sites. Erosion at BT5 and BT6 averaged 0.26 ± 0.03 and 0.10 ± 0.02 $\text{m}\cdot\text{yr}^{-1}$ respectively. The Northern sites had average erosion rates of 0.15 ± 0.01 $\text{m}\cdot\text{yr}^{-1}$ at SEB3 and 0.27 ± 0.03 $\text{m}\cdot\text{yr}^{-1}$ at CRM4. At the two extremes, Upshur Neck (UN) accreted at an average of 0.46 $\text{m}\cdot\text{yr}^{-1}$ and Elkins (Elk) eroded at 1.58 $\text{m}\cdot\text{yr}^{-1}$. Northern Fowling Point (nFP) eroded at a rate similar to the study sites while the inter island location (I-I) had almost no change despite its close proximity to the Box Tree study sites.

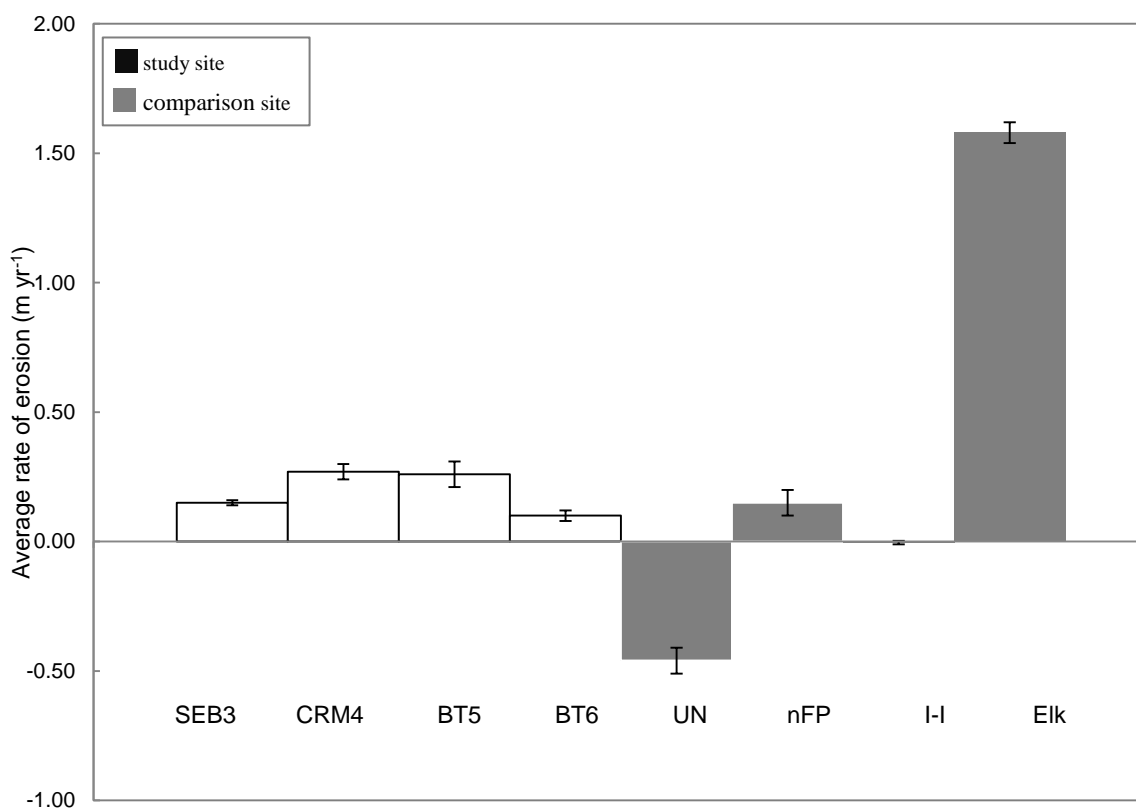


Figure 14: Average erosion rates between 1957 and 2009. Study site values fell within the range measured in other oyster reef studies and were comparable to mainland marsh erosion rates for the VCR. These rates were significantly different from each other (see Table 3) due to variance. Comparison sites varied greatly but can be explained by environmental conditions. UN was a highly developed area and the shoreline was likely influenced by the inhabitants. The environment at Elk was higher energy than the study sites and experienced greater wave power, similar to back-barrier marshes. I-I was fairly protected by the increasingly shallow waters and oyster shells that had washed ashore, and nFP rates were within the study site range.

The average erosion rates at the four study sites from 1957-2009 differed in terms of their means and variation (Figure 15). An intercomparison of the four sites indicated that the sites all had significantly different average rates. Because the SEB3 site had a much smaller variance than the other sites, it was removed for an additional test which again resulted in significance in the difference of erosion rates between the Box Tree sites and CRM4. The Northern and Box Tree pairs of sites also had significantly different erosion rates, as did CRM4 compared to the Box Tree sites. The Box Tree sites did not differ significantly at the $\alpha = 0.0083$ level, which was the only test with a p-value that exceeded the alpha.

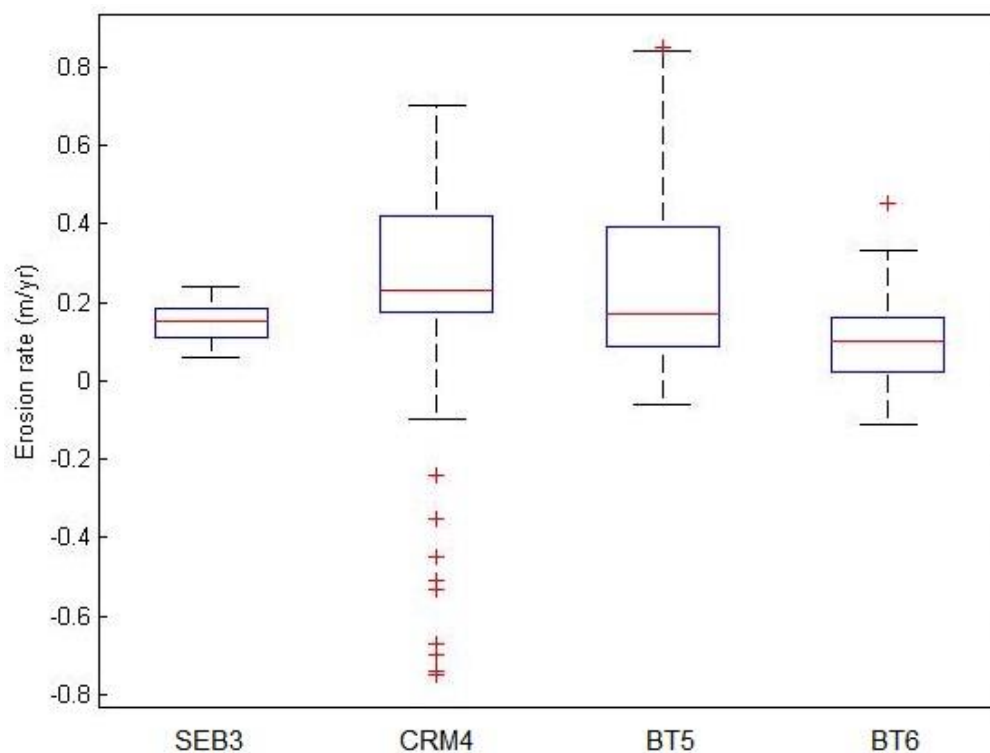


Figure 15: Box plots of erosion rates from 1957-2009 at each study site. Mean erosion rates were all significantly different from each other at the $\alpha = 0.0083$ level in a Kruskal-Wallis test (non-parametric analogue to ANOVA), which was used due to the difference in variance between sites. After removing SEB3 which caused the most heteroskedasticity, mean erosion rates were still significantly different from one another.

Table 3: Kruskal-Wallis results testing for significant differences in average erosion rates from 1957-2009. Significance at $p = 0.0083$ with the Bonferroni correction for multiple tests of the same variables. Results showed that all configurations of comparisons resulted in significantly different average rates.

	df	H	p
SEB3 · CRM4 · BT5 · BT6	3	41.10	<0.0001
CRM4 · BT5 · BT6	2	28.70	<0.0001
BT5 · BT6	1	6.52	0.0107
SEB3 · CRM4	1	24.92	<0.0001
Northern · Box Tree	1	15.27	<0.0001
CRM4 · Box Tree	1	19.95	<0.0001

Figure 16 and Figure 17 show the average erosion rate for each transect at 5 m intervals, creating a visual comparison of how rates changed along the shorelines. SEB3 had exceptionally uniform retreat between 0 and $0.5 \text{ m}\cdot\text{yr}^{-1}$ for the entire extent of the shoreline. CRM4 had the greatest variation in rates ranging from $0.0\text{-}1.0 \text{ m}\cdot\text{yr}^{-1}$ of erosion along most of the shoreline and a small section that slowly accreted at the southern end. The two Box Tree sites eroded at significantly different rates despite similar physical and ecological conditions. BT5 had less consistent erosion rates, particularly in the midsection where the island dramatically shifted shape between 1957 and 1994. BT6 mostly eroded at $0\text{-}0.5 \text{ m}\cdot\text{yr}^{-1}$ except for two swatches where it accreted slightly.

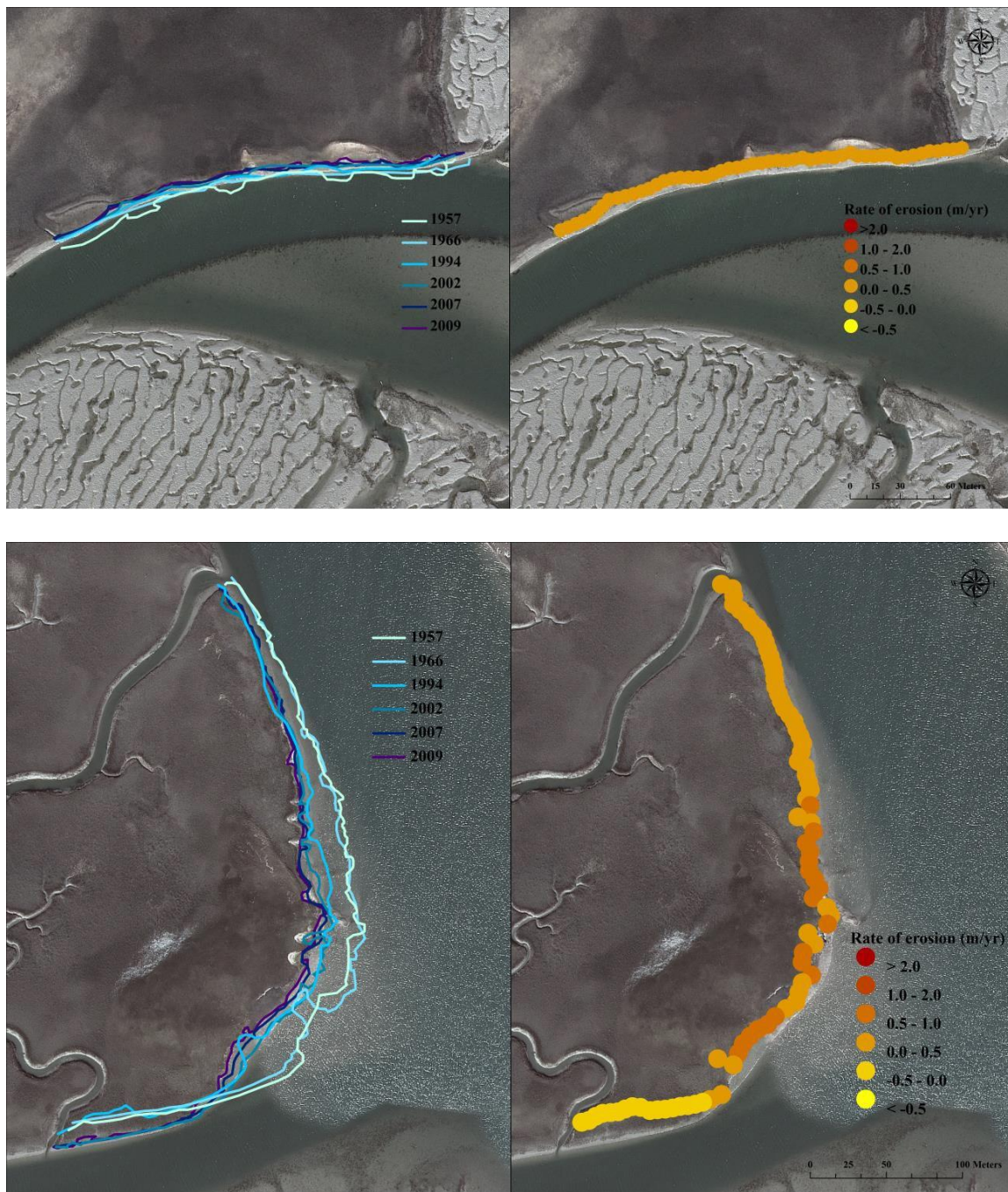


Figure 16: SEB3 (upper panel) and CRM4 (lower panel) shorelines and average erosion rates 1957-2009. Darker colors indicated more recent shorelines (left) and on the red to yellow dot spectrum (right), red dots show erosion and yellow dots show accretion. SEB3 uniformly eroded between 0 and 0.5 m per year with no variation along the length of the shoreline. By contrast, CRM4 had great spatial variability in shoreline change rates with an area of accretion at the southern end and consistent fluctuation from 0 to greater than 1 m per year of erosion through the center section.

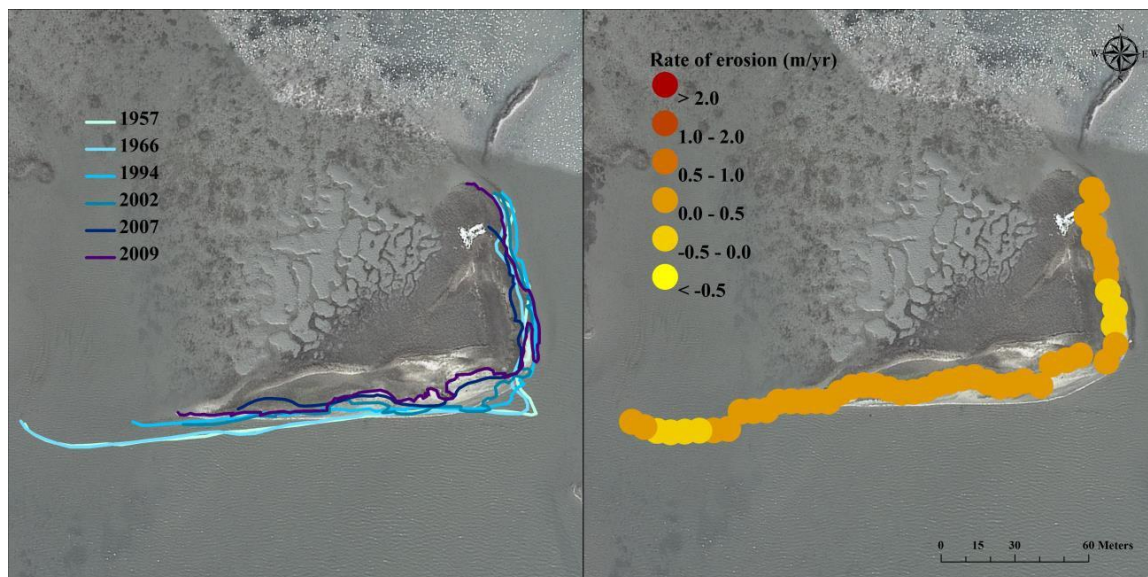
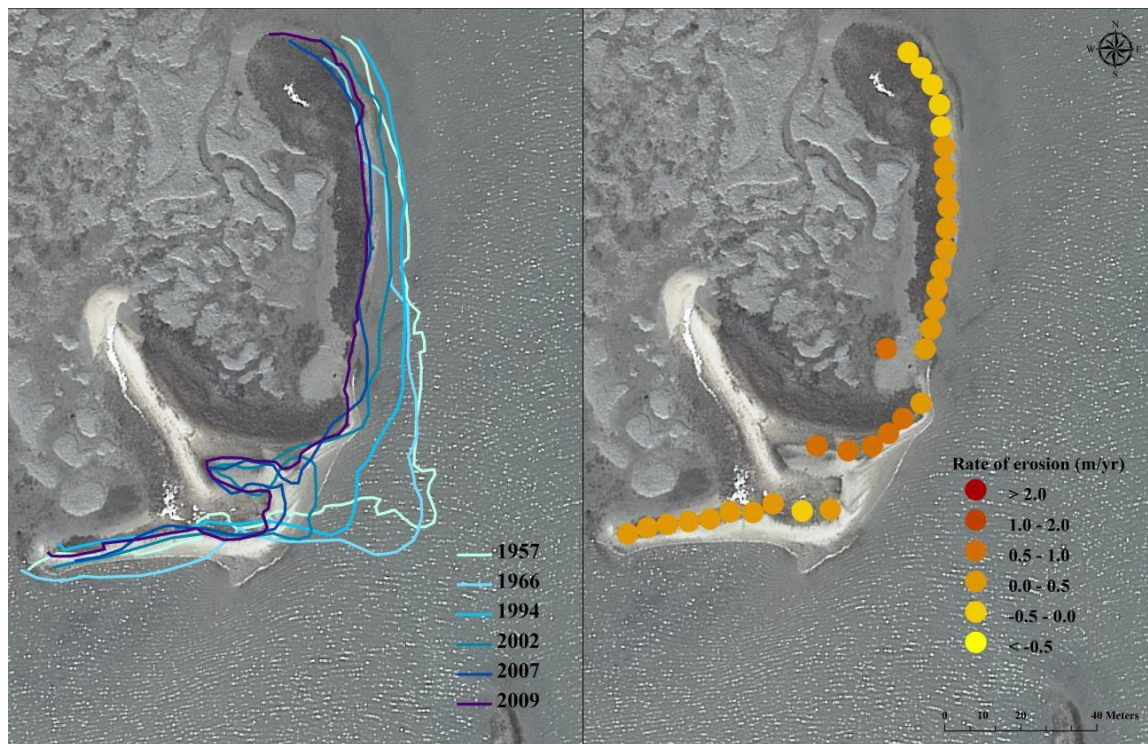


Figure 17: BT5 (upper panel) and BT6 (lower panel) shorelines and average erosion rates 1957-2009. Darker colors indicated more recent shorelines (left) and on the red to yellow dot spectrum (right), red dots show erosion and yellow dots show accretion. Both Box Tree marshes exhibited erosion rates between 0 and 0.5 m per year for the majority of the shoreline with a few areas of slight accretion due to the shift in marsh shape over the 50 year period.

With one exception (BT5 from 1957-1966), all four study sites were eroding during all time intervals with variation in those rates (Figure 18 and Figure 19). The comparison sites were more variable in their shoreline change, both accreting (UN) and eroding (I-I); Elk and nFP had limited records but all were of erosion. Comparison of differences between time intervals within each site indicated that the rates of erosion at all sites were significantly different during all periods. CRM4 and BT5 had the greatest differences between time intervals which were due in part to high variance (Table 4), however the differences at SEB3 and BT6 were also significant. SEB3 was the only site with sufficient homoscedasticity (consistent variance in data) to use an ANOVA test, therefore BT5, BT6, and CRM4 were tested using a Welch ANOVA because they did not deviate too far from a normal distribution but did have unequal variances.

Table 4: Statistics for interval erosion rate differences within a site. ^a indicates standard ANOVA, ^w indicates Welch ANOVA. Significance at $p = 0.05$. Test results were significant for all four sites.

	df	F	p
SEB3	3	6.30	0.0004
CRM4	3	18.53	<0.0001
BT5	3	8.58	<0.0001
BT6	3	6.05	0.0009

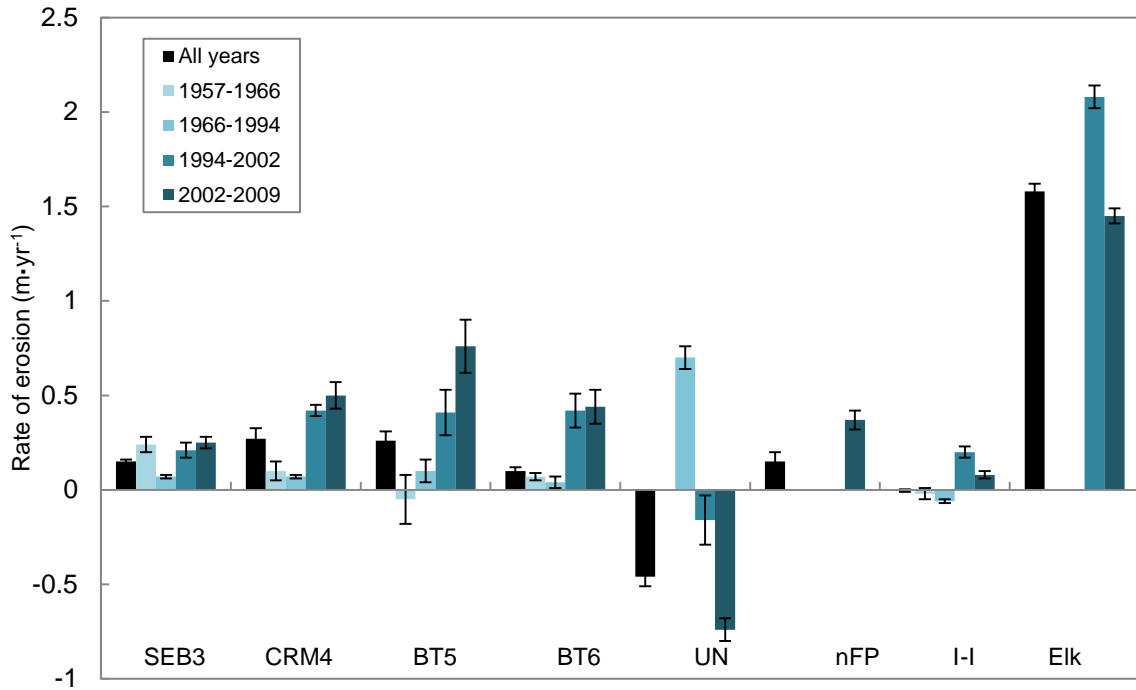


Figure 18: Average erosion rates at quasi-decadal intervals based on image availability. With the exception of BT5 from 1966-1994, all study site shorelines eroded during each time interval with a general upward trend. Greater variation in comparison sites was likely due to the influence of anthropogenic shoreline maintenance (UN) and a higher wave energy environment that was representative of the other sites (Elk). Study sites eroded at significantly different rates from each other, as well as between time intervals within each site.

Table 5: Average erosion rates in meters per year for all time intervals with standard error and sample size below. Records for UN, nFP, and Elk are incomplete due to availability and quality of images.

	All years	1957-1966	1966-1994	1994-2002	2002-2009
SEB3	0.15 ± 0.01 (52)	0.24 ± 0.04 (51)	0.07 ± 0.01 (48)	0.21 ± 0.04 (48)	0.25 ± 0.03 (51)
CRM4	0.27 ± 0.03 (81)	0.10 ± 0.05 (80)	0.07 ± 0.01 (49)	0.41 ± 0.03 (80)	0.5 ± 0.07 (83)
BT5	0.26 ± 0.05 (33)	-0.05 ± 0.13 (34)	0.10 ± 0.06 (31)	0.41 ± 0.12 (31)	0.76 ± 0.14 (33)
BT6	0.10 ± 0.02 (49)	0.07 ± 0.02 (47)	0.04 ± 0.03 (41)	0.42 ± 0.09 (38)	0.44 ± 0.09 (38)
UN	-0.46 ± 0.05 (775)	-	0.70 ± 0.06 (151)	-0.16 ± 0.13 (151)	-0.74 ± 0.06 (774)
nFP	0.15 ± 0.05 (418)	-	-	-	-0.37 ± 0.05 (414)
I-I	-0.004 ± 0.007 (118)	-0.02 ± 0.03 (117)	-0.06 ± 0.01 (117)	0.20 ± 0.03 (117)	0.08 ± 0.02 (118)
Elk	1.58 ± 0.04 (323)	-	-	2.08 ± 0.06 (87)	1.45 ± 0.04 (323)

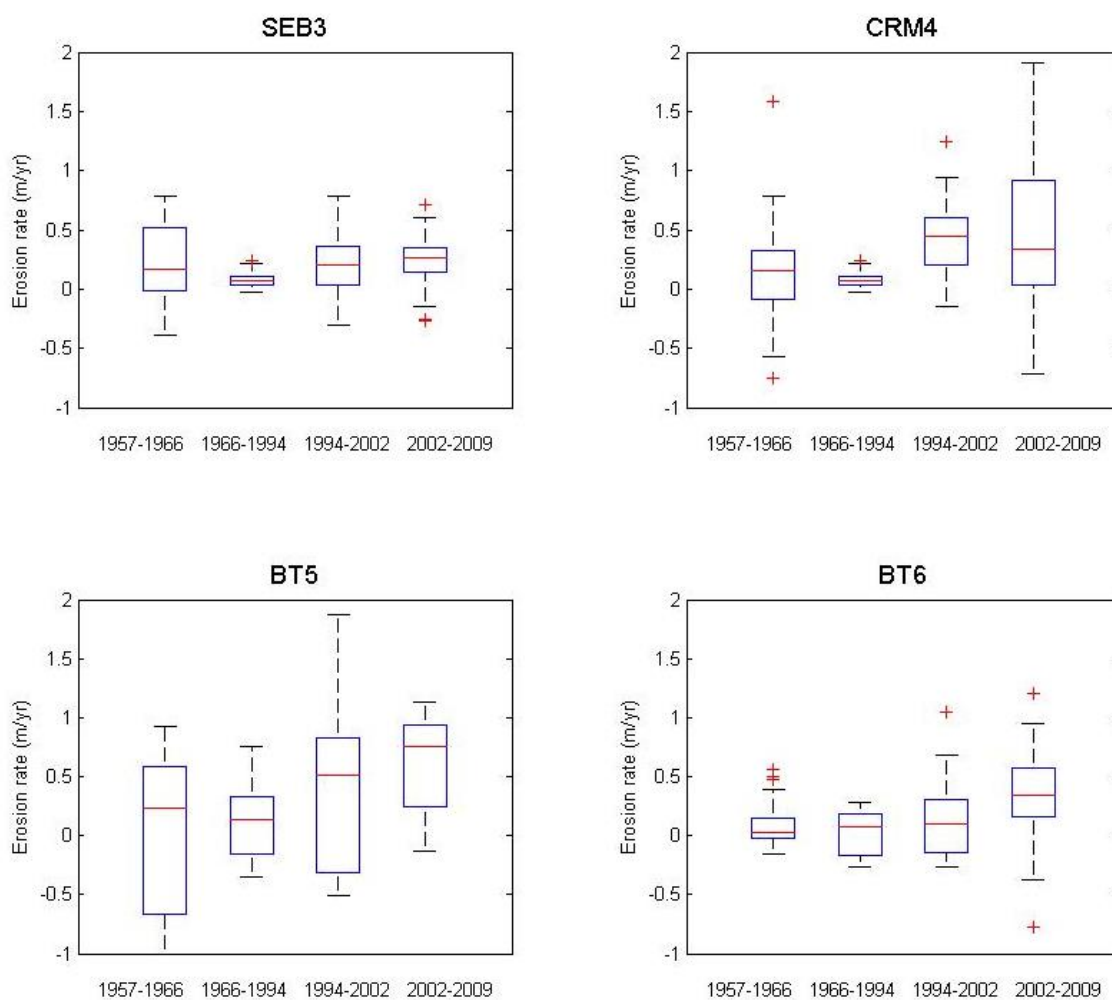


Figure 19: Time interval erosion rate statistics. NB: CRM4 and BT5 data were truncated for comparison to scale with other sites. Average erosion rates for the whole time period were significantly different between sites, as were the individual interval rates within the same site. An upward trend in erosion rate was also noted at CRM4, BT5, and BT6.

There was also a notable upward trend in the rates of erosion through time for CRM4, BT5, and BT6 with the lowest rates typically during the 1966-1994 period and the highest from 2002-2009. This trend was strong and significant at CRM4 and BT5, present at BT6 ($r^2 = 0.79$, Table 6), but no-existent at SEB3. This trend was also

significant for rates averaged over all four study sites (Figure 20). Fit plots for each site can be seen in Appendix II (Figure 59 and Figure 60).

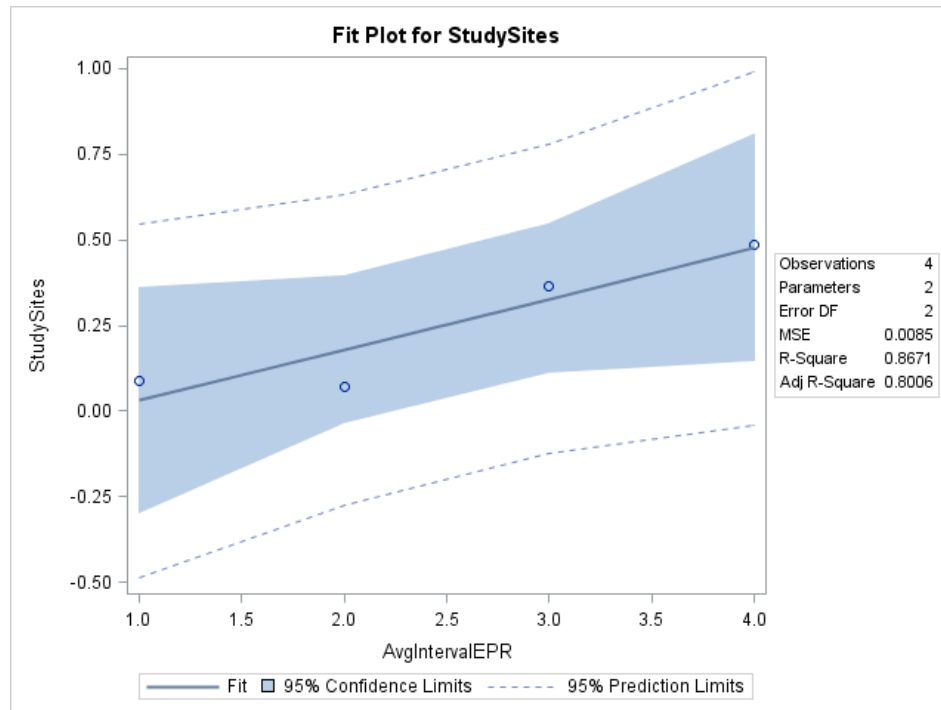


Figure 20: Fit plot of study sites average erosion rates for time intervals. There was a significant trend of increase in the erosion rate averaged over all study sites through time.

Table 6: Linear regression results of erosion rate increase with time. Significance is $p = 0.10$. Test results were significant for CRM4 and BT5. The relationship was present at BT6 though not significant, and nonexistent at SEB3.

	r^2	p	n
SEB3	0.07	0.737	4
CRM4	0.83	0.088	4
BT5	0.97	0.014	4
BT6	0.79	0.114	4
Study sites	0.87	0.069	4

Physical properties

Table 7: Physical characteristics of study and comparison sites. Northern sites tended to have similar characteristics to each other such as greater smaller grain sizes with more organic matter, greater fetch and biomass, and larger reefs. Box Tree sites were more similar to each other than compared to the Northern sites, typically with greater percentages of sand, and smaller fetches, oyster reefs, and biomass counts.

	SEB3	CRM4	BT5	BT6	UN	nFP	I-I	Elk
Shoreline length (m)	150	415	170	245	4,560	3,970	610	1,900
Percent sand	66.9%	20.7%	93.4%	86.8%	-	86.9%	71.9%	18.6%
Mean organic content	2.0%	4.6%	1.0%	1.7%	-	0.7%	2.3%	5.3%
Mean tidal range (m)	1.28	1.04	1.14	1.01	-	-	-	-
Estimated total fetch (km ²)	54.5	50.0	22.0	23.0	56.0	49.0	14.0	20.0
Reef area (m ²)	29,203	8,833	1,148	1,670	-	-	-	-
Oyster density (per m ³)	1,254	1,313	1,342	1,342	-	-	-	-
Population estimate	36,620,562	11,597,729	1,540,616	2,241,140	-	-	-	-
Reef base material	natural	natural	whelk shell	oyster castle, oyster shell	-	-	-	-
Distance from shore (m) (to nearest edge of reef)	110	110	80	50	-	-	-	-
Reef length (m)	600	800	120	230	-	-	-	-
Biomass (g·m ⁻²)					-	-	-	-
Aboveground	45	64	62	41	-	-	-	-
Belowground	1,491	1,013	644	671	-	-	-	-
Total	1,536	1,077	706	712	-	-	-	-
Burrow percent area	0.50%	0.85%	0.95%	1.30%	-	-	-	-

Sediment

The Box Tree sites exhibited similar median grain sizes and organic content (Table 19, Figure 21) with d_{50} s (median grain sizes) near 500 μm and organic content between 1-1.7%. SEB3 had on average 2% organic material and a d_{50} just under 200 μm , while CRM4 had the highest percent organic material (4.6%) and the lowest d_{50} (22 μm) of all the study sites. The distribution of grain size was quite similar between BT5 and BT6, with 85-90% sand. SEB3 had slightly less sand (~70%) and CRM4 was predominantly clay and silt (20% sand). The comparison sites fell within the range of the study sites in terms of both d_{50} and organic content. There was a clear relationship between grain size and organic matter such that locations with smaller grain sizes had greater amounts of organic material ($r^2 = 0.97$, Appendix II - Figure 22). Statistical comparisons of grain size using an ANOVA test showed that all sites were significantly different from each other except for BT5 and BT6 (Appendix II - Table 18). ANOVA results from percent organic matter showed the same, that all sites were significantly different from each other except the two at Box Tree.

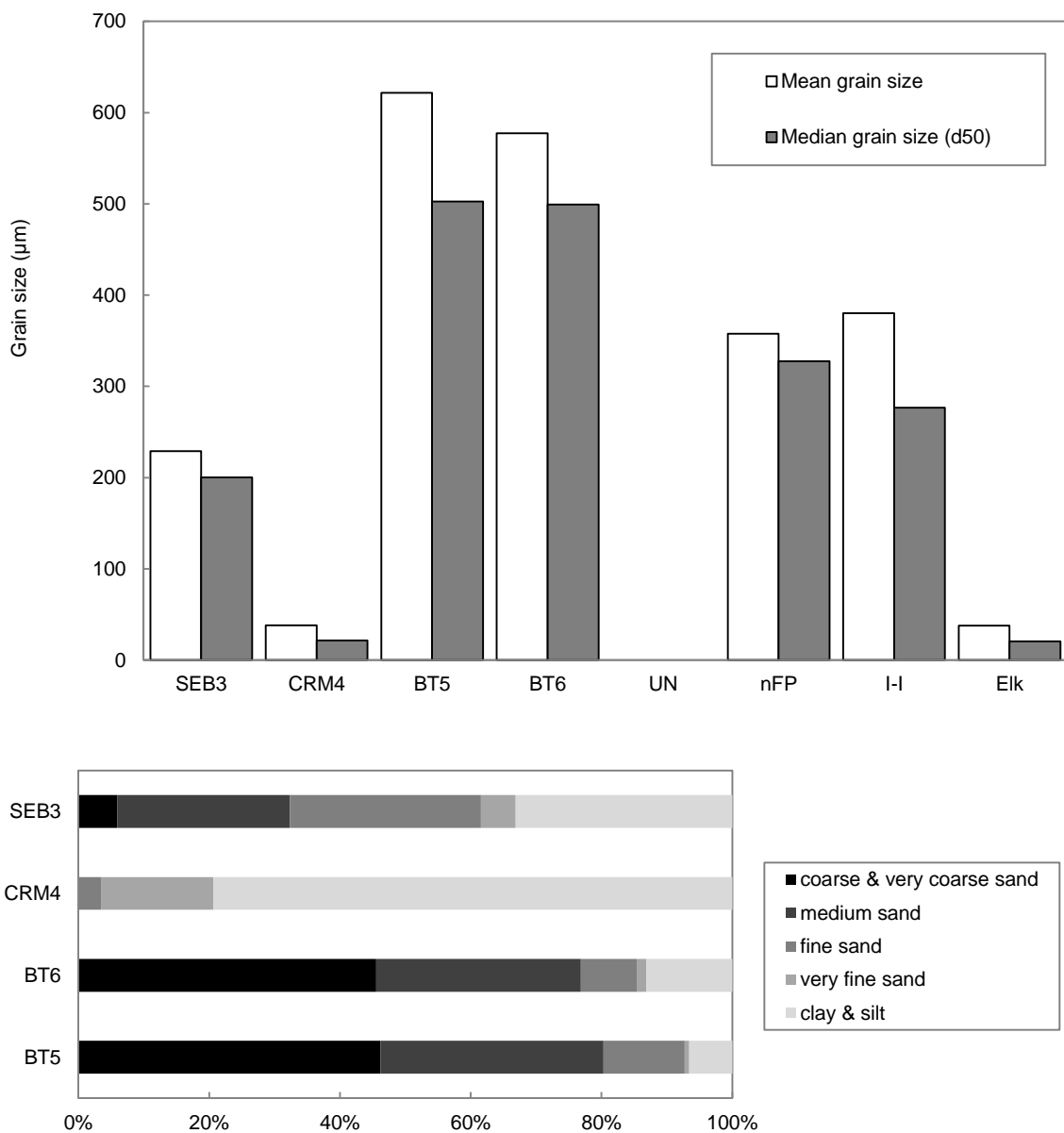


Figure 21: Upper panel: mean grain size vs. d_{50} of sediment samples. Lower panel: Grain size distributions for study sites. Box Tree sites were highly similar in grain size mean, median, and distribution, with the highest numbers overall. CRM4 had significantly different sediment properties from all other sites except Elk. There was no UN data due to property ownership and access.

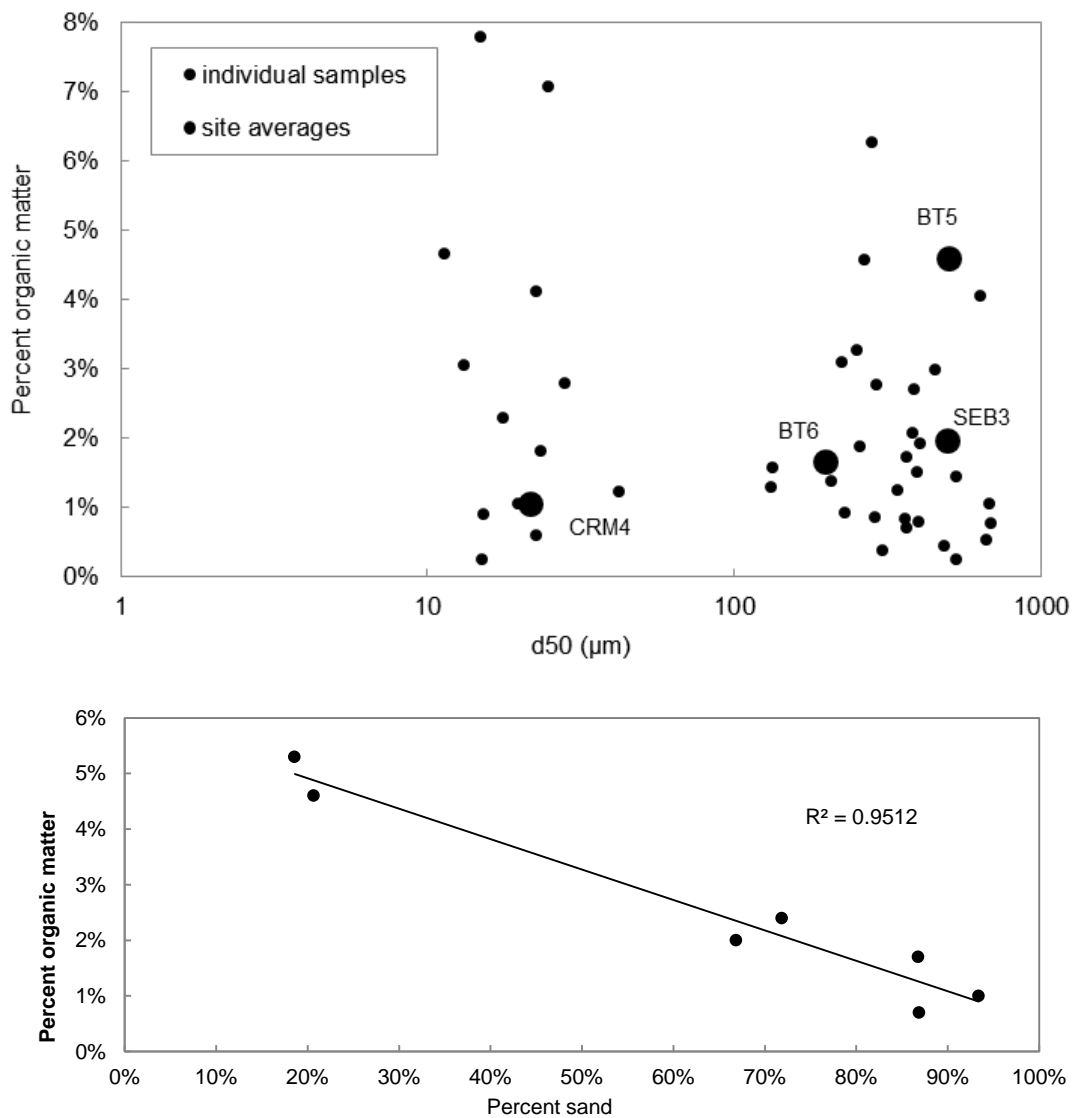


Figure 22: Upper panel: percent organic matter as a function of d_{50} . CRM4 had both the lowest percent organic material and grain size. SEB3, BT5, and BT6 fell within a similar range. Large circles are averages for study sites. Lower panel: relationship between grain size and organic content. There was a strong negative correlation between grain size and organic matter.

Ecology

Total, aboveground, and belowground biomass was not significantly different between any of the sites (Table 18). SEB3 had the greatest total biomass of $1,536 \text{ g}\cdot\text{m}^{-2}$, about 3% of which was aboveground (Table 7, Figure 23). The depth profile of the belowground biomass was the only profile that slowly declined with depth (Figure 23) as opposed to the other sites whose profiles had a sharp decline between 0-5 cm and 5-10 cm. The total biomass at CRM4 was just two thirds of the SEB3 biomass. The depth profile for CRM4 decreased rapidly between the first and second sections from the top unlike SEB3. Both Box Tree sites had only half the total biomass of SEB3, but a slightly larger portion was found aboveground (6-9%). The greatest change in their depth profiles was between the top two sections with little change below that.

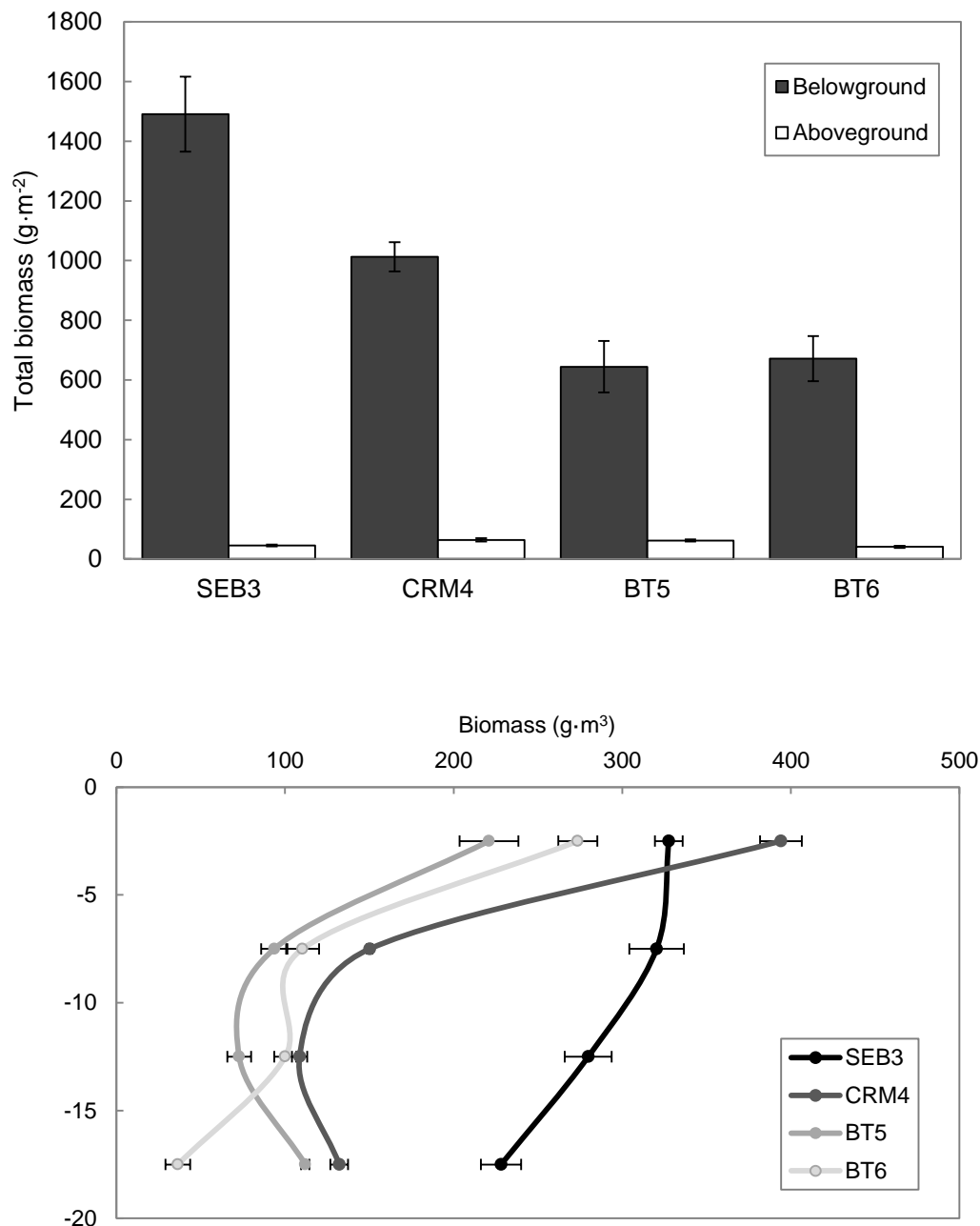


Figure 23: Upper panel: total dry weight of biomass collected above and belowground at each site. Lower panel: belowground biomass depth profiles. Dots represent mean biomass (± 1 SE) at 0-5 cm, 5-10 cm, 10-15 cm, 15-20 cm. y-axis indicates centimeters below surface. Box Tree sites were very similar to each other, as was CRM4, though SEB3 stood out because of much higher biomass counts and gentler depth profile.

Crab burrows comprised a miniscule portion of the marsh surfaces and were not significantly different between sites. The majority of burrow area was from large burrows

(Figure 24), likely attributable to *Sesarma reticulatum* and *Panopeus herbstii* based on diameter, though most of the crabs seen during the study were *U. spp.* The area covered by crab burrows was very small at each site and less than what was measured by McLoughlin (2010) at other mainland marshes in the vicinity. Statistical analyses showed no correlation between burrow area and erosion rate. The lack of correlation could be attributed to the shape of the marsh shorelines which were mainly sloping with a few interspersed scarps. McLoughlin (2010) found that destabilization caused by crab burrows was associated with locations where slumping, block detachment, and undercutting were the dominant erosion mechanisms, which required scarps. Due to the lack of scarp faces at these study sites, the presence of crab burrows likely did not have an effect on erosion.

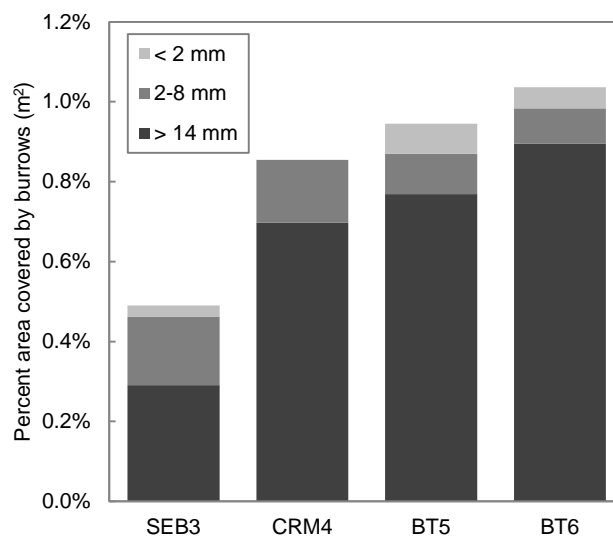


Figure 24: Mean percent area of study site shoreline covered by crab burrows. These values were very small and much lower than those measured by McLoughlin (2010) on other mainland marshes in the area. r^2 values were both small and insignificant.

Tides and currents

The mean tidal ranges recorded at the study sites by RBR wave gauges were between 1.01 and 1.28 m (Table 8), similar the NOAA buoy in Wachapreague, WAHV2 (1.2 m) (NOAA www.tidesandcurrents.noaa.gov). Water levels at SEB3 submerged the oyster reefs about 60% of the time and the vegetation line near 50% (Figure 25). Unlike SEB3, the reef at CRM4 was under water during less than half of the average tidal cycle (40%). At Box Tree, the reefs were below sea level between 70% and 75% of the time, which indicated lower-lying reefs than at CRM4, though comparable to the reef at SEB3 (Figure 26). The vegetation line on BT5 was flooded an average of 60% of the time, which was longer than both BT6 and SEB3 where the time was split evenly between above and below water. Although the Box Tree sites were in close proximity and had similar physical characteristics, BT6 had a greater difference in elevation between reef top and vegetation line than BT5 such that the BT6 reef was lower and the vegetation line on the marsh was higher.

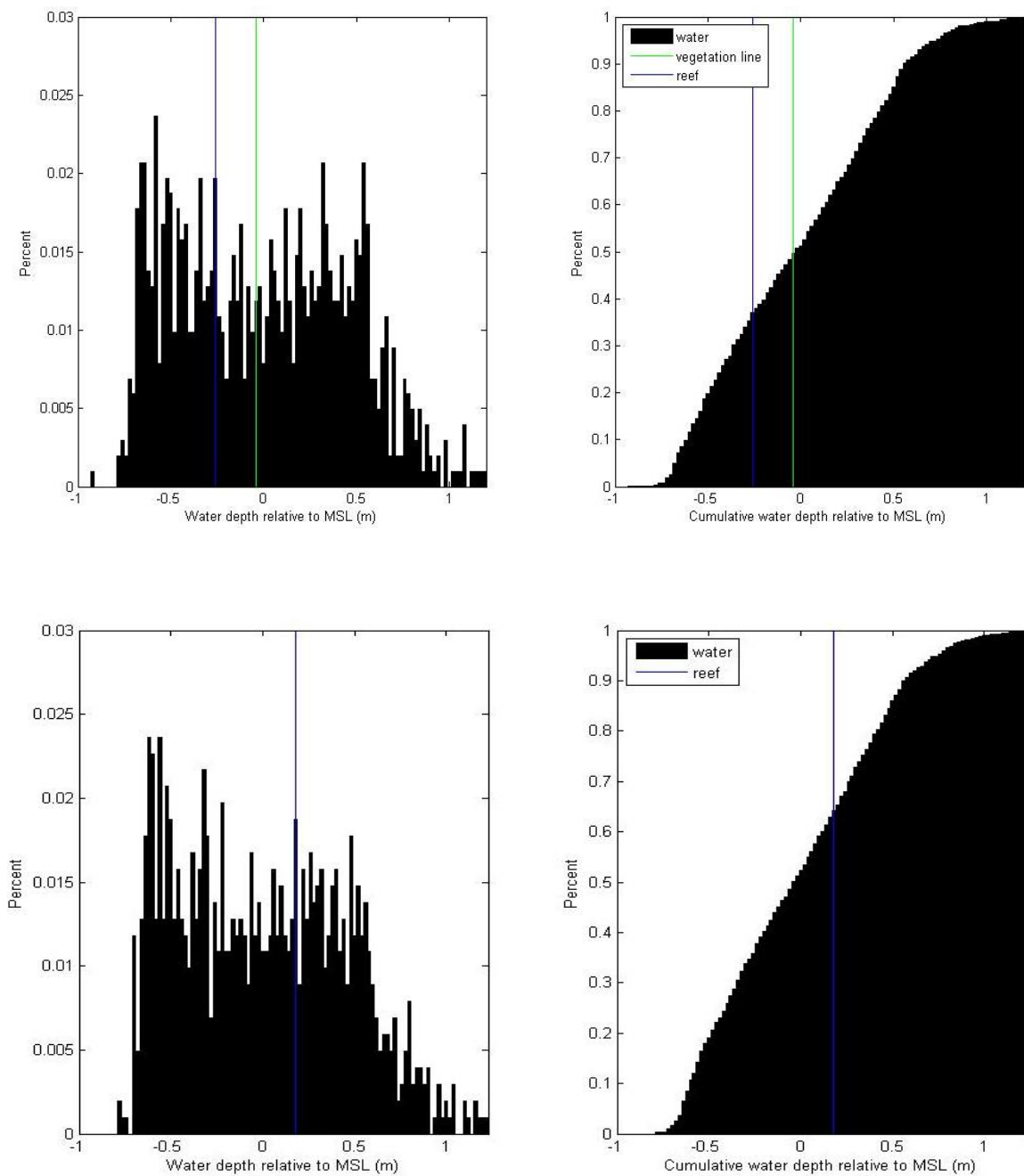


Figure 25: Sampling period water depths relative to MSL at SEB3 (upper) and CRM4 (lower); blue line indicates average reef height. No available data for CRM4 vegetation line. The tide at CRM4 in relation to the reef elevation was shallower at CRM4 than SEB3 so that the CRM4 reef was exposed over 50% of the tidal cycle. The SEB3 reef was above the water level only 35% of an average tidal cycle.

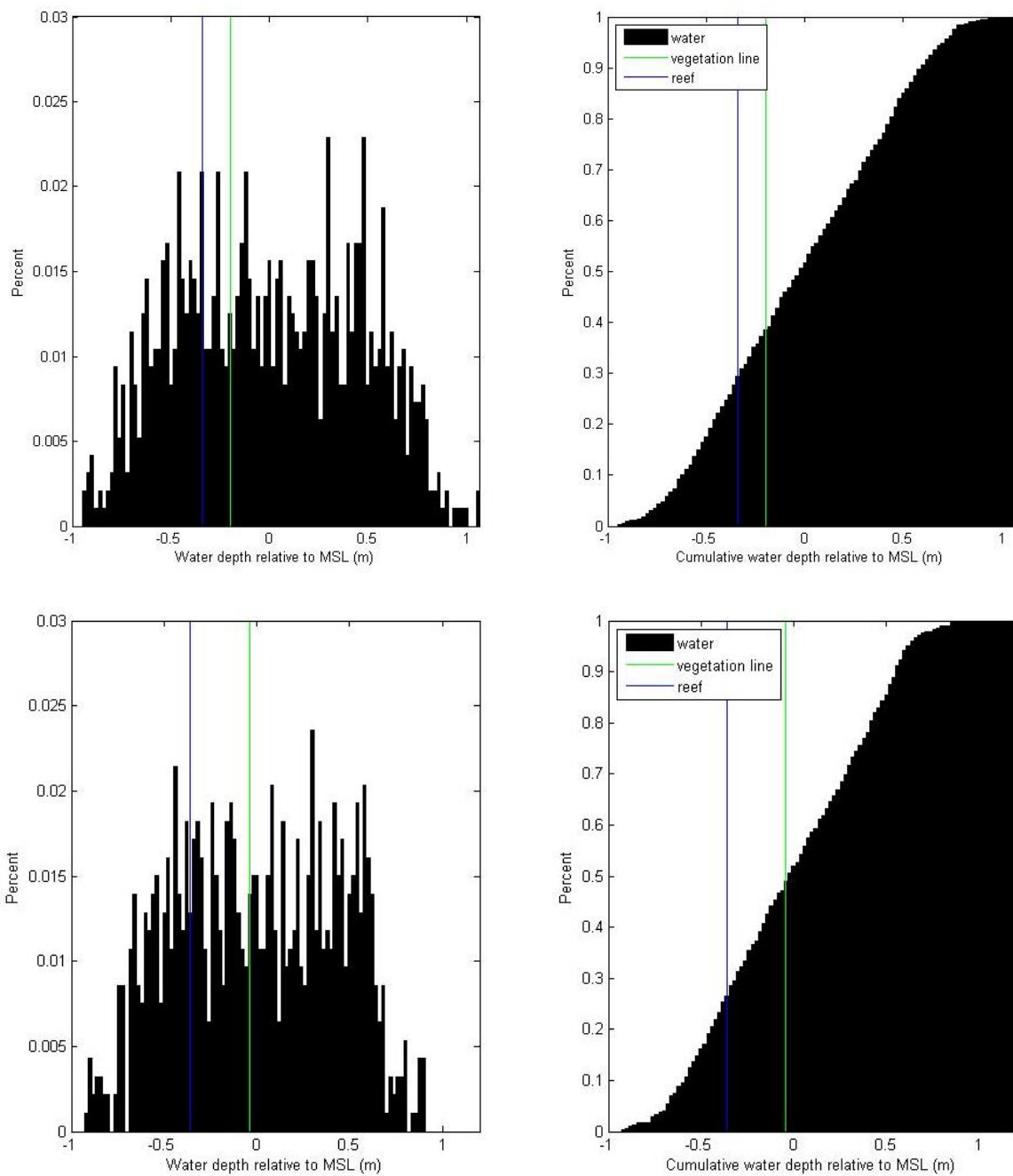


Figure 26: Sampling period water depths relative to MSL at BT5 (upper) and BT6 (lower); blue line indicates average reef height, green line indicates average vegetation line height. Cumulative water depth (right) shows reefs were below sea level about 70% of the time at both sites which is much greater than CRM4. The vegetation line was submerged only 35% at BT5 compared to 50% at BT6. Though BT5 and BT6 have similar physical and hydrodynamic characteristics, the shorelines are of different elevations relative to MSL.

A Nortek AquaDopp Profiler was deployed at each site for a period of two weeks, recording the water velocity at the end of the oyster reef closest to the marsh (Table 8, Figure 4). Root mean square (RMS) was calculated for velocity components in the east, north, and vertical directions at each site. The dominant flow axis was NE/SW which was parallel to the orientation of the shoreline in the VCR. With the shoreline to the W/NW and the oyster reef generally to the SE relative to the placement of the AquaDopp, this flow pattern was consistent with the configuration of the sites (Figure 12). Water at SEB3 flowed significantly faster than at the other sites with an average speed of $0.31 \text{ cm}\cdot\text{s}^{-1}$ compared to $0.12\text{-}0.17 \text{ cm}\cdot\text{s}^{-1}$ at CRM4, BT5, and BT6 (Table 8, Table 16). SEB3 and the Box Tree sites had higher RMS values in the E/W direction but there was no bias in water flow direction at CRM4.

Table 8: Mean tidal range, and average water speed, velocity, and direction of flow for study sites - data from RBR wave gauges and AquaDopp Profiler. Tidal ranges measured at study sites were comparable to the NOAA buoy datum in Wachapreague which was used for atmospheric information. The dominant flow axis was NE/SW which was parallel to the orientation of the VCR shoreline and consistent with the orientation of the reef and marsh to the ADP placement. Overall water moved more quickly at SEB3 than any other site.

	SEB3	CRM4	BT5	BT6
MTR (m)	1.28	1.04	1.14	1.01
RMS ($\text{m}\cdot\text{s}^{-1}$)				
East	0.33	0.12	0.13	0.12
North	0.20	0.12	0.09	0.06
Average speed ($\text{m}\cdot\text{s}^{-1}$)	0.31	0.14	0.13	0.12
Dominant flow direction	WSW, ENE	N, SW	ENE, WSW	ENE, W

Wind conditions

Winds in the VCR tended to originate from the southwest as shown by the wind rose below from station WAHV2 (Wachapreague) for the 12-month period from September 2011-2012 (Figure 27). Winds occurred most frequently from the southwest, but the highest wind speeds were disproportionately from the northeast. The average wind speed was just under $3 \text{ m}\cdot\text{s}^{-1}$ and some winds reached $12 \text{ m}\cdot\text{s}^{-1}$ which were generally associated with storm events and only accounted for 2% of all wind speeds.

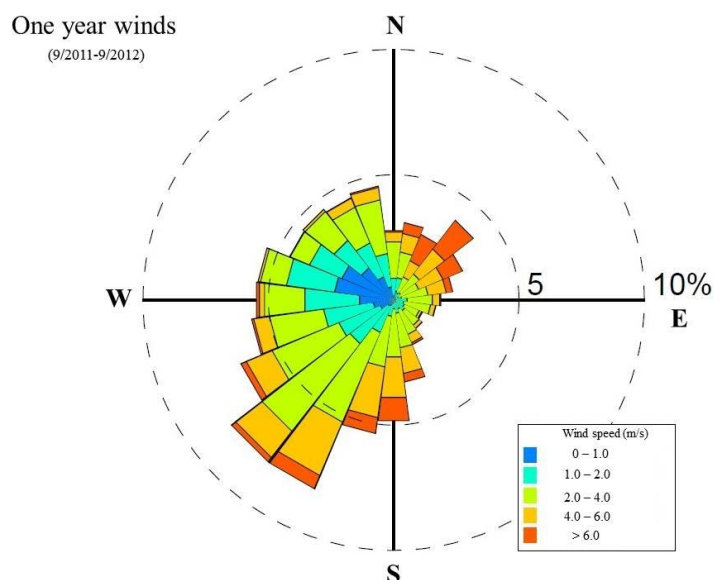


Figure 27: WAHV2 wind rose September 2011 - September 2012. Winds blew predominantly from the SW but the greatest percentage of high winds originated in the NE. This wind pattern was parallel to the shoreline orientation in the VCR.

Wind conditions during the Box Tree sampling period (2/15/2012 – 3/7/2012) (Figure 28) had the same average wind speed ($2.9 \text{ m}\cdot\text{s}^{-1}$) and similar distribution of wind direction from the September 2011 – September 2012 record (Table 17, Figure 27). However, the wind record during the sampling period for the Northern sites (12/17/2011-1/7/2012) was significantly different from the year-long record (Figure 28). The year-

long winds blew most often from the S/SW quadrant (247-336°) and the W/NW quadrant (337-66 °), 37% and 30% of the year, respectively. The least frequent winds were from the E/SE (157-246 °) and comprised only 11% of all annual winds. However, the record during the Northern sites sampling showed winds blowing from the W/NW blowing 47% of the time and only 3% from and E/SE, which was not representative of the annuals trends. In addition, the Northern sampling period average wind speed was significantly less than the annual average ($2.5 \text{ m}\cdot\text{s}^{-1}$ and $2.9 \text{ m}\cdot\text{s}^{-1}$, respectively). Because waves in the VCR are formed in response to local wind conditions, the relatively low frequencies of winds originating between the north and the southeast during the sampling periods – the directions with greatest fetch - resulted in smaller wave conditions during the study period than might be expected during a full year.

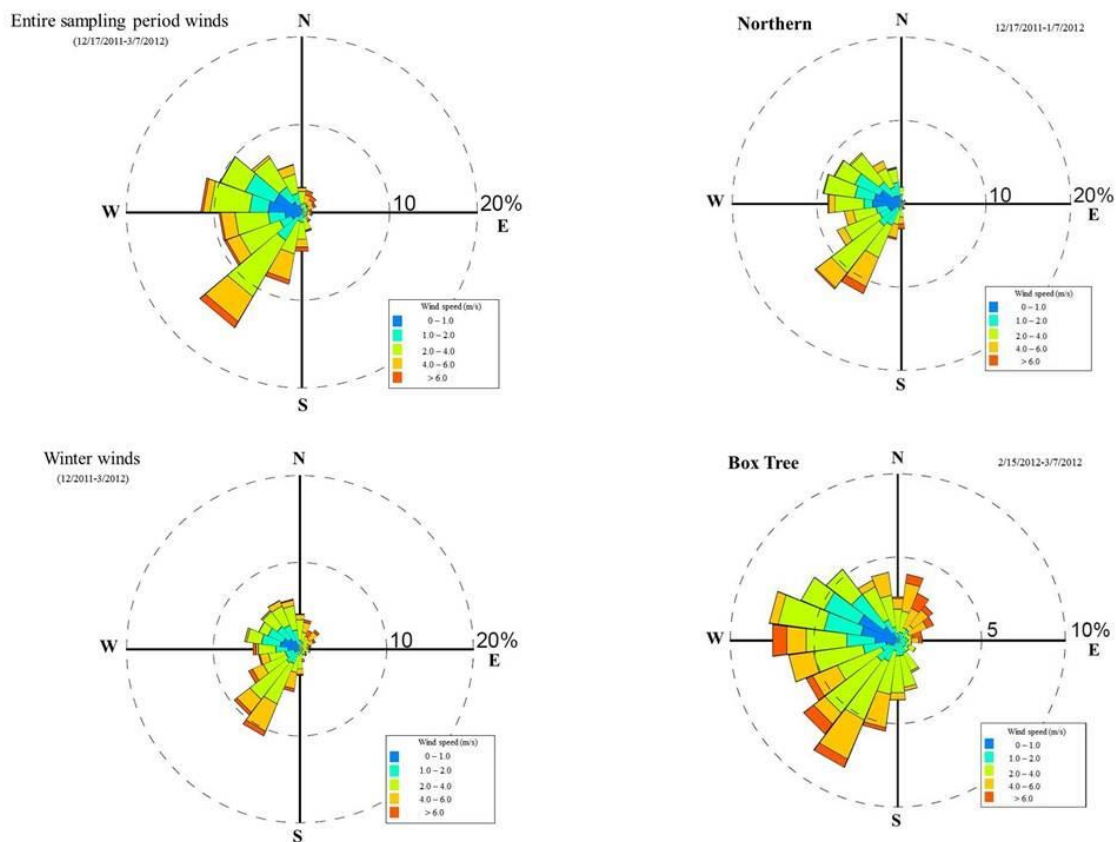


Figure 28: Wind roses during sampling periods. NB: Box Tree scale is to 10%, others are scaled to 20%. The wind speed and dominant direction during the sampling at SEB3 and CRM4 were significantly different from the annual pattern and likely caused a lower energy environment than the average for the year. Box Tree sampling period winds did not differ significantly from the annual pattern.

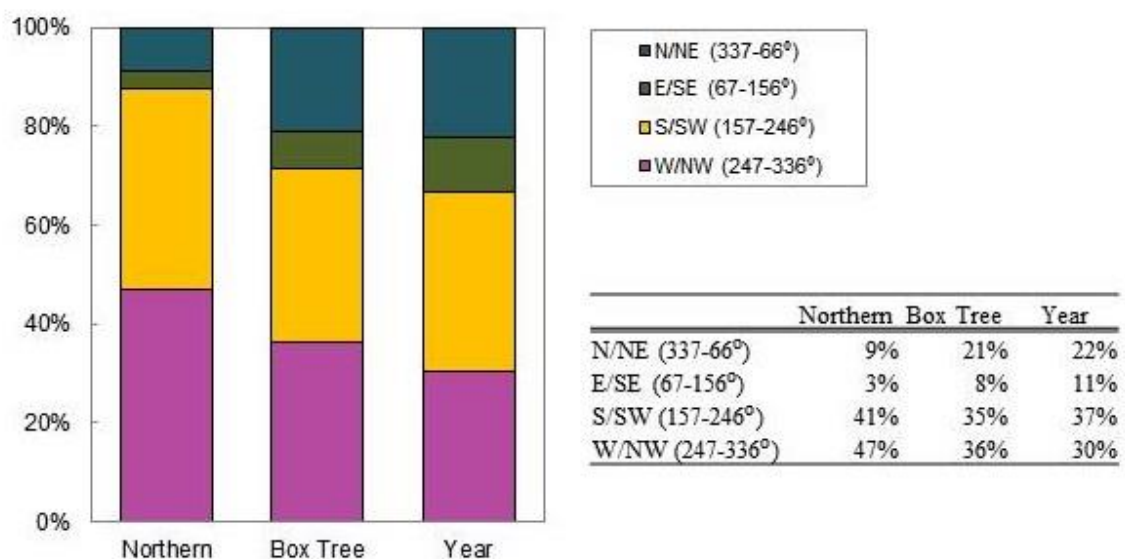


Figure 29: Wind direction frequencies at each location during sampling period. Wind patterns were significantly different during the Northern site sampling period from the Box Tree sampling period and year-long average, likely creating an atypically lower energy environment during that time.

Fetch

The estimated fetch areas varied widely among the study and comparison sites (Figure 30, Table 21). Both Northern sites had fetch areas around 50-55 km², most of which were from stretches that are ≥ 6 km in length. The Northern comparison sites had similar fetch area estimates to the study sites. The Box Tree sites were estimated to have less than 50% of the Northern sites fetch area (22-23 km²), which was a product of shorter distances (4-8 km) rather than a lack of space around the marsh. Elkins had a similar fetch to the Box Tree sites but the inter-island site had only about 14 km² because it was farther inland and slightly protected by the study sites. Woodhouse and Knutson (1990) considered low-energy environments to have fetch distances of less than 9 km in

their study of successful marsh restoration along the Atlantic and Gulf coasts, which was comparable to the fetch range at each of these sites.

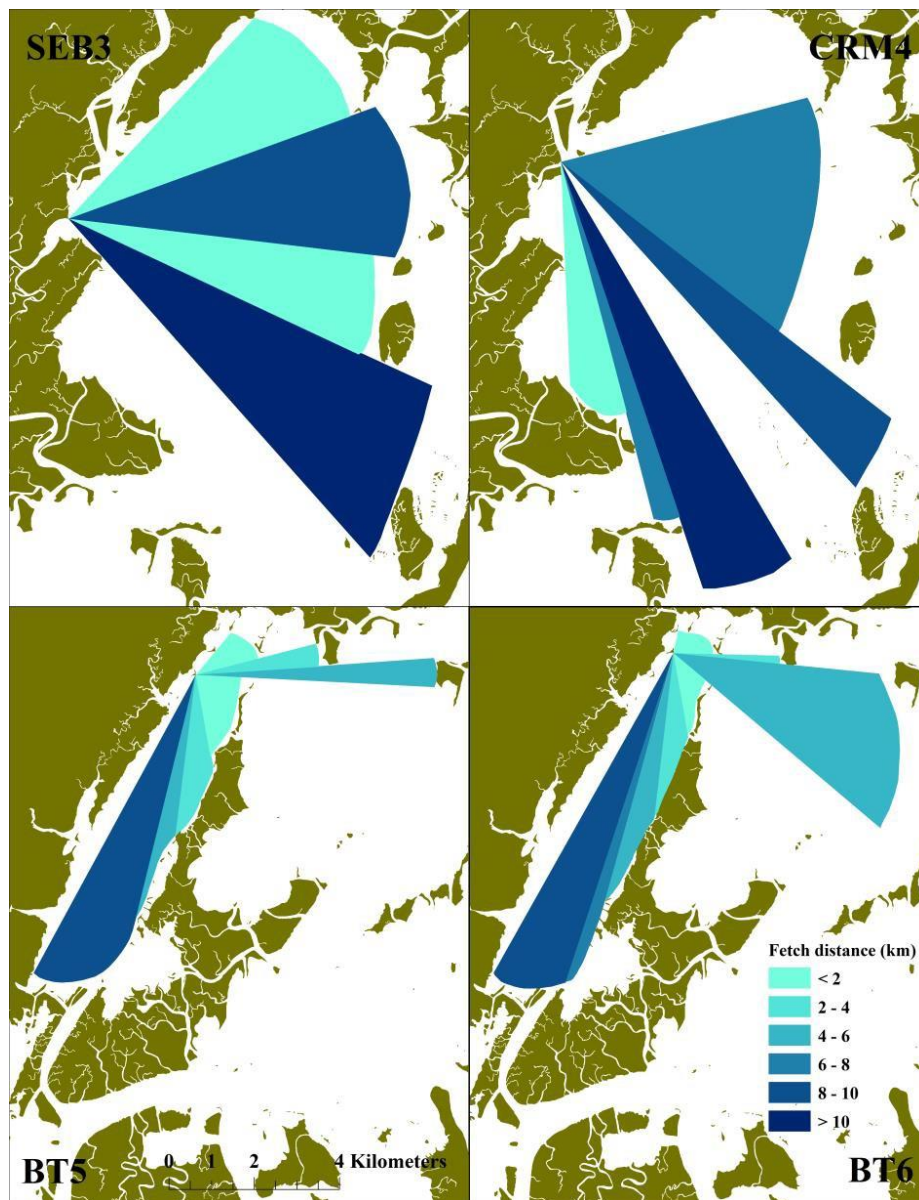


Figure 30: Fetches at study sites. Box Tree sites had roughly half the fetch area of the Northern sites which was mostly attributable to shorter fetch lengths.

Wave environment

RBR gauges placed at each of the four study sites recorded wave conditions for a period of two weeks (Table 2). Mean significant wave heights were used to compare wave conditions between sites which had varying reef shapes, sizes, and water depths (Table 7) along with the wind conditions at the time of sampling (Figure 28). Figure 31 shows a time series combining significant wave height (H_s) and wind speed at BT5. BT5 experienced average significant wave heights of 0.03 m at the marshside gauge (M_{sig}) and 0.04 m at the bayside gauge (B_{sig}). This differed from BT6 which had wave heights of 0.03 m on both marshside and bayside (Table 9). CRM4 had average significant wave heights comparable to those at the Box Tree sites despite the difference in wind activity (Figure 28). Waves at SEB3 were notably smaller than at the other sites. Shallow water depth in relation to the reef and the predominance of winds from the west where there was little fetch may explain the relatively small waves at SEB3. This site also appeared to be more of a tidal creek environment than one dominated by wind-waves. The water level that produced the greatest frequency of waves with $H_s > 0.03$ m was roughly 1 m in depth. Differences in H_s between sites were difficult to see using the complete data sets (Figure 32 upper panel). The lower panel of Figure 32 shows only those records where $H_s > 0.03$ m, where it is apparent that on average the largest waves were recorded by the marshside gauge of CRM4 and the bayside gauge of BT5.

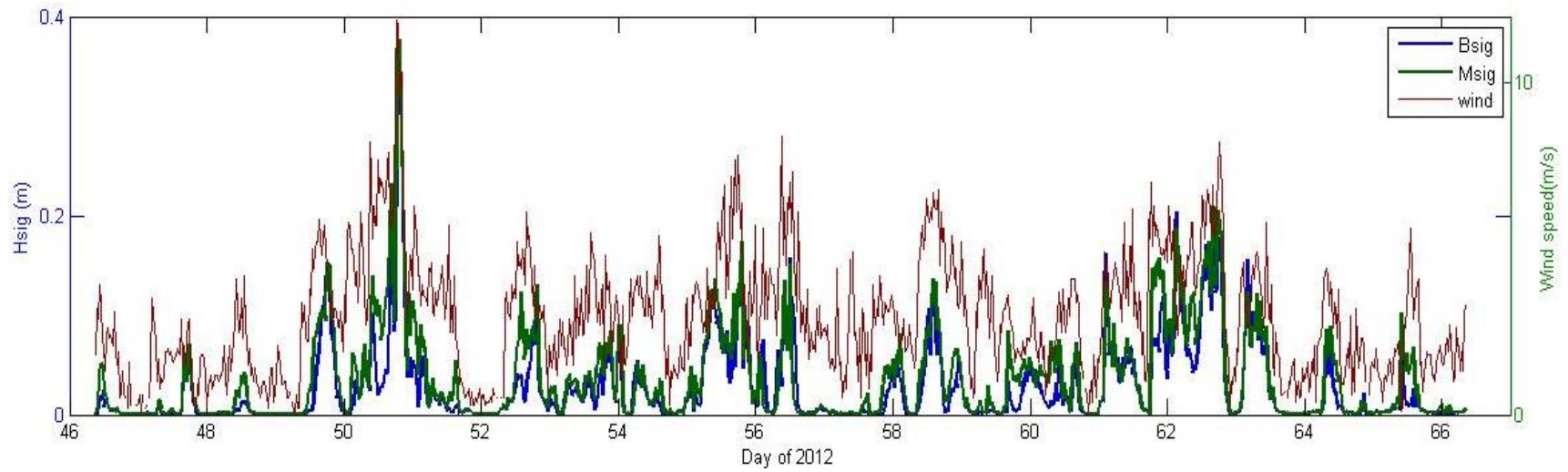


Figure 31: Example of H_s and wind speed time series from BT5. Wave heights were responsive to changes in wind speed, particularly from the E/SE.

Table 9: Significant wave height statistics. SEB3 waves were exceptionally small but significant wave heights at the other three sites were similar to one another (~ 0.03 m). A water level of about 1 m produced the greatest number of larger than average waves ($H_s > 0.03$ m).

	<i>Bsig</i>	<i>Msig</i>	h with greatest frequency $H_s > 0.03$ m (m)
SEB3			
H_s (m)	0.007	0.004	
ΔH_s (m)		0.003	1.4
CRM4			
H_s (m)	0.031	0.028	
ΔH_s (m)		0.029	1
BT5			
H_s (m)	0.036	0.027	
ΔH_s (m)		0.011	1
BT6			
H_s (m)	0.028	0.028	
ΔH_s (m)		0.028	0.9

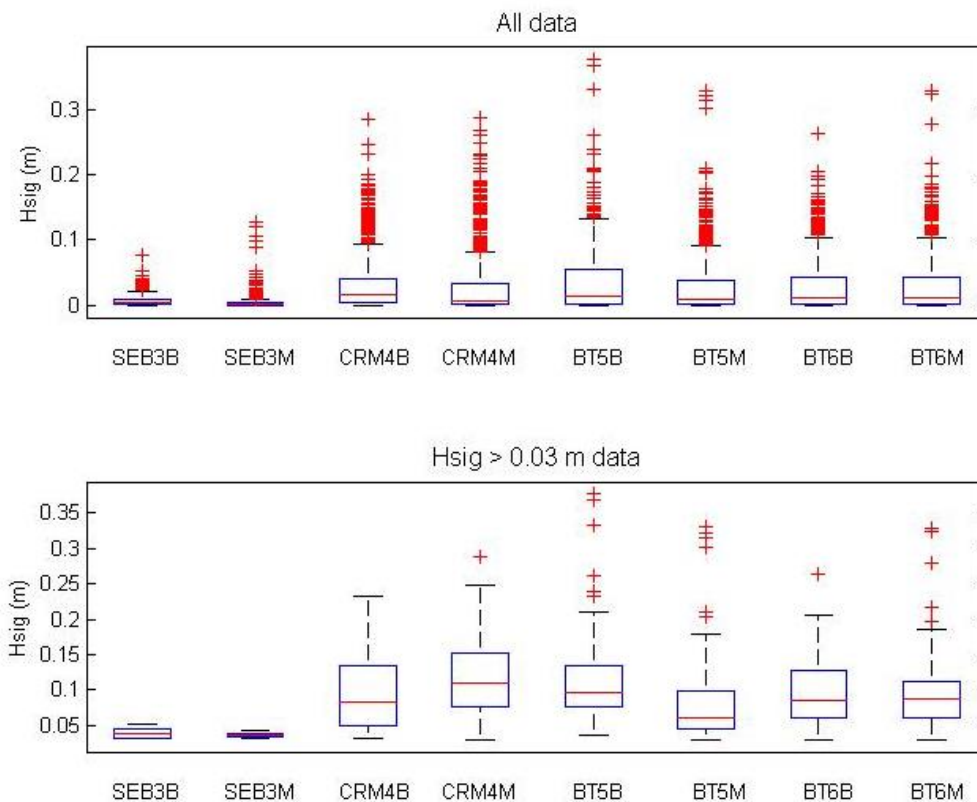


Figure 32: Significant wave height statistics for full data sets (top panel) and just Records of Interest (bottom panel). Differences in wave characteristics between sites is difficult to determine from the full data set. Viewing just records of greater than average waves, it is clear the marshside of CRM4 experienced the largest waves on average, followed by the bayside of BT5.

Waves in the Virginia Coast Reserve are mainly produced by winds blowing across the water surface; therefore the fetch at each site was influential on the formation of waves recorded on either side of the oyster reef. The Northern sites have fetches almost exclusively to the east and southeast, which make westerly winds of any sort fairly ineffective at generating waves across the water surface. It should be noted that the fetch at CRM4 changes with high and low tide on the marshside because of its proximity to a mud flat. Combining the fetch and wind data at the Northern sites (Figure 33, Figure 34), larger waves were likely to form due to easterly and southeasterly winds, though the occurrence of winds from those directions was infrequent. Winds from the west/southwest were the most common but had little potential to create large waves because of the limited fetch in that direction. At Box Tree (Figure 35 and Figure 36), there is a small slice of open water in the southwest that could have been responsible for the creation of frequent waves because the wind blew from that direction so often. Southeasterly winds were infrequent but had sufficient fetch to build up sizeable waves. From the significant wave height and wind data, it is apparent that winds from the E/SE (quadrant with an average wind direction of 112°) generally produced the largest waves despite the low frequency of occurrence. However, based on wind speed and frequency alone, southwesterly winds had the greatest capacity for creating large waves.

Data showed that SEB3 wave heights were unresponsive to increases in wind speed and did not show a preferential wind direction. Conversely, waves at CRM4 had a strong response to increased wind speed, particularly from the E/SE and S/SW. E/SE was the quadrant with the greatest fetch and S/SW was the quadrant with the most frequent

winds so this site appeared to react as predicted to changes in the environment. BT5 waves increased with higher wind speeds from all directions, though as at CRM4, the highest waves were created by winds from the E/SE. The same occurred at BT6 but to a lesser degree, possibly because waves from the E/SE would arrive at BT5 before reaching BT6.

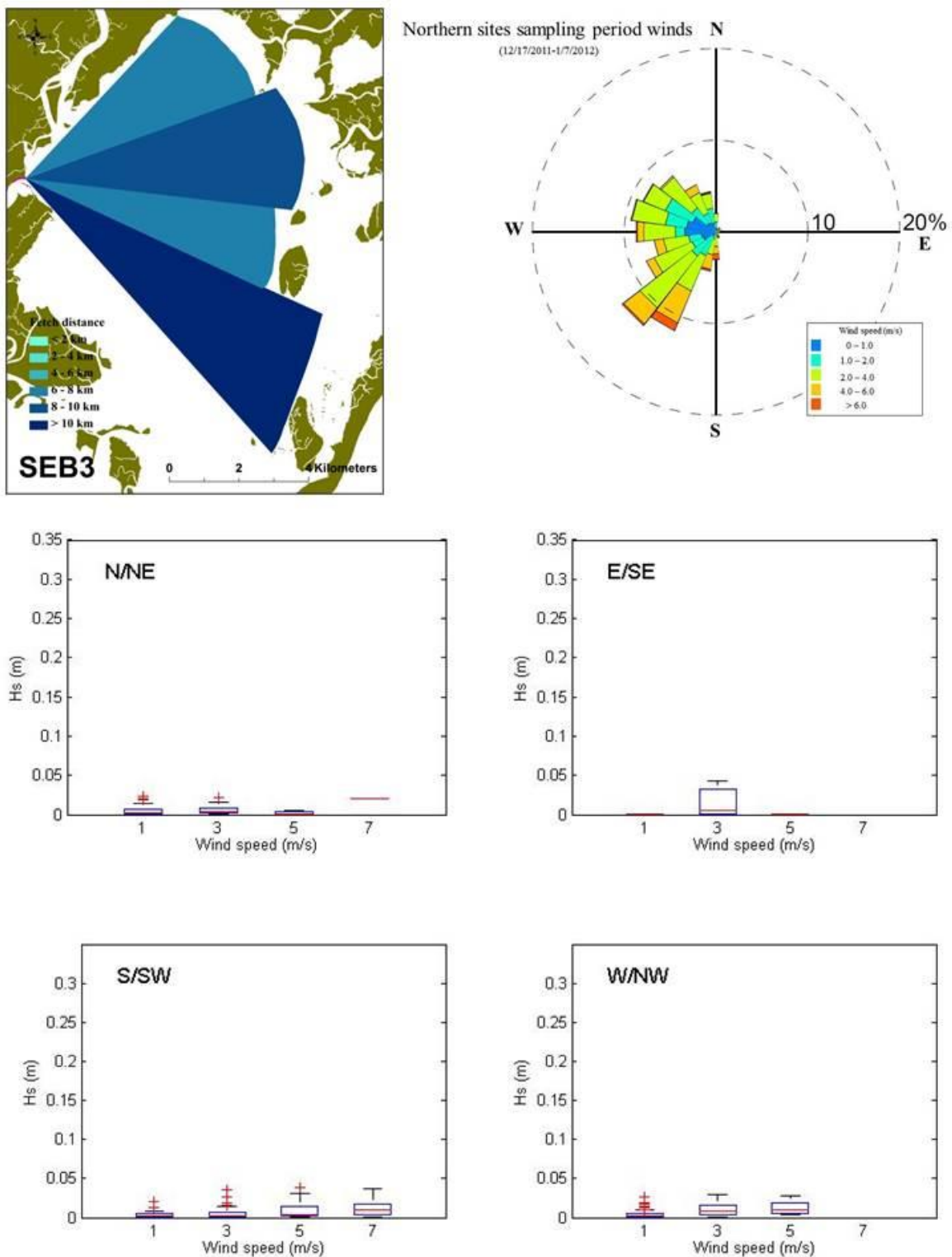


Figure 33: Fetch, winds, and significant wave height by wind direction for SEB3. Though the fetch at this site was more than sufficient to build up waves from the east, significant wave heights were miniscule potentially due to the majority of winds coming from the west.

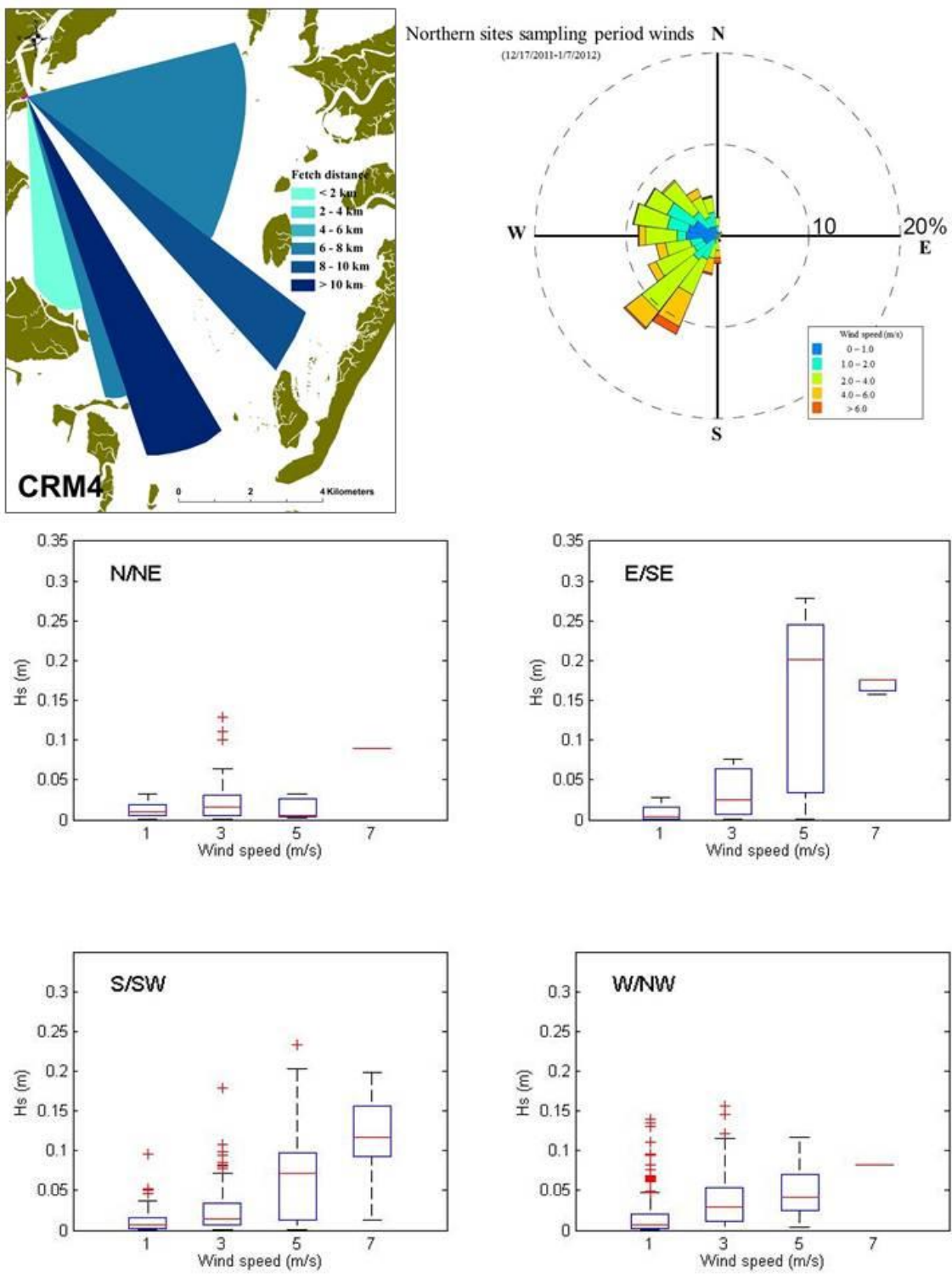


Figure 34: Fetch, winds, and significant wave height by wind direction for CRM4. There were strong wave height responses to increases in wind speed from E/SE and S/SW winds, the directions of greatest fetch and most frequent winds, respectively.

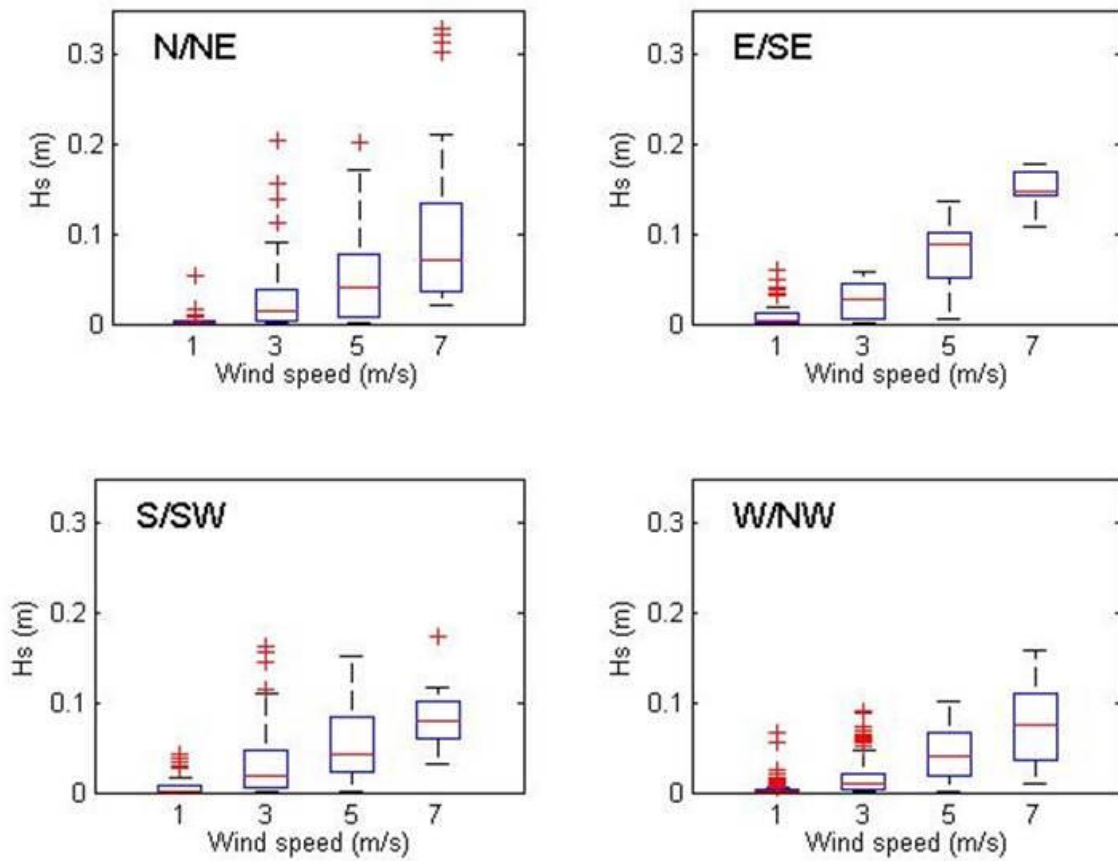
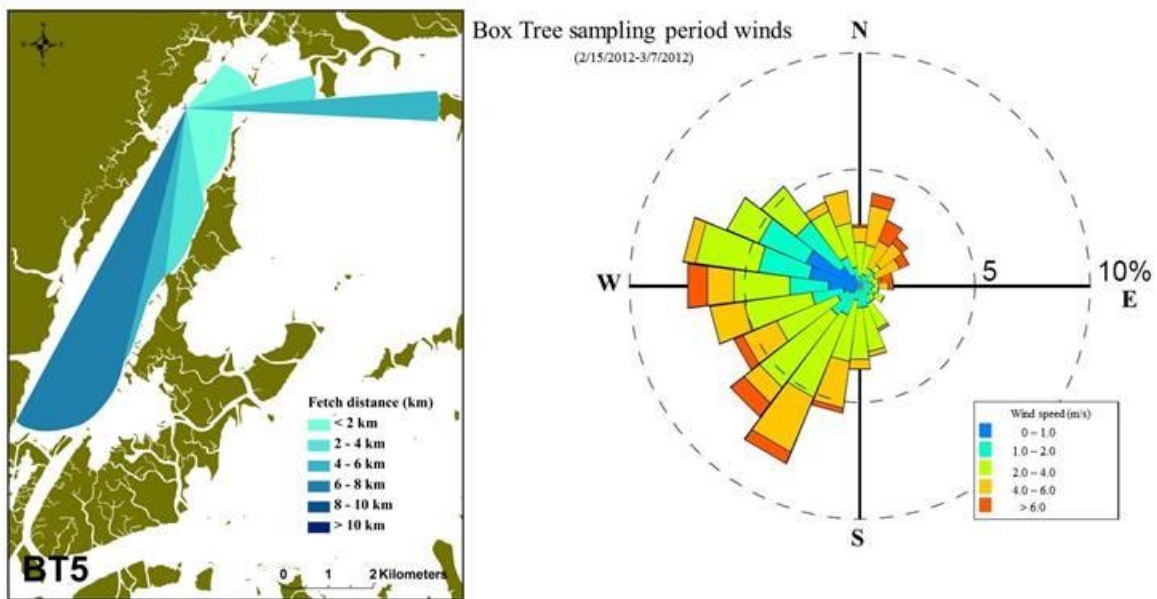


Figure 35: Fetch, winds, and significant wave height by wind direction for BT5. Winds from all directions elicited larger waves from increased wind speed with the most noticeable rise due to winds from the E/SE despite the low frequency and fetch.

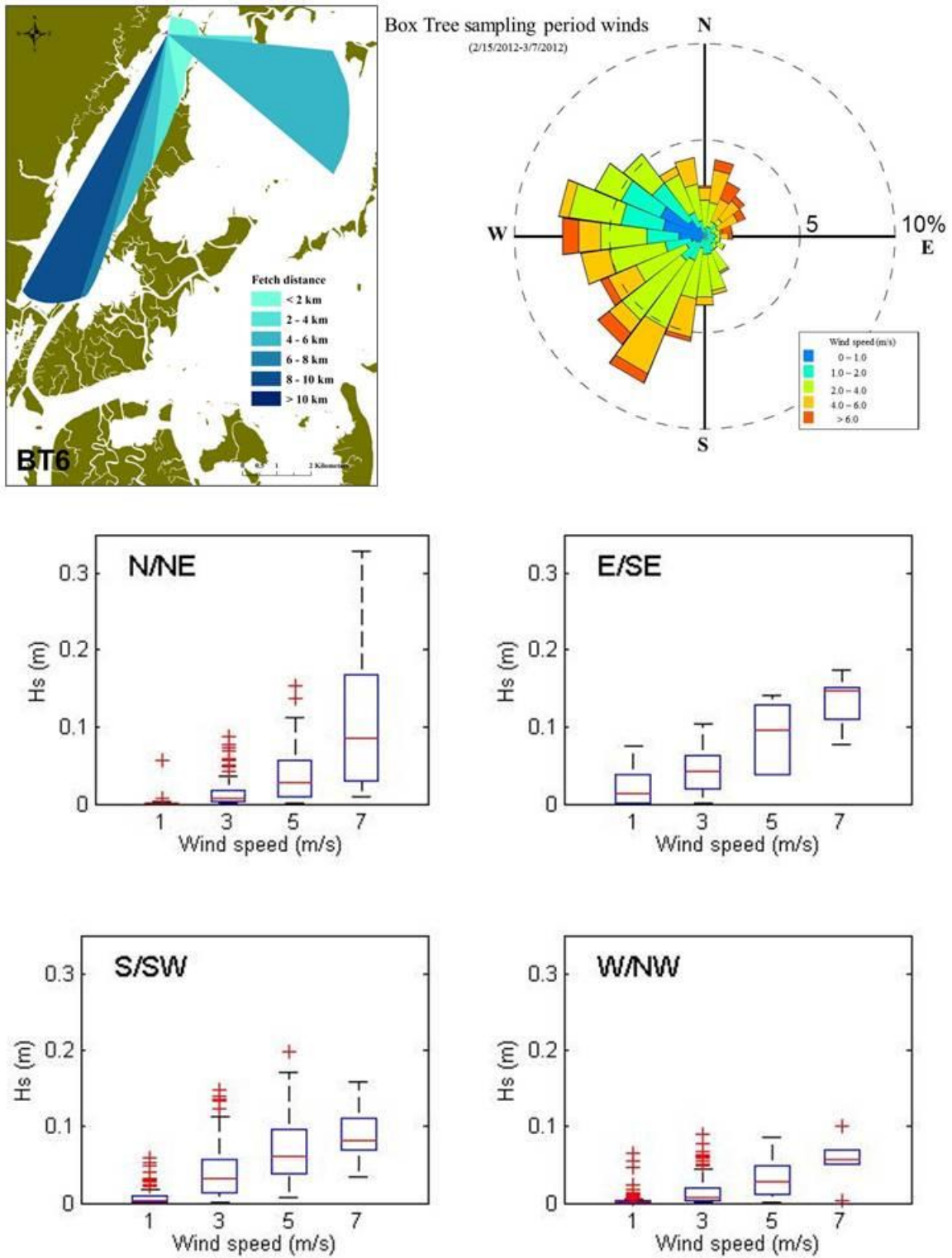


Figure 36: Fetch, winds, and significant wave height by wind direction for BT6. Wave heights reacted positively to increased wind speeds from all directions, particularly E/SE.

The upper and middle panels on Figure 37 show that water depths measured by all four gauges at the Box Tree sites tracks together, as do the significant wave heights. This supports the idea that the environments at the two locations were highly similar. The lower panel shows the wind speed during the same time period which reflects the trends in significant wave height. In Figure 38, water levels measured by the four gauges at SEB3 and CRM4 follow each other well, but SEB3 waves were much less responsive to changes in wind speed than waves at CRM4. Both significant wave height on the bayside (B_{sig}) and marshside (M_{sig}) at SEB3 are barely visible in the middle panel, especially towards the end of the sampling period because the values were so small. CRM4 B_{sig} and M_{sig} were not as tightly coupled as those at BT5 or BT6, but were much higher than values measured at SEB3. It is readily apparent that the wave environments at the two Northern sites were not similar.

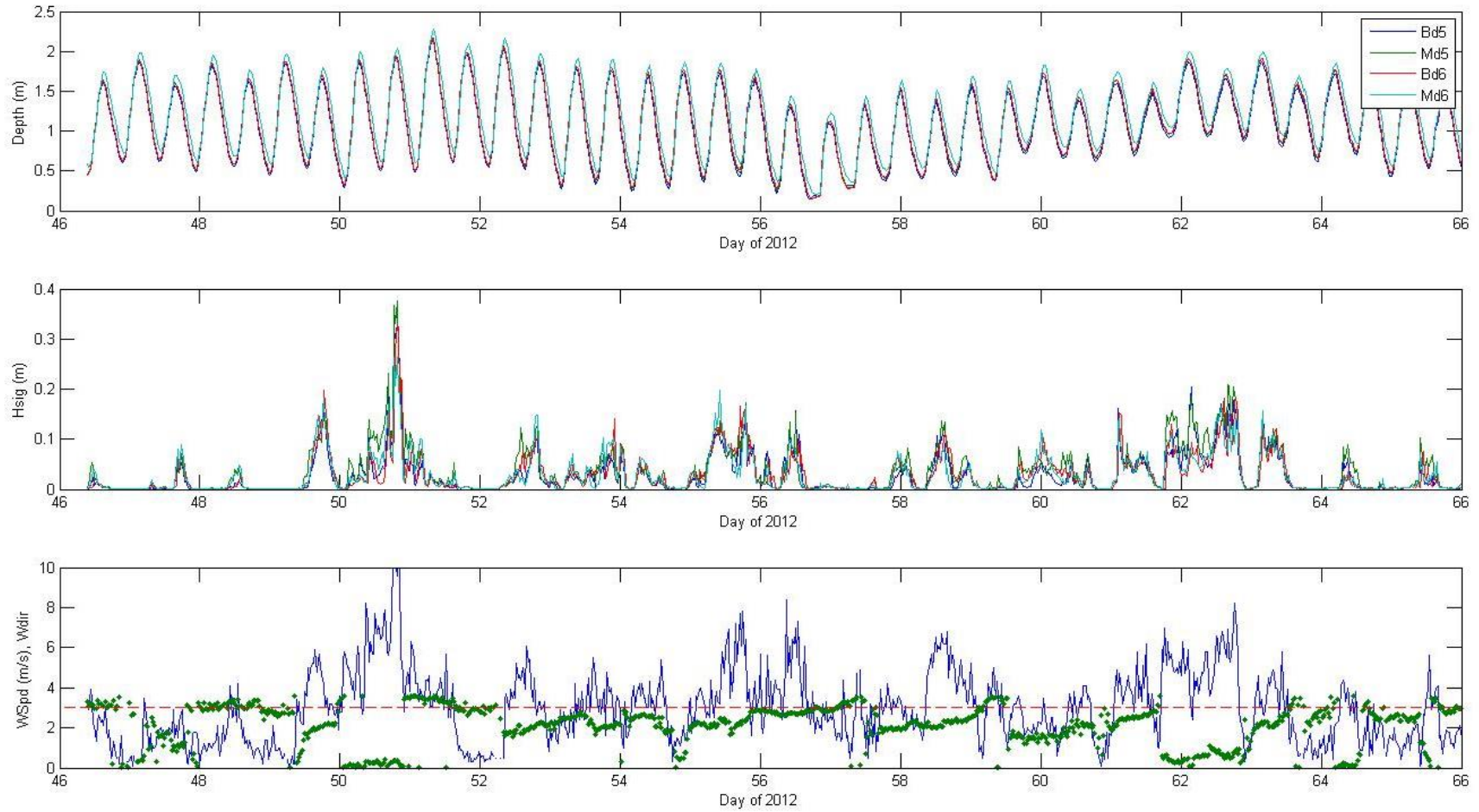


Figure 37: Water depth (upper), significant wave height (middle), and wind (lower) time series for sites BT5 and BT6. Green dots in bottom panel indicate wind direction (degree divided by 100) and dashed red line is 300 degrees. Wave heights recorded by each gauge tracked with each other and in response to wind speed. The greatest wind speeds produced the highest waves as seen between 50 and 52 along the x-axis.

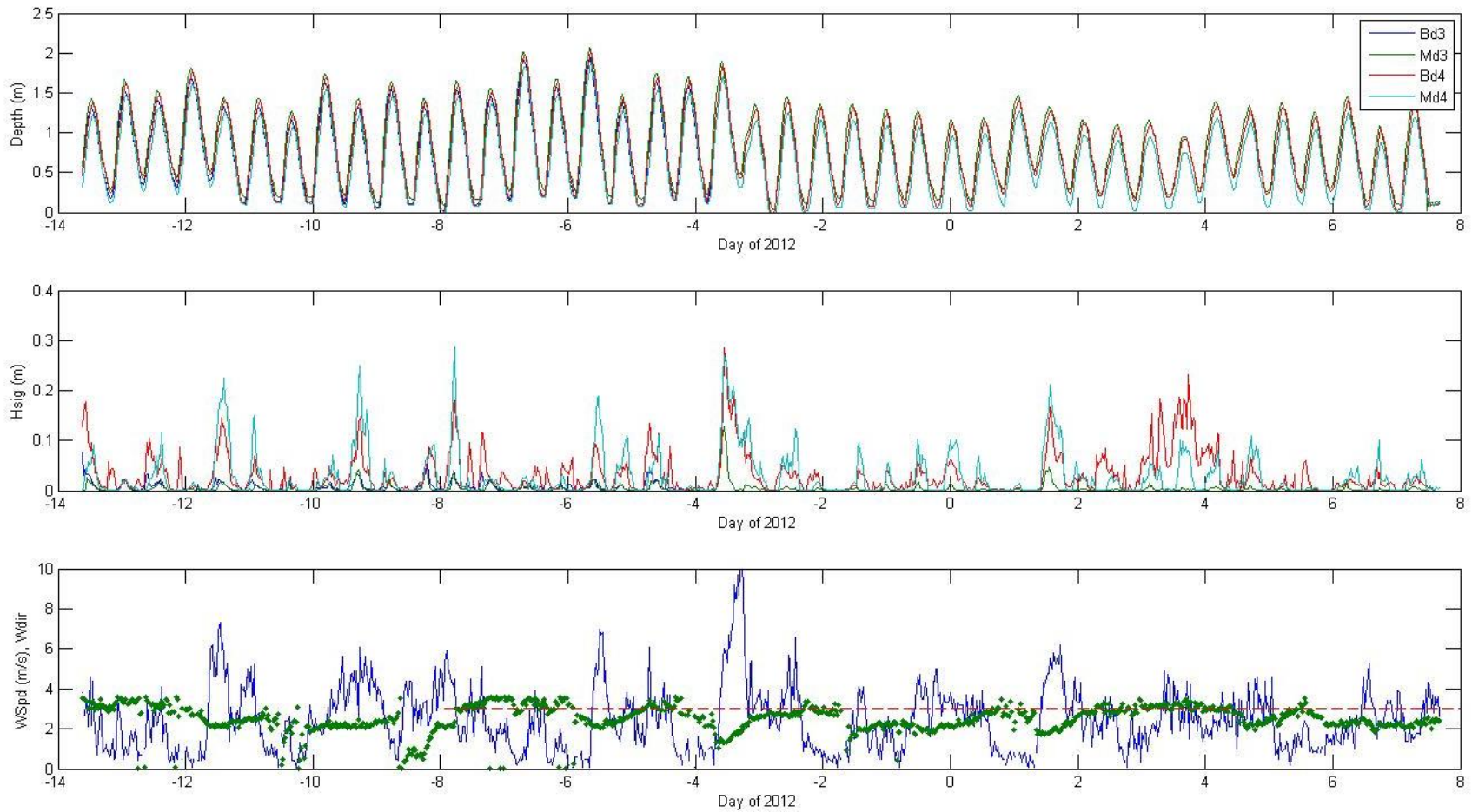


Figure 38: Water depth (upper), significant wave height (middle), and wind (lower) time series for sites SEB3 and CRM4. Green dots in bottom panel indicate wind direction (degree divided by 100) and dashed red line is 300 degrees. Water depths measured by all four gauges tracked well with each other and with the wind speed but waves at SEB3 did not respond to the same extent as those at CRM4.

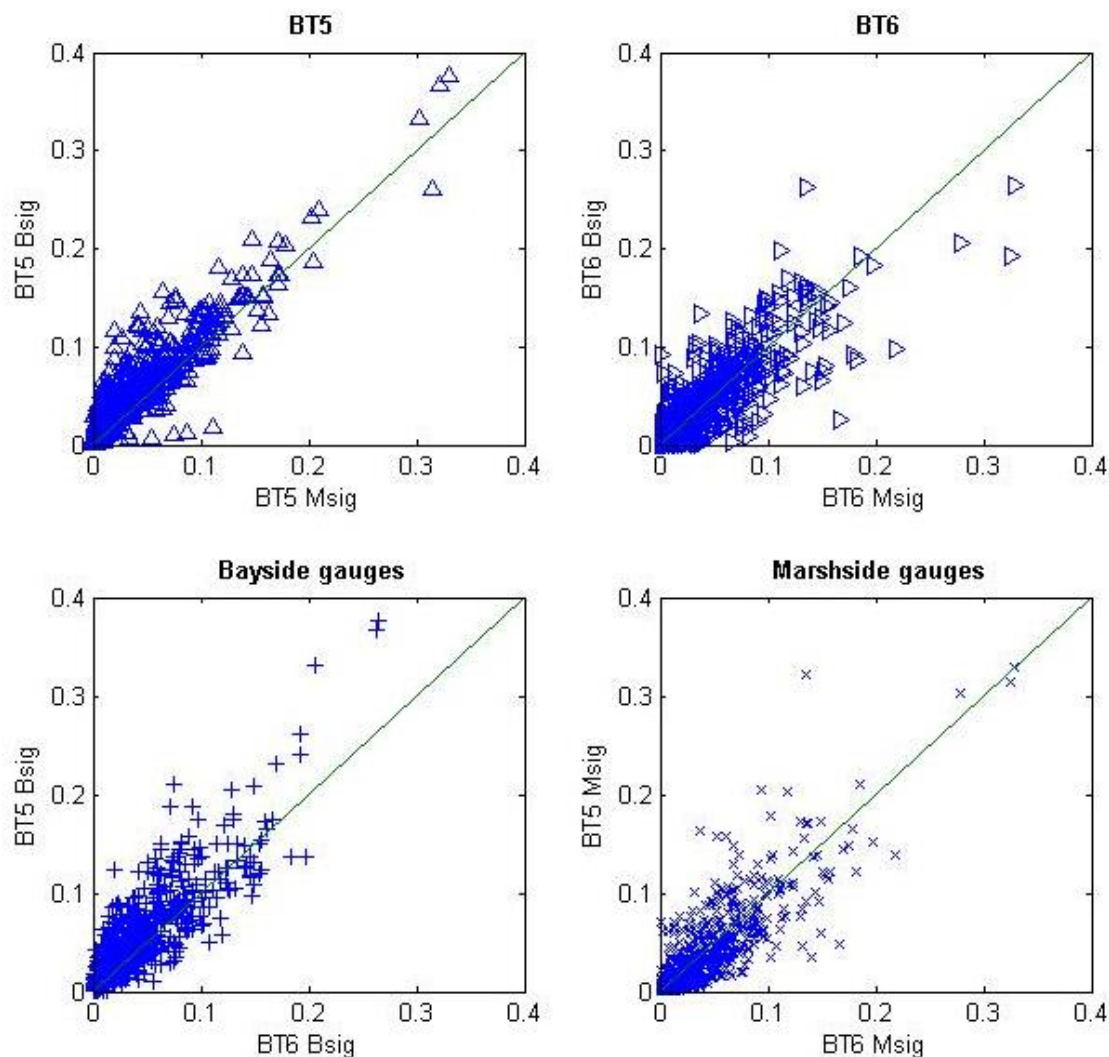


Figure 39: BT5 and BT6 significant wave heights; green line is a 1:1 ratio. Bayside waves at BT5 were higher than marshside waves, consistent with the idea that waves would propagate towards the marsh and dissipate over the reef. Bayside waves at BT5 were larger than bayside waves at BT6 because waves produced by SE winds that would place bayside gauges upwind of the reef would encounter BT5 before making it to BT6. Minimal scatter around the 1:1 lines means the wave environments were essentially the same.

Though the wave environments at BT5 and BT6 appear to be fairly similar, Figure 39 shows there was a trend of larger waves at BT5. At that site, bayside waves were almost always larger than marshside waves (top left), consistent with the expectation that waves would propagate from the bay towards the marsh and dissipate over the reef. If the wave heights were the same on both sides of the reef, points would

fall directly on the green line that shows a 1:1 ratio. However, the greater density of points to the left of the line indicates a bias towards larger waves on the bayside. This bias was not seen at BT6 (upper right) based on the even spread of data points. This could have been the case because winds from the SE that would have put the bayside gauge at BT6 upwind had already encountered the reef at BT5, decreasing the size of the waves. The highest waves at BT6 were on the marshside of the reef which could be attributed to winds from the NE that would have put that gauge upwind. Comparing the two bayside gauges at Box Tree sites shows BT5 wave heights were slightly larger than BT6, particularly when wave heights were greatest. Winds from the SE would put the BT5 bayside gauge upwind of all other gauges, so it would be expected that the highest waves would be recorded by this gauge (lower left plot). Marshside gauges did not have the same sort of lopsided relationship as the bayside gauges, suggesting that winds from the S, SW, and W, placing the marshside gauges upwind, affected both similarly (lower right). The scatter between the marshside and bayside plots did not vary greatly, indicating that the wave environment was essentially the same at BT5 and BT6.

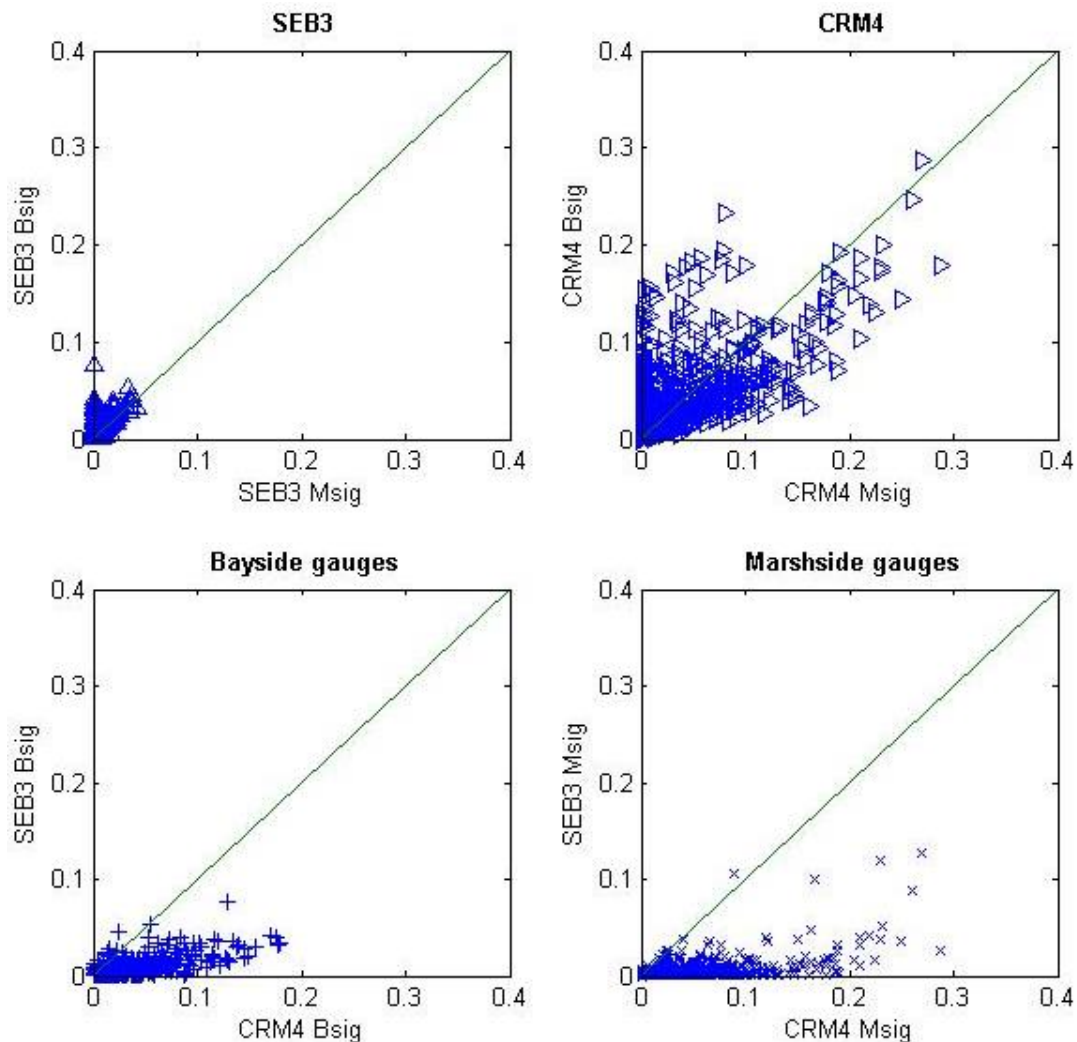


Figure 40: SEB3 and CRM4 significant wave height correlation plots.

CRM4 and SEB3 wave environments were distinctly unlike judging by the marked differences in significant wave heights between the sites (Figure 32, Figure 38, Figure 40). The two upper plots in Figure 40 show that there were no SEB3 records when significant wave height from either side of the reef reached 0.1 m. The values recorded were so small that it was difficult to make out any sort of pattern between the two gauges, though the largest wave in the SEB3 data set was recorded on the bayside. CRM4 waves (upper right) looked much more like the BT5 or BT6 records in terms of range and

variance. Smaller waves tended to be higher on the bayside gauge but the largest waves were recorded on the marshside. This could be accounted for by the fact that some of the highest wind speeds were from the S and SW, placing the marshside gauge upwind. Clearly the wave environments were dissimilar at SEB3 and CRM4, making temporal comparisons futile between the two sites.

Wave events

After removing wave records with low significant wave heights ($H_s < 0.03$ m), roughly 10% of the original data remained. The characteristics of the remaining records and the full data set are summarized in Table 10. The SEB3 data was of little use because there were only 3 wave records, with $H_s > 0.03$ m, so this site was not considered in the analysis of wave dissipation. CRM4 and BT6 had a sufficient number of usable records (81 and 94) however BT5 was likely the most valuable for this analysis with 91 records and strong trends of waves from one side. Most of the records of interest fell in series that combined to form “wave events” or periods of noticeably higher wave action. Records were broken down by their attributes (high/low tide, rising/falling tide, wind direction, etc.) to help compare to each other and between sites.

Within the ROI data sets, tidal motion (rising or falling) was inconsequential and appeared to have no bearing on wave height. BT5 was the only location where the data set showed a strong trend of waves originating in the bay (NE/E/SE). BT6 had slightly more wave records originating on the marshside, and CRM4 had twice as many records of waves originating on the marshside. Of the 91 ROI from BT5, 84 came in from the bay towards the marsh, consistent with winds from the N, E, and SE, under which conditions

the bayside wave gauge was upwind. The other 7 records corresponded to winds from the west when the marshside gauge was upwind. This agreement between wind direction and wave propagation held for the majority of records at other sites (Table 9). The series were also internally consistent in that the wind direction was the same for the entire wave event.

Table 10: Statistics for wave data sets before and after selecting records of interest (all numbers in upper panel are averages). Records from SEB3 were too few to analyze due to weak response to wind but CRM4, BT5, and BT6 had a number of wave events. Clearest signals were recorded at BT5.

Averages	SEB3		CRM4		BT5		BT6	
	initial	> 0.03 m	initial	> 0.03 m	initial	> 0.03 m	initial	> 0.03 m
Wind speed (m/s)	2.5	2.7	2.5	3.8	3.0	5.0	3.0	4.9
d (m)	0.81	1.18	0.72	1.23	0.99	1.10	1.11	1.37
$Bsig$ (m)	0.01	0.04	0.03	0.08	0.04	0.12	0.03	0.10
$Msig$ (m)	<0.01	0.02	0.03	0.12	0.03	0.09	0.03	0.09
ΔH_s (m)	<0.01	0.02	0.02	0.05	0.01	0.11	0.02	0.04
Records	1014	3	1015	81	957	91	957	94
Tide								
rising		2		46		34		41
falling		1		35		57		53
high		1		11		4		5
low		0		0		2		1
Direction								
from bayside	371	3	604	16	781	84	512	56
from marshside	643	0	411	65	176	7	445	38

At all locations, H_s was significantly responsive to increases in wind speed (Figure 41, Table 25) particularly at BT5. B_{sig} and M_{sig} at BT5 had the highest correlations ($r^2 = 0.43$ each) which were nearly twice as large as those at BT6 ($r^2 = 0.24, 0.25$) (Figure 42). Waves at CRM4 were also strongly related to winds speed but much more so on the marshside ($r^2 = 0.39$) than the bayside ($r^2 = 0.15$) (Figure 43). Waves in the VCR are wind-driven so a correlation between H_s and wind speed was expected. The weaker relationship between CRM4 B_{sig} and wind speed may have been a result of the infrequency of winds from directions that would have put that gauge upwind during the sampling period (NE, E). Wave height is also a function of water depth as well as wind speed so the positive correlations between wave height and water depth reflected the theoretical expectation. Both gauges at BT5 had a significant $r^2 = 0.25$ in relationship to water depth above the reef (d_{reef}) as did the bayside gauge at BT6 ($r^2 = 0.15$). This relationship was weak but still significant marshside at BT6 and non-existent at CRM4. Wind direction was difficult to correlate because both high and low values were indicative of the same direction (360° and 0° are from N). In place of statistical analysis, the directions of wave propagation was compared to wind direction during the recording period and were found to be consistent with each other for more than 95% of the records from all sites.

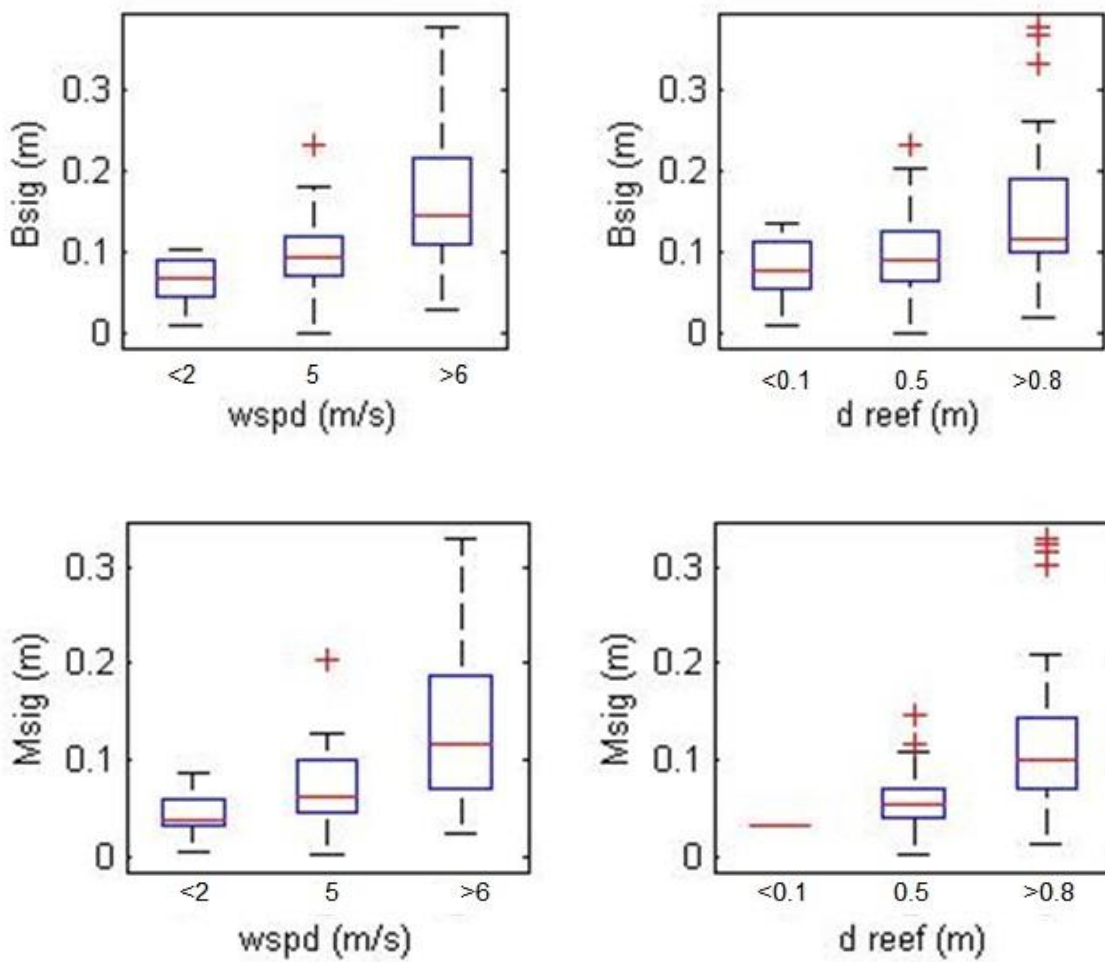


Figure 41: BT5 B_{sig} (upper) and M_{sig} (lower) response to wind speed (left) and reef water depth (right). Waves measured by both gauges were responsive to changes in wind speed and water depth.

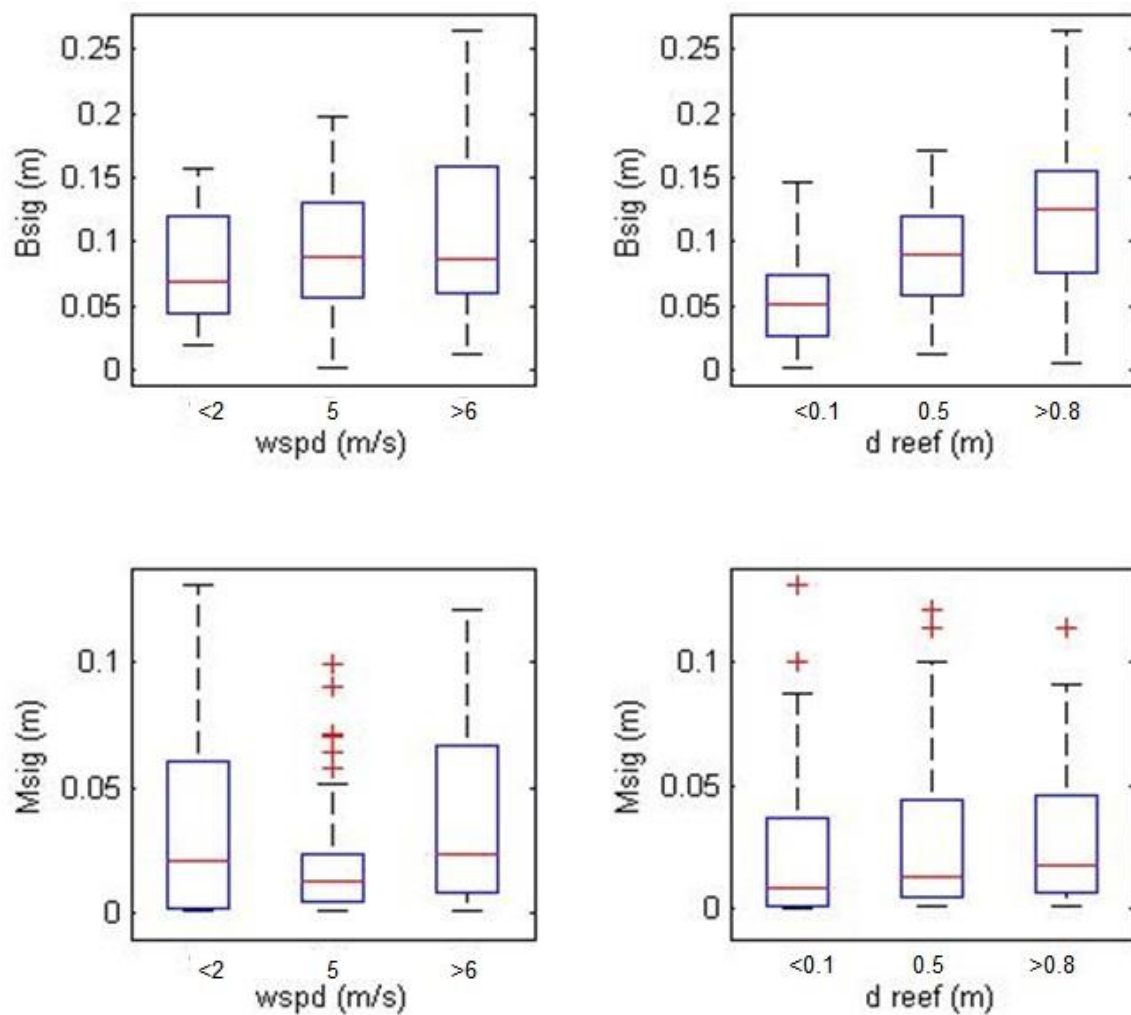


Figure 42: BT6 B_{sig} (upper) and M_{sig} (lower) response to wind speed (left) and reef water depth (right). Waves measured by both gauges were responsive to changes in wind speed and water depth but only the bayside gauge plot averages showed a consistently positive reaction to increased wind speeds. Statistical analysis indicated there was a significant positive relationship between wave height and wind speed on the marshside as well.

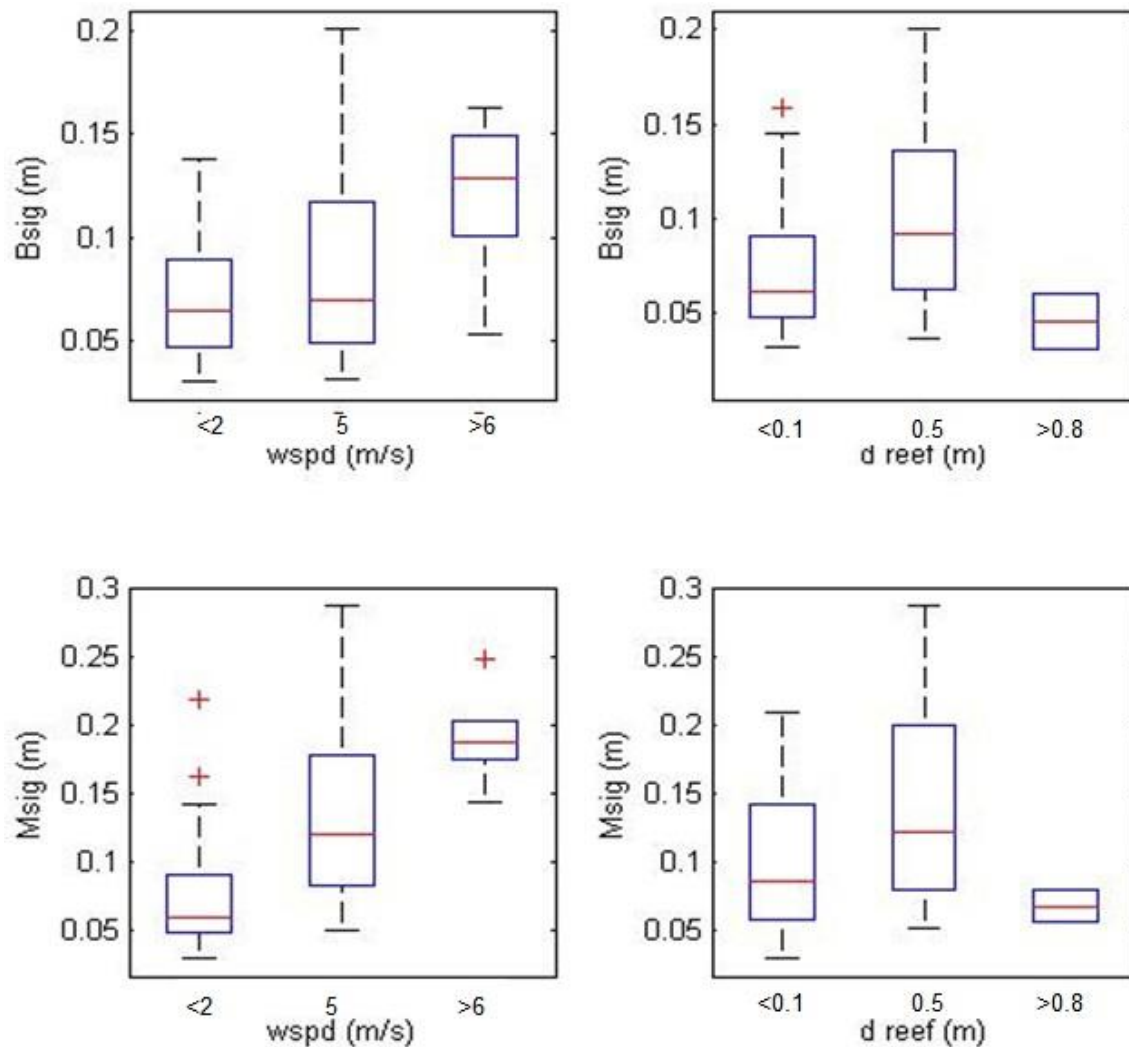


Figure 43: CRM4 *Bsig* (upper) and *Msig* (lower) response to wind speed (left) and reef water depth (right). Waves measured by both gauges were responsive to changes in wind speed and but not as expected to water depth.

Wave power

Wave power density was calculated in order to compare conditions at these sites to data from McLoughlin (2010), the VCR model by Mariotti et al. (2010), Venice Lagoon, and Delaware and Rehoboth Bays. As with the significant wave height analysis, SEB3 was excluded

from wave power calculations. The average wave power density for the full set of wave records at CRM4, BT5, and BT6 was $5\text{-}6 \text{ W}\cdot\text{m}^{-1}$ which was significantly smaller than values for the records of interest (Table 11). At BT5, the power generated on the bayside of the reef was $36 \text{ W}\cdot\text{m}^{-1}$ on average and $26 \text{ W}\cdot\text{m}^{-1}$ on the marshside for the ROI (Figure 44) which was consistent with higher H_s values on the bayside. CRM4 wave power distribution also matched the difference in significant wave height on either side of the reef with $23 \text{ W}\cdot\text{m}^{-1}$ on the bayside and $30 \text{ W}\cdot\text{m}^{-1}$ on the marshside. BT6 was more evenly divided, $23 \text{ W}\cdot\text{m}^{-1}$ bayside and $28 \text{ W}\cdot\text{m}^{-1}$ marshside, again reflective of the significant wave height statistics. Measurements from McLoughlin (2010) reached maxima between 50 and $80 \text{ W}\cdot\text{m}^{-1}$ whereas during high wind events, wave power at BT5 was calculated to be over $350 \text{ W}\cdot\text{m}^{-1}$ which was more on the order of estimates from Mariotti et al. (2010). Figure 1 shows these estimates by Mariotti et al. (2010) of wave power for shorelines in the VCR weighted by wind statistics. Their model predicted that wave power at these locations would be less than $50 \text{ W}\cdot\text{m}^{-1}$ as an annual average, which was in agreement with our data.

Overall, the mean reduction in wave power from the upwind to the downwind sides of the reefs for the ROI was 49% regardless of the direction of propagation. This amount differed depending on the direction of the waves for CRM4 and BT5, but not BT6 (Table 11). BT5 and BT6 had very similar average reductions in wave power - 44% and 42% respectively. However the mean reduction value at CRM4 was 61% which was significantly larger than BT5 and BT6.

Table 11: Wave power density averages for sites CRM4, BT5, and BT6 records of interest. Reefs reduced wave power by an average of 49% regardless of the direction of propagation. Percent reduction was influenced by the side on which the wave originated. There was no significant difference between power reduction rates at the Box Tree sites but CRM4 was significantly higher.

All records	CRM4		BT5		BT6	
	Bay	Marsh	Bay	Marsh	Bay	Marsh
P_{avg} ($W \cdot m^{-1}$)						
by side	5	6	7	5	5	5
site	5.5		6		5	
ROI	CRM4		BT5		BT6	
	Bay	Marsh	Bay	Marsh	Bay	Marsh
P_{avg} ($W \cdot m^{-1}$)						
by side	23	30	36	26	23	28
site	27		31		26	
ΔP_{avg} ($W \cdot m^{-1}$)						
by origin	10	25	10	13	11	22
site	18		12		16	
$\% \Delta P_{avg}$						
by origin	67%	60%	46%	24%	42%	42%
site	61%		44%		42%	

High values of wave power were recorded exclusively in conjunction with deep water while low values were associated with all water depths. This trend was particularly strong on the bayside of BT5 (Figure 45) but could be seen in the other locations as well. The ratio of P_B to P_M was plotted as a function of water depth for waves originating in the bay and in the marsh separately (lower plots in Figure 44-Figure 46). At CRM4 and BT5 there was a visible downward trend as the two values grew closer together as water depth increased. This trend was observed on the bayside of BT6 after a brief increase but was not apparent for waves propagating from the marsh.

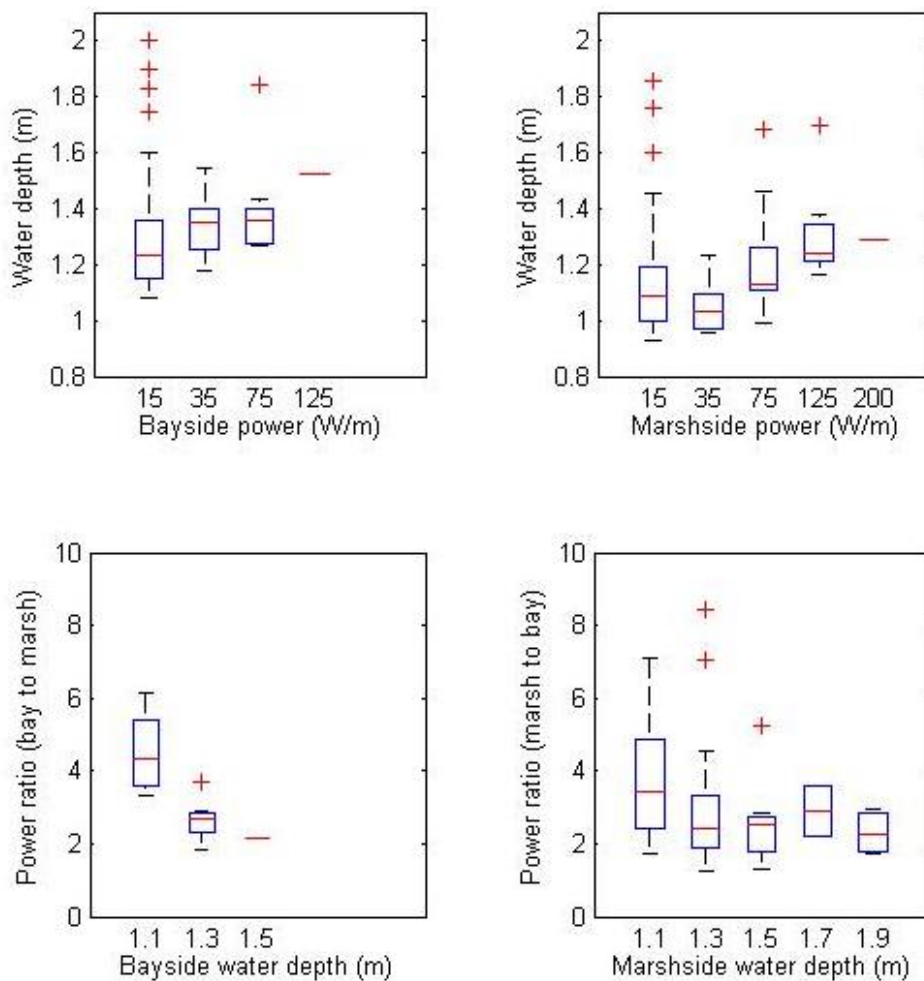


Figure 44: CRM4 wave power statistics. Wave power density as a function of water depth (upper) exhibited the expected positive relationship between high power and deep water. The ratio P_B to P_M for waves originating in the bay (lower left) showed a strong negative relationship, as did P_M to P_B for waves from the marshside (lower right), indicating less reduction of wave power with greater water depth. NB: Bins appear to be “missing” from bayside plots because there were no data for that interval.

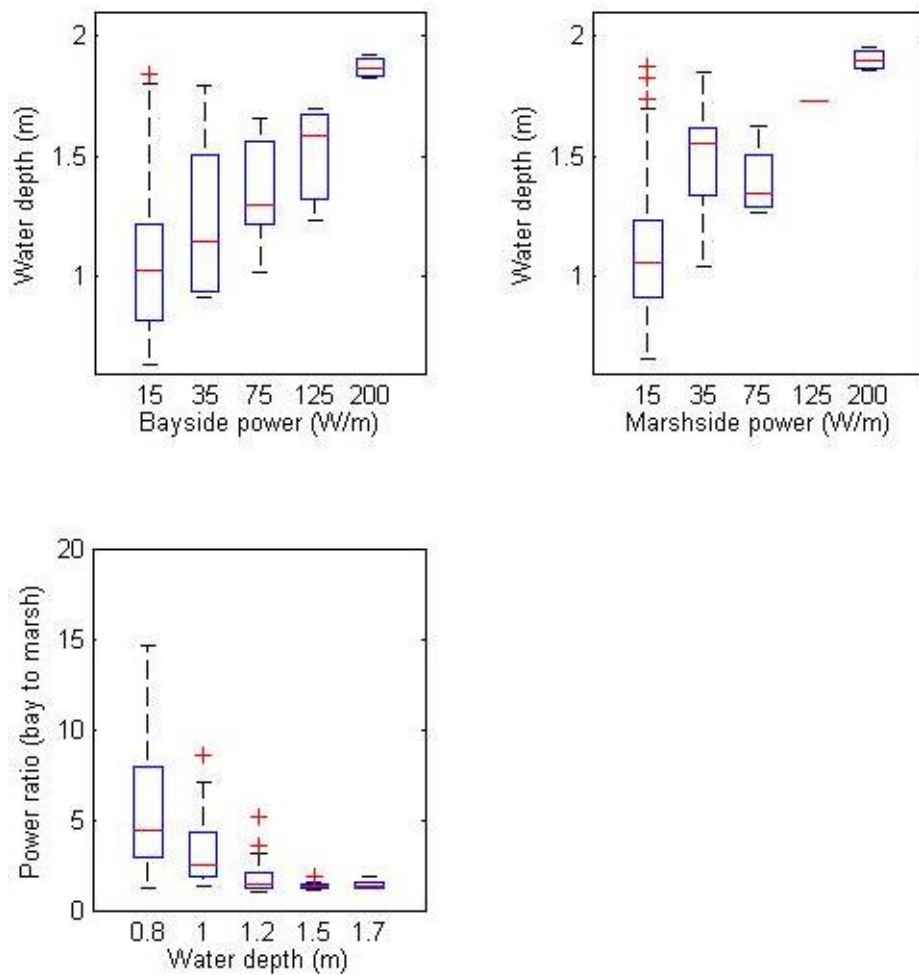


Figure 45: BT5 wave power density statistics. Wave power density as a function of water depth (upper) showed the expected positive relationship between high power and deep water. The ratio P_B to P_M for waves originating in the bay (lower left) showed a very strong negative relationship indicating less reduction of wave power with greater water depth. There were too few records of waves from the marshside to plot.

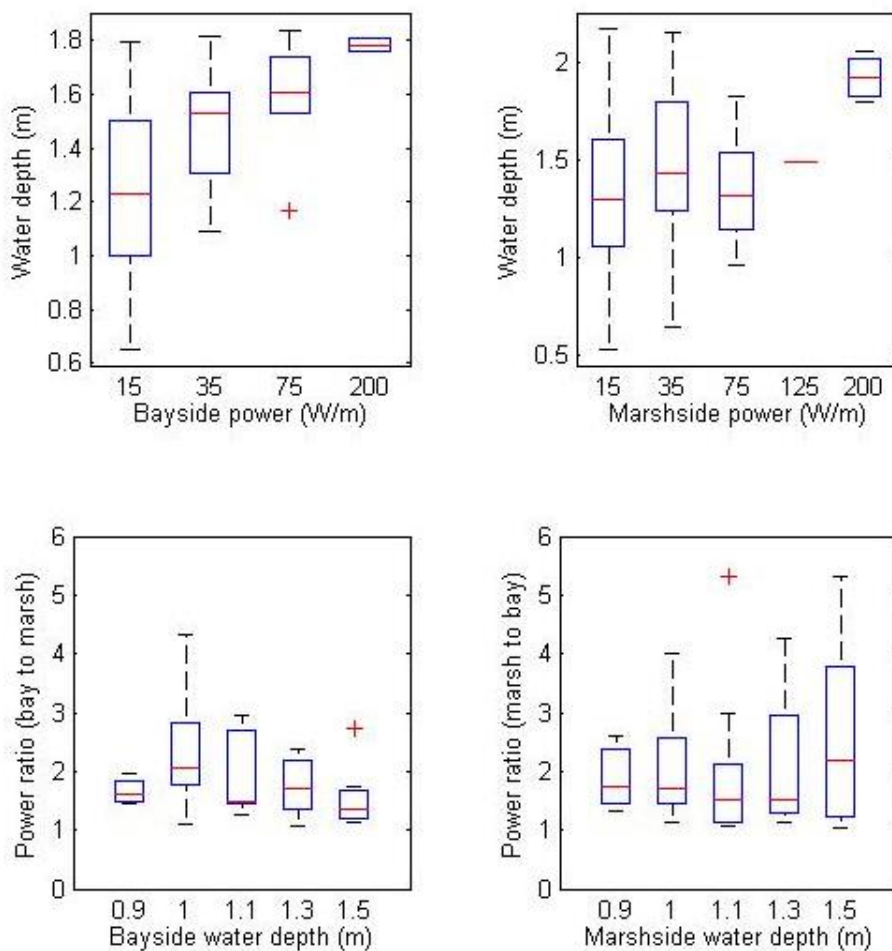


Figure 46: BT6 wave power density statistics. Wave power density as a function of water depth (upper) showed the expected positive relationship between high power and deep water. The ratio P_B to P_M for waves originating in the bay (lower left) grew then declined with greater water depth. This trend was not apparent on the marshside.

Reef dissipation of wave energy

Statistical analysis did not identify any variables that had a significant relationship to ΔH_s . However, visual analysis of box plots showed that in general, ΔH_s exhibited positive relationships with H_s , wind speed, and bottom orbital velocity (u_{br}), and a more complex relationship with d_{reef} . In terms of change in the actual spectrum, h and Δh had increasingly important roles as ΔH_s increased, and well as a corresponding decrease in the importance of w . These variables also tracked well with the median frequency, f_{50} , which exhibited similar tendencies to w .

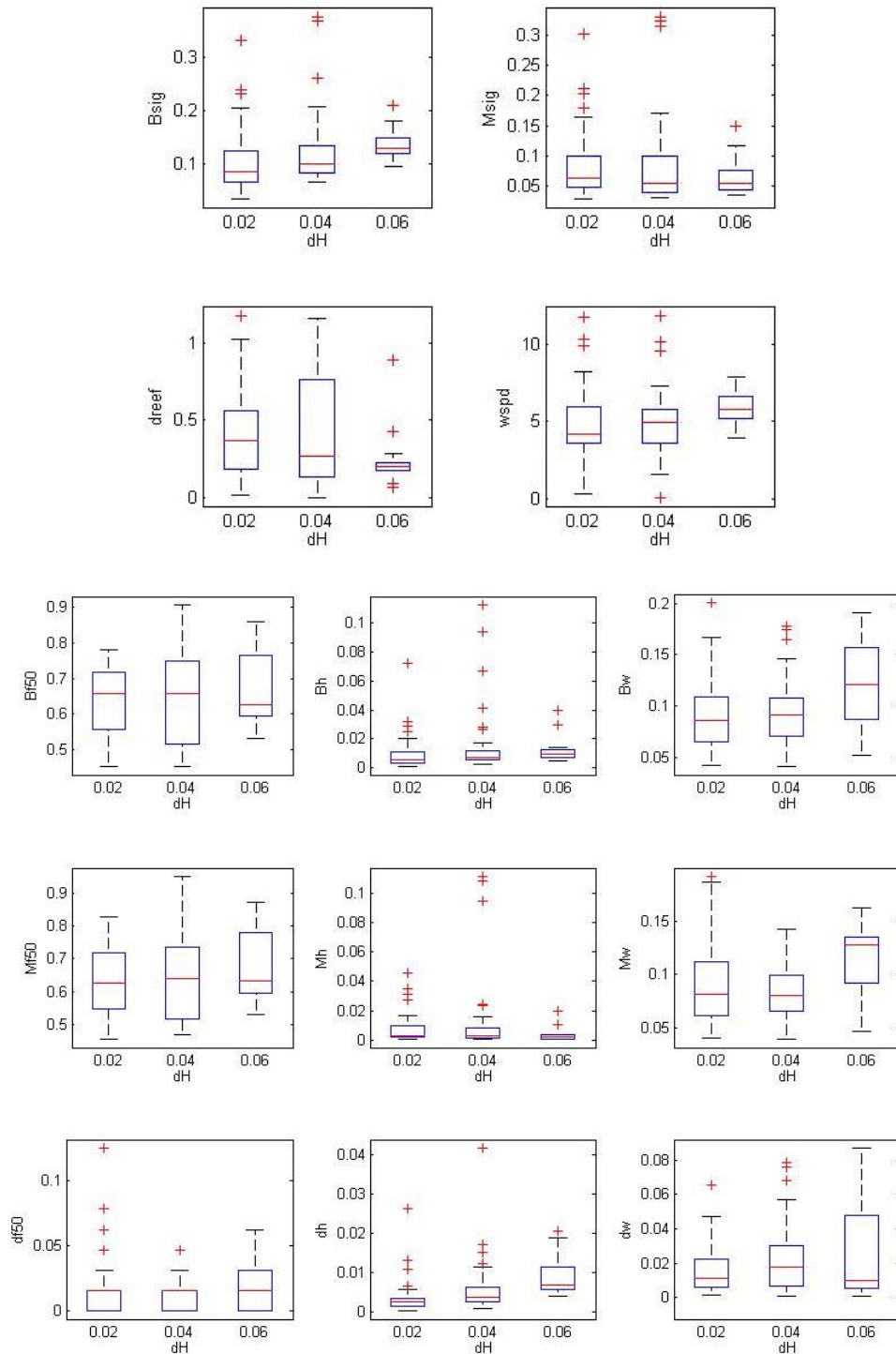


Figure 47: Change in significant wave height as a function of various factors. ΔH_s had a positive relationship with H_s , wind speed, and Δh . There was a negative correlation with d_{reef} .

There is a possible explanation for the lack of statistically significant trends at BT5. A finer examination of this data using more divisions of ΔH_s as a function of water depth above the reef revealed a maximum in Δh at $d_{reef} = 0.15$ m followed by decreasing values of Δh . This may signal a progressive decoupling of the interaction between waves and reef for values of $d_{reef} > 0.15$ m such that wave orbital motion when $d_{reef} > 0.50$ m was insufficient to significantly modify the passing waves (Figure 49). This pattern was not apparent in plots using only three divisions.

Wave base calculations were performed for BT5 where strong relationships in significant wave height and wave power data were most apparent. Wavelengths for ROI ranged from 2.1-7.3 m. The relationship $WB = \lambda/2$ for deep water waves was inconsistent with results from dissipation analysis. Using d_{reef} as the effective wave base, the relationship at BT5 was analyzed by locating x , the ratio of wavelength to depth above the reef, where wave dissipation began to decline. This depth was between 0.15 and 0.30 cm and resulted in the relationship

$$WB_{reef} = \lambda/15.$$

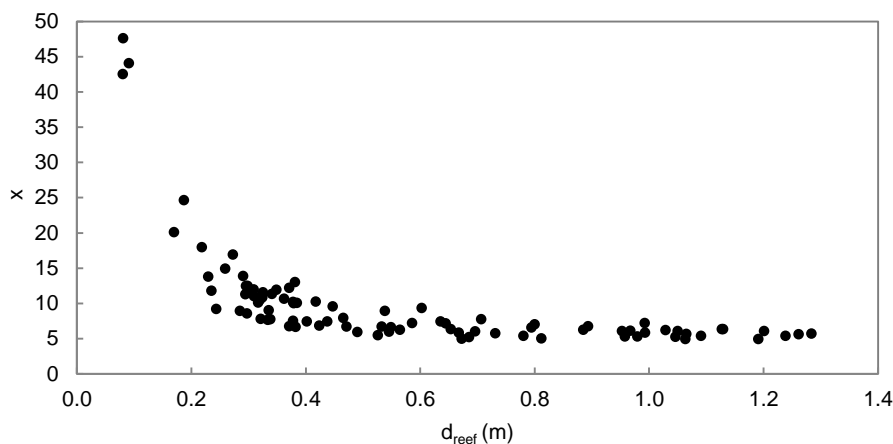


Figure 48: Wave base for BT5. Cut off point for decreased wave dissipation between 0.15 and 0.30 m where x is roughly 15.

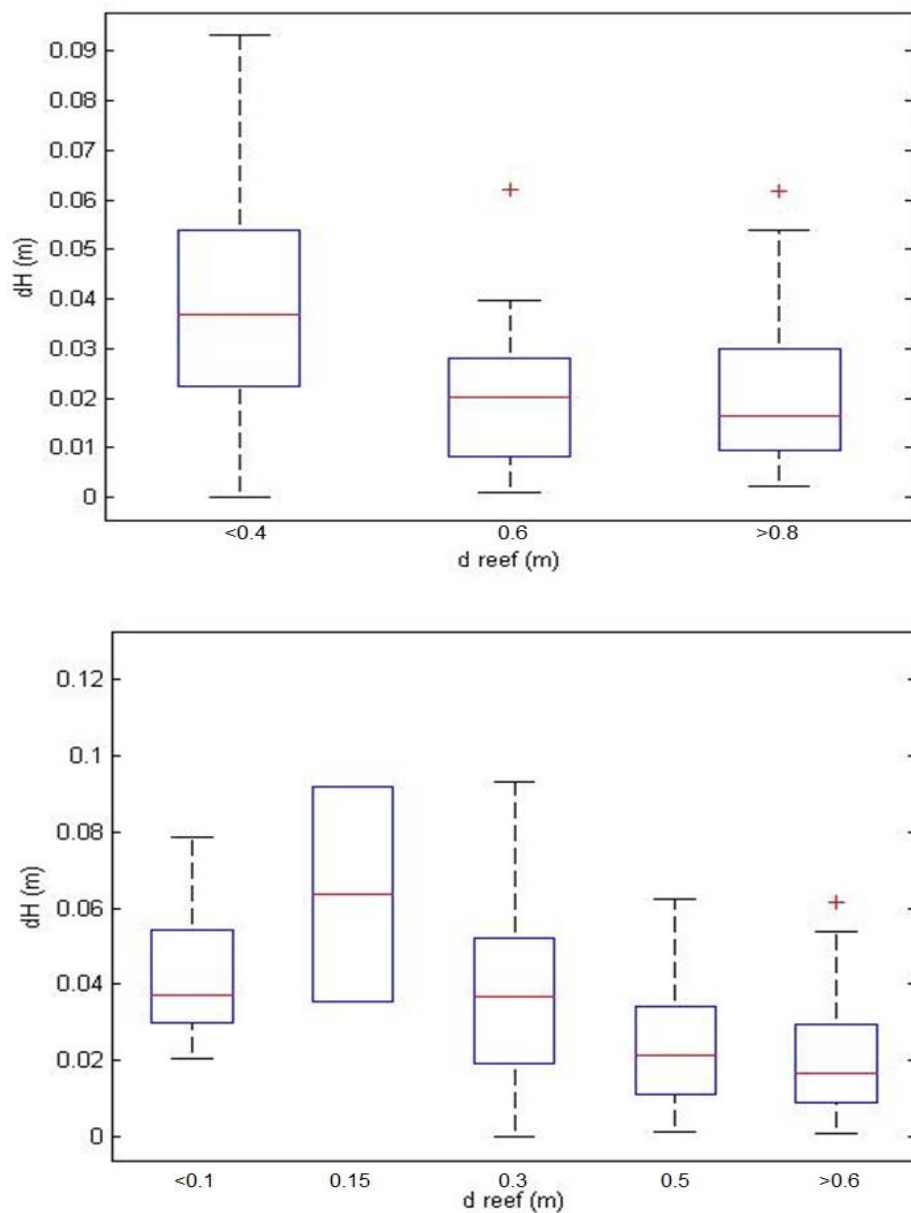


Figure 49: BT5 wave dissipation as a function of water depth to the reef. The upper panel trends suggest a strong negative relationship between ΔH_s and d_{reef} which was not reflected in the statistical analysis results. Using more data divisions revealed a tipping point at which ΔH_s decreased after initially increasing with depth.

Discussion

Rates and variability of erosion

Shoreline change on the mainland marshes of the Virginia Coast Reserve was highly variable, ranging from areas of high erosion rates like Elkins Island ($1.5 \text{ m}\cdot\text{yr}^{-1}$) to locations of accretion such as Upshur Neck ($+0.4 \text{ m}\cdot\text{yr}^{-1}$). McLoughlin et al. (2011) used digital shoreline analysis over a 50-year period to determine erosion rates of 10 other mainland marsh locations within the VCR. Those results showed that sites eroded from 0.02 - $1.62 \text{ m}\cdot\text{yr}^{-1}$ with an average of $0.2 \text{ m}\cdot\text{yr}^{-1}$ on mainland marshes (Table 12). Both the range and average rate of erosion were comparable to results from this study. Although there was a general trend of erosion along the length of the VCR that did not necessarily indicate a net loss of marshland as the study did not include lagoonal marshes or marsh gained by progradation, just that there was greater lateral erosion than accretion at the bay-marsh edge (McLoughlin et al. 2011).

Table 12: Mean rates of change along marsh edges and corresponding standard error and deviation. Adapted from McLoughlin et al. (2011).

Marsh site	Mean change ($\text{m}\cdot\text{yr}^{-1}$)	Standard error	Standard deviation
Gargathy Bay	-0.35	0.02	0.28
Cedar Island Bay	-0.70	0.02	0.41
Hummock Cove	-0.07	0.01	0.20
Wachapreague	-0.75	0.04	0.56
North Matulakin	-0.71	0.03	0.41
Short and Long Prong	-0.78	0.03	0.53
Crabbing	-0.04	0.06	0.88
Oyster	0.17	0.03	0.39
Mockhorn	0.01	0.03	0.42
Marion Scott Cove	-0.61	0.04	0.70

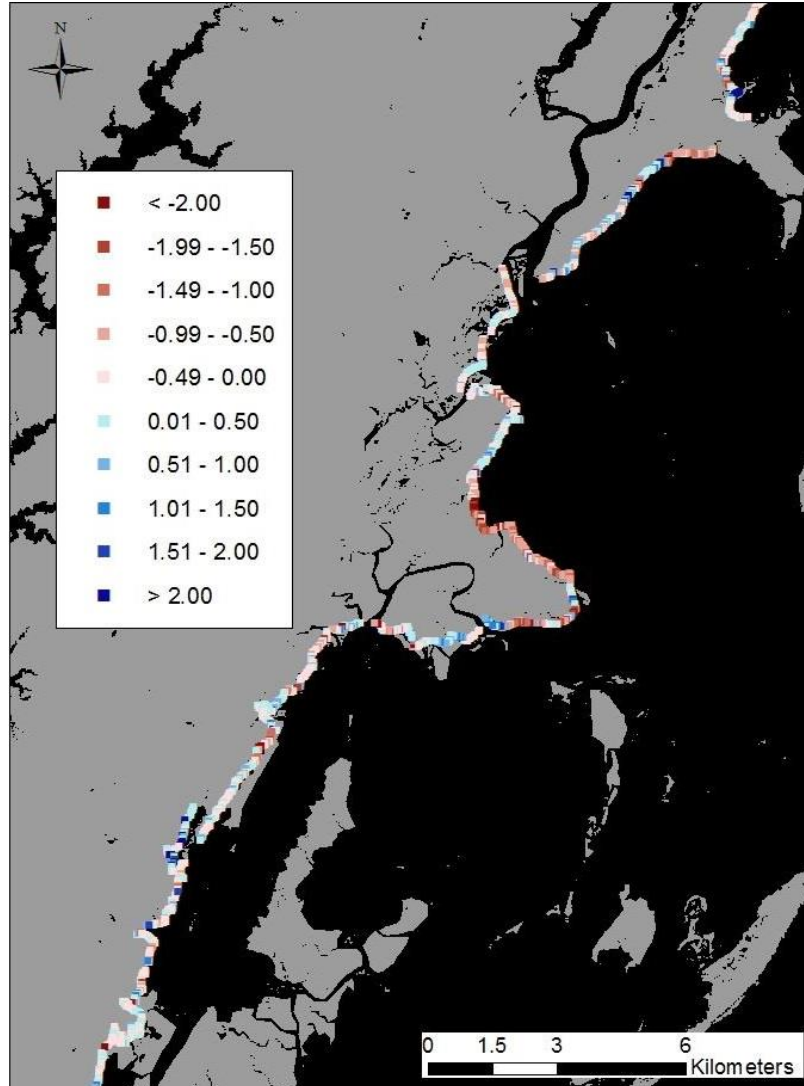


Figure 50: From McLoughlin et al. 2011 - variation in mainland marsh erosion rates in the south-central VCR.

Day et al. (1998) conducted a study in the Venice Lagoon which is similar to the VCR in many regards: it is a shallow coastal lagoon separated from the open sea by barrier islands, has a mean water depth of 1.1 m, mean tidal range of 0.6-1.0 m, 7.5 km mean fetch, and wave attack-dominated erosion. Erosion rates were recorded between 0.6-2.2 m·yr⁻¹, which are higher than the oyster reef sites measured in this study but not

dissimilar. In Rehoboth Bay, DE, Schwimmer (2001) found that marshes eroded between 0.14-0.43 m·yr⁻¹ and an overall average of 0.24 m·yr⁻¹ which is comparable to the range from our study sites, though there were no reefs at that location.

One objective of this study was to determine erosion rates at study sites with oyster reefs as well as how these rates varied through space and time. High variability of erosion rates both spatially and temporally were seen between and within sites in this study (Figure 14), similar to the McLoughlin et al. (2011) measurements for other mainland locations in the VCR (Figure 50). Like this study, they reported no significant spatial trend in erosion rates between Northern and Southern sites. Schwimmer (2001) noted great variability in erosion rates at the Rehoboth Bay sites during the 3-year study. Erosion rates decreased markedly between years 1 and 2, and increased between years 2 and 3 in that study. Most of our study sites showed significant upward trends in shoreline retreat though there were some instances of decline between periods (Table 5, Figure 18). The erosion rates from 1957-1966 had the greatest variability between study sites; SEB3 was eroding nearly at its maximum rate and BT5 was accreting as part of the major shift of the island point, which was the only record of any study site accreting on average. From 1966 onward, there was a trend of increasing erosion rates at all four sites with the greatest increase between the 1966-1994 and 1994-2002 periods.

Marsh and reef attributes

Though wave attack may be the dominant factor in marsh erosion, it was not the only one to have a meaningful effect (McLoughlin 2010, Schwimmer 2001). Feagin et al. (2009) stated that marshes with greater amounts of coarse sediment would have higher

rates shoreline retreat. This was not supported by results from this study, which showed no relationship between grain size and erosion rate (Table 22), nor in the McLoughlin (2010) results which showed a strong negative trend for other marshes in the VCR ($r^2 = 0.97$). These results suggested that sediment size did not play a large role in the erosion rates at marshes in this study or if it did, it was complicated by other factors.

In this study organic matter was highly negatively correlated with grain size. Because grain size did not have much bearing on erosion rates, it was no surprise that organic matter did not either. The relationship between erosion rate and amount of *S. alterniflora* was also insignificant. Feagin et al. (2009) stated vegetation was unlikely to be a primary control in erosion rates, however root stabilization capacity had been cited in other studies (e.g. Rosen 1980, van Eerd 1985, Allen 1989, Goodbred and Hine 1995). Dense root mats bound sediment which increased marsh platform stability and erosion resistance (Pestrong 1969), though it was not reflected in these statistical analyses. Belowground biomass was probably more important in this context because of the root/rhizome stabilization, though aboveground vegetation was shown to significantly reduce wave energy on marsh edges (Knutson et al. 1982). The first 2.5 m of the shoreline was reported to have the potential to attenuate over 50% of wave energy with the presence of *S. alterniflora* (Knutson et al. 1982).

Ecological factors did not appear to predispose any of the marshes to greater erosion. The percent area of marsh surface covered by crab burrows also did not have a significant relationship with erosion rate though there were holes in the structure which reduced cohesiveness and strength, making the marsh more susceptible to slumping and

block detachment (McLoughlin 2010). The area covered by crab burrows was very small at all sites and had little effect on the soundness of the marsh infrastructure. Population was the only oyster reef property that showed a relationship to erosion rates though it was not significant. Population combined both reef area and density of oysters which lead us to believe that larger and denser reefs might have had a greater capacity to attenuate waves before they reached the shore.

These comparisons were also conducted with erosion rates from the most recent period, 2002-2009 (Table 22), because current physical characteristics of the study sites and reefs may have changed since 1957. Using only the most recent erosion rates, r^2 values increased and p-values decreased, indicating a stronger relationship between physical factors and erosion, but none of these relationships were statistically significant. From this data, it did not appear there was a strong direct relationship between oyster reef properties and erosion rates. Because natural pre-existing reefs were the only type used in this study, it is possible that a planned reef may have greater impact on erosion control. Results from the wave dissipation analysis showed that reefs did decrease wave energy as they propagated across. There may not be a single physical reef factor or two that explains wave dissipation, but a complex interaction of many reef aspects. Overall, none of the physical properties of the marsh itself predisposed the location to erosion.

Work by Whitman and Reidenbach (2012) investigating the *C. virginica* recruitment in the VCR reported that the coefficient of drag was five times greater over the oyster reefs than over mud beds. We do not have an estimate for the drag coefficient at our study reefs made of *C. virginica*, but they were likely similar to or greater than

those measured by Whitman and Reidenbach based on area, height, and density of reefs used in that study ($A = 270 \text{ m}^2$, $h \sim 0.75 \text{ m}$, $\rho \sim 700\text{-}900 \text{ oysters per m}^2$ – compare to Table 7).

VCR erosion rate comparison

The wave environment in the VCR appeared to be similar to those in previous studies investigating oyster reef erosion control. The Meyer et al. (1997) study site in North Carolina was also an Eastern Seaboard location with sea-level rise of $2.57 \text{ mm}\cdot\text{yr}^{-1}$ and predominantly wind driven waves with some boating traffic. The Louisiana study by Piazza et al. (2005) was set in an area with water depths between 1-3 m, regional erosion rates around $1 \text{ m}\cdot\text{yr}^{-1}$ (Wilson and Allison 2008), and fetches described as “quite large.” However, the sea-level rise was on the order of $9.5 \text{ mm}\cdot\text{yr}^{-1}$ which was almost three times as fast as the VCR. The Stricklin et al. (2010) site in Mississippi was a microtidal area that could be wind influenced and was eroding at $0.5\text{-}4 \text{ m}\cdot\text{yr}^{-1}$ with a rate of sea-level rise near $3 \text{ mm}\cdot\text{yr}^{-1}$. Rehoboth Bay was the least similar location to the VCR because it was a mid-level energy environment with deeper water but smaller tidal range ($< 0.5 \text{ m}$). Though there was no data in these papers specific to the wave environments, the tidal and erosion metrics were similar to those for Virginia (Table 13). However, it should be noted that aside from Scyphers et al. (2011), these other studies and current projects “armored” shorelines by placing the oyster reefs directly on the marsh whereas this study examined reefs that were separated from the shoreline by a stretch of water. These reefs were examined because there were no locations where reefs were situated directly on the marsh edge in the VCR.

Table 13 contains a large range of erosion rates measured at various locations in the USA in relation to fringing oyster reefs. The average rates of erosion for the last fifty years in the VCR were akin to rates from the other low-energy environment studies (all but Scyphers et al. 2011). The numbers from the Scyphers et al. (2011) study were much larger than any of the others because of the higher energy and failed oyster reef structure. Our 52-year study was considerably longer than the others though the average rates were similar. However, erosion rates over the shorter time intervals, 2007-2009 and 2011-2012, were markedly higher, mostly outside the range seen in the other low-energy oyster reef studies. One explanation for this may be the different methods used to measuring shoreline change. All other studies measured the distance between shoreline and marker stakes placed at the original shoreline at the beginning of the study. This technique was used for the 2011-2012 analysis in the VCR and resulted in much higher rates. There were a number of possible sources of error associated with this method such as having different people measure the change over the course of the study or the risk of poles shifting around in the mud and coming loose which was noted by Stricklin et al. (2010). When measuring the stake distance for the VCR study, one stake was in a marsh block that had detached and some stakes were missing altogether. Data from these other studies would be in question if similar events happened during the course of the sampling periods. Marker stake rates from our study from 2011-2012 were much higher than rates from 2007-2009 that were measured using DSAS. This jump in erosion rates may have been influenced by the method (DSAS to marker stakes) or they could have been an accurate reflection of the shoreline retreat. Five years passed from the beginning of the

first sampling period to the end of the second with a two year gap in between which was sufficient time for the environment to change. The increased erosion rates from 2011-2012 could also have been the result of hurricane Irene (H2) which struck the coast in August of 2011.

Table 13: Comparison of average erosion rates from oyster reef studies ($\text{m}\cdot\text{yr}^{-1}$), observation methods, and relevant statistics. No data for BT6 2007-2009 because 2007 orthograph was taken at high tide and skewed results. Average erosion rates from this study of oyster reefs was in the range of rates reported in previous studies excluding Scyphers et al. which was located in a higher energy environment.

Comparison of oyster reef studies												
	Scyphers et al.		Meyer et al.		Piazza et al.		Stricklin et al.		Taube & Wiberg			
Average erosion rates ($\text{m}\cdot\text{yr}^{-1}$)	2.1	breakwater reef	-0.39*	cultched	0.02	cultched	0.42	natural	0.15	0.25	0.45	SEB3
	2.5	control	0.65	non-cultched	0.10	non-cultched	0.02	constructed	0.27	0.87	1.72	CRM4
									0.26	0.76	1.05	BT5
									0.10	-	0.70	BT6
Duration	24 months		20 months		13 months		21 months		52 years	24 months	15 months	
Years	2007-2009		1992-1994		2002-2003		2006-2008		1957-2009	2007-2009	2011-2012	
Method	marker stakes		marker stakes		marker stakes		marker stakes		GIS	GIS	marker stakes	
Regional erosion rate	~1		0.8-0.9		~1		~1		1.2			
SLR ($\text{mm}\cdot\text{yr}^{-1}$)	2.10		2.57		9.40		2.98		3.48			
MTR (m)	0.36		~0.9		1.90		0.42		1.2			

Erosion rates and storm events

Wave energy can be amplified by higher local sea-level, storm surge, and extreme wind conditions which are all aspects of hurricanes and tropical storms (Mariotti et al. 2010). In the VCR, winds blowing strongly from the northeast, along the same axis as the shoreline, produced statistically high storm surge (Fagherazzi et al. 2010). The resulting waves affected the marsh as they propagated down the shoreline to the southwest. Ekman transport from along-shelf winds created storm surge that increased coastal water depths and wave energy. Because wave energy is the driving erosive force in the VCR large storm events could have had an impact on shoreline stability. Schwimmer (2001) found that marsh shoreline erosion rates were related to storm events both in magnitude and frequency in a review of other studies of shoreline retreat and storm events (Swisher 1982, French 1990, Maurmeyer 1978, Phillips 1985, Ramsey et al. 1998).

The number of hurricanes and tropical storms with paths within 100 km of the study sites were determined from the NOAA Historical Hurricane Tracks database (Appendix II - Table 23). The frequency of storm events during each quasi-decadal interval used in the digital shoreline analysis was calculated by dividing the number of storm records by the years covered in the interval (Table 14). Mean storm intensity for each interval was calculated by assigning a value to each class of storm (tropical storm = 0, category 1 hurricane (H1) = 1, etc.) and averaging all events that took place during that time (Table 14). The impact value represented mean storm intensity weighted by frequency which accounted for both aspects of storms that were likely to have an impact on erosion rates (Table 14).

The compiled data revealed that the frequency of tropical storms and hurricanes (referred to as storm events hereafter) increased with time. The greatest change in frequency (0.43-0.63 events per year) occurred between the same periods as the greatest increase in erosion (0.07-0.37 m·yr⁻¹ between 1966-1994 and 1994-2002). Storm intensity also increased after 1966 as did impact value, suggesting that hurricanes may have destabilized the marshes sufficiently to increase the rate of erosion over time. Linear regressions showed that storm frequency was highly correlated with average erosion rate, as was storm impact (Figure 51, Table 15). Data from the Meyer et al. (1997) and Piazza et al. (2005) studies showed that oyster reefs were ineffective wave buffers in high energy situations which would have made them unlikely to be successful erosion deterrents during tropical storms and hurricanes. Other studies also found that marsh erosion was positively correlated with storm events (McLoughlin 2010, Meyer et al. 1977). It has been suggested that intermediate grade storms may be likely to have had the greatest impact on erosion because of the mid-sized waves they create. These waves potentially do the most damage because they impact the shoreline rather than overtopping the marsh surface and propagating toward the interior (Wray et al. 1995). Further analysis using only “major” hurricanes according to the Saffir-Simpson Hurricane Wind Scale (H3 and greater) resulted in even higher r^2 values which suggested major storms were more important than minor to mid-sized storms in influencing erosion rates, particularly in terms of frequency (Appendix II - Table 24).

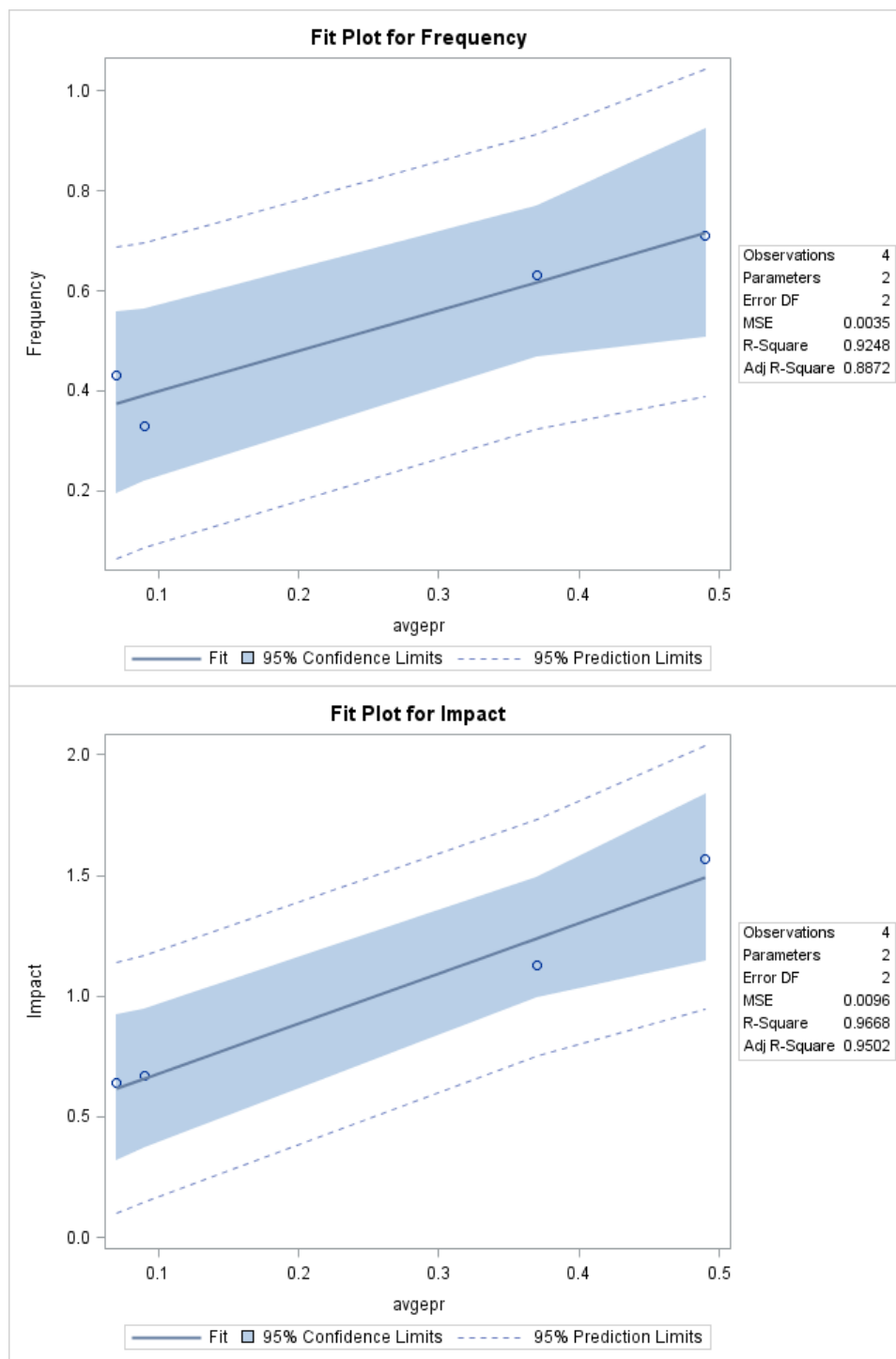


Figure 51: Fit plots for average erosion rates at study sites and storm frequency (upper) and impact (lower). x-axis labels are actually time intervals; first point is 1957-1966 and so on. avgepr is the average erosion rate for all study sites during time period. Frequency of storm events were strongly related to erosion rates as was storm impact value. Impact value would inherently have a strong correlation because it is a product of frequency, however it should be noted that the r^2 value of storm impact was greater than that for frequency, indicating that storm intensity also played a role, though a slight one.

Table 14: Frequency of storm events within 100 km of study sites during each interval. Storm events were ranked such that tropical storm (TS) = 0, class 1 hurricane (H1) = 1, etc. Impact value is intensity weighted by frequency.

Years	Frequency (events per year)	Mean intensity	Impact value	Mean erosion rate (m·yr ⁻¹)
1957-1966	0.33	2.0	0.67	0.09
1966-1994	0.43	1.5	0.65	0.07
1994-2002	0.63	1.8	1.13	0.37
2002-2009	0.71	2.2	1.57	0.49

Table 15: Linear regression results testing the relationship of hurricane frequency and intensity with erosion rates.

	r ²	p	n
Frequency	0.93	0.039	4
Mean intensity	0.40	0.372	4
Impact value	0.97	0.015	4

Wave environment

The wave and water heights recorded during the sampling periods may have been smaller than what would usually have been observed throughout the year. There were significant differences between wind records during the sampling periods and the entire year. A vast majority of the winds recorded during the sampling period were from the southwest, which would have created atmospheric forcing conditions that lowered the regional water levels (Fagherazzi et al. 2010). However this was not reflected in the difference between measured and predicted tides as recorded by NOAA during deployments. The Atlantic Coast experiences storm surges driven by high northeasterly winds blowing parallel to the axis of the shoreline (Fagherazzi et al. 2010). The sampling period was almost entirely devoid of winds from the northeast which are more prevalent

at other times during the year. Because of these wind patterns, the recorded wave environments were likely lower in energy than average.

Despite the skewed wind representation, there were a number of notable relationships between wave heights on either side of the reefs at the Box Tree sites. Bayside waves at BT5 were consistently the largest recorded for the entire Box Tree area. Trends in wave response to wind from a particular direction suggested that BT5 bayside waves were the highest because of its upwind position during E/SE winds which tended to create the significant wave heights (Figure 35). BT6 bayside waves were not as well correlated with wind speed as waves at BT5; BT5 would have been upwind of BT6 during winds from the E/SE, dampening waves as they propagated towards BT6. The lack of bias in significant wave height between marshside gauges at BT5 and BT6 indicates that winds affected both gauges to a similar degree. The reaction of significant wave height to winds from the S/SW and W/NW, the directions that would put the marshside gauges upwind, was not as pronounced as for E/SE winds.

Wave power

Values of wave power calculated in this analysis were similar to values reported by Marani et al. (2011) for the Venice Lagoon which has frequently been compared to the VCR. Their wave power density value averages ran from approximately 5-50 $\text{W}\cdot\text{m}^{-1}$. The binned time series average was on the order of 20 $\text{W}\cdot\text{m}^{-1}$, similar to the low end of averages measured in this study (25-30 $\text{W}\cdot\text{m}^{-1}$).

Wave power density in the VCR modeled by Mariotti et al. (2010) and estimates from Schwimmer (2001) of the Delaware and Rehoboth Bays are interesting comparisons

because of their locality. Values from Mariotti et al. (2010) and Schwimmer (2001) were two to three orders of magnitude larger than the averages in this study. Though Mariotti et al. (2010) also calculated wave power using $P = c_g E$, wind speed was held constant throughout a 48 hour simulation period at $10 \text{ m}\cdot\text{s}^{-1}$ and $20 \text{ m}\cdot\text{s}^{-1}$ which are on the high end for the area. The maximum recorded wind speed during this study was $12 \text{ m}\cdot\text{s}^{-1}$ and the annual mean was $3 \text{ m}\cdot\text{s}^{-1}$ (Sept. 2011- Sept 2012). It seems the sustained wind speeds used in the model are unrealistic as a general representation of wave power for this area but may be reflective of storm conditions. The upper model estimates of power density using winds of $10 \text{ m}\cdot\text{s}^{-1}$ are in line with the highest values recorded in this study, $350\text{-}400 \text{ W}\cdot\text{m}^{-1}$, which occurred during times of maximum wind speeds ($10\text{-}12 \text{ m}\cdot\text{s}^{-1}$). However, these study sites were estimated by Mariotti et al. (2010) to have wave power densities less than $75 \text{ W}\cdot\text{m}^{-1}$ by the $10 \text{ m}\cdot\text{s}^{-1}$ wind model (Figure 1).

Schwimmer (2001) does not provide details of how he determined average wave power for his sites. His range of values was $660\text{-}921,000 \text{ W}\cdot\text{m}^{-1}$ which overlaps with the upper bounds of the Mariotti et al. (2010) model but not at all with Marani et al. (2011) or values from this study. Due to the demonstrated relationship between erosion and wave power (Kamphius 1987, Gelinas and Quigley 1973), it stands to reason that regions with very high shoreline retreat rates would experience very high wave power, thereby explaining to some extent the departure of oyster reef study site values from those of the Delaware and Rehoboth Bays, where retreat rates were as high as $7.3 \text{ m}\cdot\text{yr}^{-1}$.

Schwimmer (2001) fit an equation to the relationship between shoreline retreat and wave power density to his data based on power law relationships generated by

Kamphius (1987) and Gelinas and Quigley (1973) regarding erosion of glacial till bluffs at Lake Erie. The Schwimmer (2001) relationship, $R = 0.35P^{1.1}$, where R is the linear rate of shoreline retreat ($\text{m}\cdot\text{yr}^{-1}$) and P is wave power density ($\text{kW}\cdot\text{m}^{-1}$), is quite similar to those found by Kamphius (1987), $R = 0.35P^{1.37}$, and Gelinas and Quigley (1973), $R = 0.35P^{1.31}$ (Figure 52). Marani et al. (2011) suggest that differences in sediment properties (glacial till versus Delaware marshes versus Virginia marshes) could account for the various slopes of these trend lines.

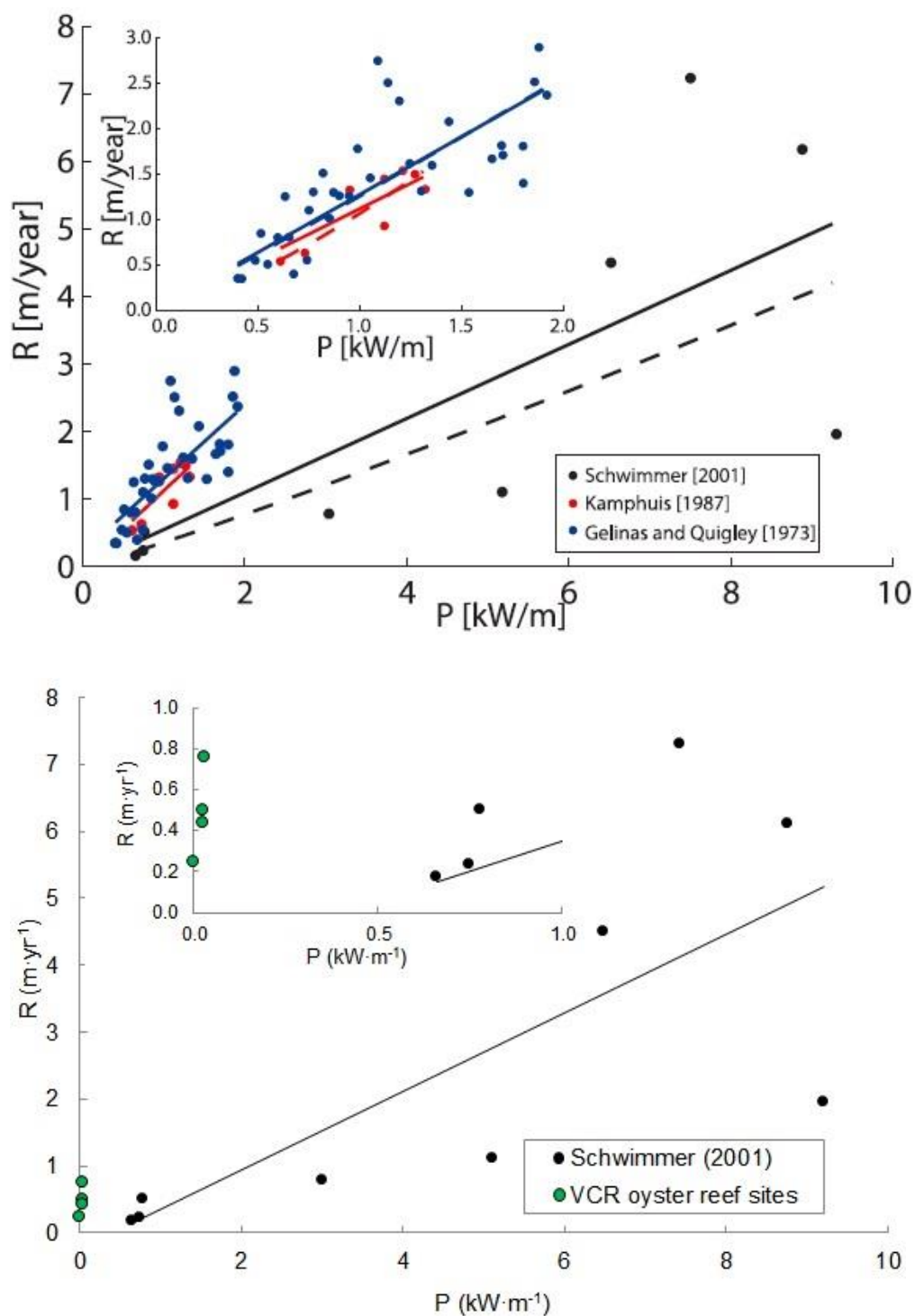


Figure 52: Upper panel: linear and power law fits of wave power density to edge erosion rates. Reproduced from Marani et al. (2011). Dashed lines indicate power law fits and solid lines are linear fits. Trend lines from all three studies are in fair agreement. Lower panel: data from this study plotted with Schwimmer's (2001). VCR oyster reef site values are considerably smaller but not completely out of line.

Plotting the erosion rates from 2007-2009 and 2012 wave power values in VCR with Schwimmer's (2001) data shows that the VCR rates and powers are much lower than his but not out of line when plotted on linear axes. Marani et al. (2011) argued that the relationship between wave power and marsh erosion should be linear. However, they used volumetric erosion instead of linear retreat as a measure of marsh edge change which cannot be compared erosion rates at the oyster reef sites owing to lack of marsh elevation data. Marshes in the Venice Lagoon are primarily scarps and the eroded volume can easily be calculated whereas the VCR study site marsh edges gently rise from the water and have few vertical faces. Despite this, if it is assumed that the marsh edge height stays constant, there is an implied linear relationship between power density and linear margin retreat as well.

Reef dissipation of wave energy

Wave attenuation over coral reefs has been studied to the point that the mechanism is well-understood, particularly in regard to the reef rim. Lowe et al. (2005) and Huang et al. (2012) successfully calculated energy dissipation coefficients for coral reefs that stretched over an entire lagoon or significant length of space. Their methods have not been applied directly to our case because the oyster reefs are much narrower than a full-scale reef. In addition, much of what is understood about coral reef wave dissipation would not translate well to oyster reefs because the majority of work done with coral was at the reef rim where there is an large and abrupt drop in water depth and significantly larger waves than in the VCR near our reefs. Future work in this area could

include a modified method of calculating an energy dissipation factor based on equations for coral reefs but adapted to suit the discrete nature of the oyster reef structure.

The measurements presented here suggest that attenuation of wave energy by oyster reefs depends on complex interactions among variables that are often interrelated. From plots and statistics for these data sets, it was apparent that significant wave height was the most prominent and consistent influence on wave dissipation, and often the crux that explained other relationships. In order to have large changes in significant wave height, there must be large waves to dissipate. Most waves in the VCR are wind-waves, with H_s closely tied to wind speed and water depth. Many of the other correlations with ΔH_s were a product of association with H_s . Because u_{br} scales with H_s it too has a positive relationship with ΔH_s , as do wind speed and water depth. H_s and f_{50} had a negative relationship because as water over the reef deepened, larger waves could be sustained (H_s) that often had lower frequencies (longer periods).

The manner in which spectra changed as they interacted with the reef varied depending on significant wave height and water depth above the reef. In all instances the change in maximum spectral density exceeded effects due to changes in frequency or spectral width. We can conclude that when an oyster reef is submerged, it decreases the energy across the entire spectrum of the wave frequencies as opposed to acting as a filter and removing energy at certain frequencies. Times when the reef was above the water line were not analyzed in this study because the presence of the reef disconnected the waves on either side. In this case, the reef likely acted as a breakwater.

As water depth over the reef grew, there was a decoupling between the surface waves and the reef structure. This idea is supported by findings by Fagherazzi and Wiberg (2009) on the influences of wave-generated shear stress in shallow intertidal location which were modeled on the VCR. They identified four tidal states in which increased water depth either hindered or promoted bottom shear stress. For tidal levels above mean higher high water (MHHW), an increase in wave height was offset by increased water depth, causing bottom shear stress to decrease. The third zone, between MSL and MHHW, produced the greatest amount of sediment resuspension because wave-generated bottom shear stresses reached maximum values in this range of water depths. This is analogous to what was seen with the oyster reefs, that there was a range of water depths for maximum interaction between waves and reefs.

Wavelengths for ROI did not reach values such that $\lambda/2$ was less than d_{reef} , indicating that the wave base ratio for this environment was less than for deep water waves. Analysis of the wave data for BT5, low-energy lagoon setting, indicated that the effective wave base was equal to approximately $\lambda/15$, shallower than the threshold for deep water waves, $\lambda/2$. This reduced reach of waves into the water column corresponded to the depth range 0.15-0.03 m where decoupling of waves and reefs from deep water observed for both wave power and significant wave height.

Because oysters are intertidal dwellers, water depth will fall in and out of this ideal range with the tide. Oyster reefs can only survive at certain zones within the intertidal such that the oysters are submerged and exposed for sufficient amounts of time. This means reefs will tend to be successful in locations where the water depth above the

reef is limited, particularly in environments with low wave energy and small to mid-sized tidal ranges.

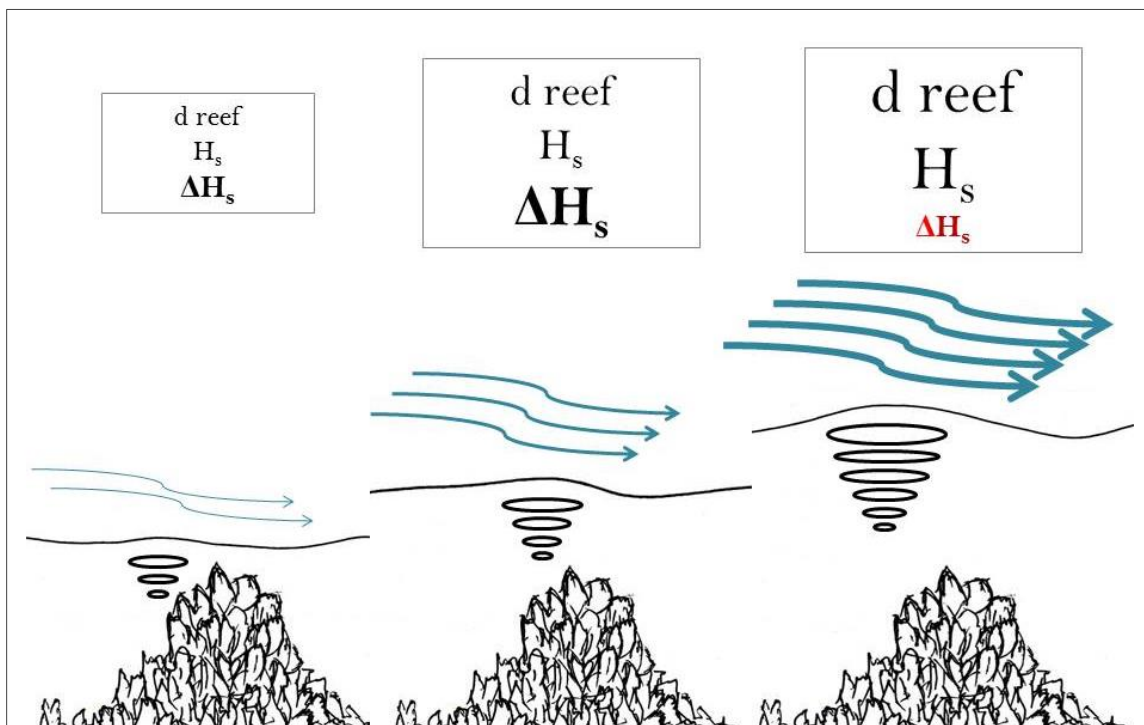


Figure 53: Conceptual diagram of decoupling between waves and reef surface. This diagram illustrates that with increasing water depth above the reef, waves grew and interacted with the reef, producing some amount of dissipation. When water depths were at a mid-level, the water column could support larger waves with wave bases that still interacted with the reef surface. This resulted in greater wave dissipation (positive relationship between H_s and ΔH_s). Once water depths exceeded a certain level, waves continued to grow but their bases did not extend far enough into the water column to interact with the reef surface, leading to decreased wave dissipation.

The reduction of wave power density by the study oyster reefs for significant wave records was 49% averaged over the three sites. This value was significantly higher at CRM4, 61%, than the Box Tree sites, 42-44%. A possible explanation for this difference is the CRM4 reef elevation relative to MSL. The Box Tree reefs are roughly 0.3 m below MSL but the crest of the CRM4 reef sits approximately 0.2 m above MSL. This reef is also significantly larger in both length and width than the Box Tree reefs,

providing a larger surface over which to dissipate the wave power. There was a positive but insignificant correlation between oyster reef population, which incorporated both area and shell density, and erosion rate, which could be related to the power reduction exhibited here.

Patterns observed in the box plots of wave power and water depth show similarities to trends in significant wave height dissipation. High values of wave power were recorded only when there was also deep water, which mirrors the positive correlation between significant wave height and water depth. Differences in percent reduction based on wave propagation direction could also be likened to the relationship between H_s and ΔH_s . In order to have large dissipation values, there needed to be high waves with great potential for dissipation to begin with. In terms of wave power, this analogy would suggest that the side of the reef with overall greater power would tend to have higher percentages of reduction because there was initially more to be dissipated. This observation holds for both CRM4 and BT5 which had uneven reduction percentages, but not at BT6 where the percentage was independent of propagation direction. The lack of real bias at BT6 was also observed in significant wave height patterns (B_{sig} and M_{sig} averages were 0.10 m and 0.09 m, respectively) and this site had the smallest difference in wave power between the two sides ($5 \text{ W}\cdot\text{m}^{-1}$).

Reduction of wave power was observed to decline with increasing water depth. Change was quantified as a ratio based on the side with greater initial power (i.e. $P_B : P_M$ for waves propagating from the bayside to the marshside). As water levels deepened, the power ratio became closer and closer to 1 (power values were more similar to each

other), which could be interpreted as a decrease in dissipation. BT5 is a strong example of this (Figure 45) particularly because waves propagated almost strictly from the bay which reduced noise in the data. This trend is similar to what was seen with ΔH_s and reinforces the theory of waves decoupling from the reef surface with increased water depth.

If oyster reefs are placed in low-energy environments with suitable tidal ranges, they have the potential to decrease wave energy impact on marsh shorelines, and thus erosion, in locations where wave attack is the primary agent of marsh-edge retreat. On average, oyster reefs in this study dissipated wave power density of significant waves by 49%. Both power law and linear fit equations have shown wave power density to be a robust predictive indicator of shoreline erosion rates. Extrapolating from these models, oyster reefs could reduce erosion rates by almost half in ideal settings. However, because of the decoupling effect between waves and reef that is triggered by deepening water, oyster reefs will not profoundly decrease wave energy during periods of sizable storm surge brought on by hurricanes and tropical storms. These high-energy events appear to trigger rapid marsh-edge erosion despite the presence of oyster reefs.

Conclusion

Marshes at all of the primary study sites experienced gradual rates of shoreline retreat between 1957 and 2009. Average rates ranged from $0.10 \text{ m}\cdot\text{y}^{-1}$ to $0.27 \text{ m}\cdot\text{y}^{-1}$ at the study sites and $0.46 \text{ m}\cdot\text{y}^{-1}$ of accretion to $1.58 \text{ m}\cdot\text{y}^{-1}$ of erosion at the comparison sites. Erosion rates differed significantly between sites as well as between analysis intervals

within each site (1957-1966, 1966-1994, 1994-2002, 2002-2009). There was a statistically significant upward trend in the average rate of erosion between the time intervals. This increase strongly corresponded to higher frequency and intensity of tropical storms and hurricanes passing within 100 km of the VCR. Wave attack is the primary mechanism of marsh-edge erosion for this region and large-scale storm events are known to amplify this with greater wind speeds, wave heights, and water depths through storm surge. No physical characteristics of the marshes were identified as relating strongly to erosion. Oyster reef size and density were the only factors that had a relationship with erosion rate though it was not a strong one. The erosion rates from the sites with oyster reefs are comparable to measurements from other studies involving oyster reef wave attenuation. However, they were also very similar to the average rate of erosion for mainland marshes in the VCR regardless of if there were oyster reefs present or not (McLoughlin et al. 2011).

The hydrodynamics differed between the Northern sites and the Box Tree sites, but BT5 and BT6 experienced a similar environment. Winds during the sampling periods at the Northern site likely created a lower-energy environment than average for the area. At CRM4 and Box Tree sites, waves tended to be most responsive to winds from the E/SE though that was the least frequent direction during the sampling periods. SEB3 experienced substantially lower significant wave heights than the other three sites and was determined to be more consistent with tidal creek systems than lagoonal marshes and was therefore excluded from further hydrodynamic analyses.

Oyster reef dissipation of wave energy was correlated to significant wave height and water depth above the reef. There was an optimal range of water depths for maximum wave attenuation where the water column was deep enough to support large waves but not so deep as to separate the waves from the reef surface and decouple the interaction. Analysis of power spectrum densities indicated that wave interaction with oyster reefs result in an overall reduction in wave spectral energy rather than at selective frequencies. On average, the study site reefs reduced wave power of significant waves by 49%. The wave power density values for these sites were comparable to values from the McLoughlin (2010) study of the VCR and the Marani et al. (2011) study of the Venice Lagoon in Italy. Compared to linear erosion rates and wave power densities from Schwimmer (2001), VCR values fell on the low end but did not deviate drastically from the proposed relationship between wave power and erosion when plotted on a linear axis.

Though oyster reefs reduced wave energy, any impact of these reefs on marsh erosion rates was too small to identify within the high variability of the erosion rates for mainland marshes in the VCR. More intentional placement of reefs in regard to both tidal levels and orientation to the shoreline has the potential to increase the efficacy of oyster reefs as an erosion control method in low-energy environments. Reefs are unlikely to be beneficial if water becomes too deep or waves too large like those seen in storm surges from tropical storms and hurricanes. Barring these large-scale weather events, oyster reefs could have a positive impact on shoreline retreat based on our understanding of the relationship between wave power reduction and erosion rates, particularly in low-energy

settings such as those where Living Shorelines are being implemented along the Gulf and Atlantic Coasts.

Despite all of the relationships covered in this study, there is still much we do not understand about oyster reef impacts on salt marshes. The next step in this process would be to apply the hydrodynamic sampling methods and wave spectra analysis from this study to trial reefs built in the VCR which TNC has already begun. Trial reefs should be constructed at various orientations including parallel to the shoreline, perpendicular to the dominant wind direction, and perpendicular to the direction with greatest wave response to winds (in this case, E/SE). These reefs should also be created with different widths in order determine whether the effect of oyster reef width on energy dissipation factor equations is similar to that found in coral reef studies. Because the current practice of constructing Living Shorelines is to place oyster reefs directly against the shoreline, energy dissipation over these near-shore reefs should be compared to data from this study to determine the most effective distance between marsh and reef for maximum wave attenuation and marsh protection.

References

- Allen, E. A. and H. A. Curran. 1974. Biogenic sedimentary structures produced by crabs in lagoon margin and salt marsh environments near Beaufort, North Carolina. *Journal of Sedimentary Petrology* 44:538-548.
- Allen, J.R.L. 1989. Evolution of salt-marsh cliffs in muddy and sandy systems: a qualitative comparison of British west-coast estuaries. *Earth Surface Processes and Landforms* 14:85-92.
- Byrne, R.J. and G.L. Anderson. 1978. Shoreline erosion in tidewater Virginia. Special Report in Applied Marine Science and Ocean Engineering. No. 111, Virginia Institute of Marine Science, Gloucester Point, VA. p. 102.
- Castillo, J. M., P. Leira-Doce, A. E. Rubio-Casal, and E. Figueroa. 2008. Spatial and temporal variations in aboveground and belowground biomass of *Spartina maritima* (small cordgrass) in created and natural marshes. *Estuarine, Coastal and Shelf Science* 78:819-826.
- Chesapeake Bay Foundation. 2007. Living shorelines for the Chesapeake Bay Watershed. Public distribution. 12 pp.
- Coen, L. D., R. D. Brumbough, D. Bushek, R. Grizzle, M. W. Luckenbach, M. H. Posey, S. P. Powers, and S. G. Tolley. 2007. Ecosystem services related to oyster restoration. *Marine Ecology Progress Series* 351:303-307.
- Cossett, K.M., T.J. Culliton, P.C. Wiley, and T.R. Goodspeed. 2004. Population Trends Along the Coastal United States: 1980-2008. *NOAA's Coastal Trends Report Series*. Sept 2004.
- Cox, R., R. A. Wadsworth, And A. G. Thomson. 2003. Long-term changes in salt marsh extent affected by channel deepening in a modified estuary. *Continental Shelf Research* 23:1833-1846.
- Dame, R. F. and B. C. Patten. 1981 Analysis of energy flows in an intertidal oyster reef. *Marine Ecology Progress Series* 5:115-124.
- Day Jr., J. W., F. Scarton, A. Rismondo, and D. Are. 1998. Rapid deterioration of a salt marsh in Venice Lagoon, Italy. *Journal of Coastal Research* 14:583-590.
- Downs, L. L., R. J. Nicholls, S. P. Leatherman, and J. Hautzenroder. 1994. Historic evolution of a marsh island: Bloodsworth Island, Maryland. *Journal of Coastal Research* 10:1031-1044.

- Fagherazzi, S. and P. L. Wiberg. 2009. Importance of wind conditions, fetch, and water levels on wave-generated shear stresses in shallow intertidal basins. *Journal of Geophysical Research* 114:12pp.
- Fagherazzi, S., G. Mariotti, J.H. Porter, K.J. McGlathery, and P.L. Wiber. 2010. Wave energy asymmetry in shallow bays. *Geophysical Research Letters* 72, L24601. doi:10.1029/2010GL045254.
- Feagin, R. A., S .M. Lozada-Bernard, T. M. Ravens, I. Moller, K. M. Yeager, and A. H. Baird. 2009. Does vegetation prevent wave erosion of salt marsh edges? *Proceedings of the National Academy of Sciences* 106:10109-10113.
- Fletcher, C., J. Rooney, M. Barbee, S. Lim, and B. Richmond. 2003. Mapping shoreline change using digital orthophotogrammetry on Maui, Hawaii. *Journal of Coastal Research* 38:106-124.
- French, G.T. 1990. Historical shoreline changes in response to environmental conditions in west Delaware Bay. M.S. thesis, University of Maryland College Park, p. 240.
- The Galveston Bay Foundation and Texas Coastal Watershed Program. Living shorelines brochure.
http://tcwp.tamu.edu/files/2012/06/LivingShorelineBrochureFinal_3.pdf.
Accessed Mar 12, 2013.
- Gelinas, P. and R. Quigley. 1973. The influence of geology on erosion rates along the north shore of Lake Erie. *Proceedings of the 16th Conference on Great Lakes Research*. Pp. 421-430. International Associate for Great Lakes Research, Ann Arbor, MI.
- Goodbred, S.L. Jr. and A.C.Hine. 1995. Coastal storm deposition: salt-marsh response to a severe extratropical storm, March, 1993, west-central Florida. *Geology* 23:679-682.
- Gross, M. F., M. A. Hardisky, P. L. Wolf, and V. Klemas. 1991. Relationship between aboveground and belowground biomass of *Spartina alterniflora* (smooth cordgrass). *Estuaries* 14:180-191.
- Hobbs, C. H. III, D. E. Krantz, and G. L. Wikel. In press. 44 pp in *The Geology of Virginia*. Chuck Bailey (Ed.) College of William and Mary.
- Huang, Z.-C., L. Lenain, W.K. Melville, J.H. Middleton, B. Reineman, N. Statom, and R.M. McCabe. 2012. Dissipation of wave energy and turbulence in a shallow coral reef lagoon. *Journal of Geophysical Research* 117, C03015. doi:10.1029/2011JC007202.

- Hughes, M.L., P.F. McDowell, and W.A. Marcus. 2005. Accuracy assessment of georectified aerial photographs: Implications for measuring lateral channel movement in a GIS. *Geomorphology* 74(2006): 1-16.
- IPCC, 2007: Summary for Policymakers. In: *Climate Change 2007: The Physical Science Basis. Contribution of Working Group I to the Fourth Assessment Report of the Intergovernmental Panel on Climate Change* [Solomon, S., D. Qin, M. Manning, Z. Chen, M. Marquis, K.B. Averyt, M.Tignor and H.L. Miller (eds.)]. Cambridge University Press, Cambridge, United Kingdom and New York, NY, USA.
- Kamphius, J. 1987. Recession rate of glacial till bluffs, *Journal of Waterway, Port, Coastal, and Ocean Engineering*, 113:60-73.
- Kastler, J. A. 1993. Sedimentation and landscape evolution of Virginia salt marshes. MS Thesis. University of Virginia, Charlottesville, VA.
- Kastler, J. A. and P. L. Wiberg. 1996. Sedimentation and boundary changes of Virginia salt marshes. *Estuarine, Coastal and Shelf Science* 42:683-700.
- Kearney, M. S., R. E. Grace, and J. C. Stevenson. 1988. Marsh loss in Nanticoke Estuary, Chesapeake Bay. *Geographical Review* 78:205-220.
- Knuston, P. L., R. A. Brochu, W. A. Seelig, and M. Inskeep. 1982. Wave dampening in *Spartina alterniflora* marshes. *Wetlands* 2:87-104.
- Law, Brent. Personal communication via P.L. Wiberg. Nov. 9, 2012.
- Lowe, R.J., J.L. Falter, M.D. Bandet, G. Pawlak, M.J. Atkinson, S.G. Monismith, and J.R. Koseff. 2005. Spectral wave dissipation over a barrier reef. *Journal of Geophysical Research* vol. 110, C04001, doi:10.1029/2004JC002711.
- Marani, M., A. D'Alpaos, S. Lanzoni, and M. Santalucia. 2011. Understanding and predicting wave erosion of marsh edges. *Geophysical Research Letters* 38:L21401. doi:10.1029/2011GL048995.
- Mariotti, G., S. Fagherazzi, P. L. Wiberg, K. J. McGlathery, L. Carniello, and A. Defina. 2010. Influences of storm surges and sea level on shallow tidal basin erosive processes. *Journal of Geophysical Research*. doi:10.1029/2009JC005892.
- Maurmeyer, E.M. 1978. Geomorphology and evolution of transgressive estuarine washover barriers along the western shore of Delaware Bay. Ph.D. dissertation, University of Delaware, Newark, p. 274.

- McDonald, J.H. 2009. Handbook of Biological Statistics (2nd ed.). Sparky House Publishing. Baltimore, Maryland. pp. 165-172.
- McLoughlin, S. M. 2010. Erosional Processes along Salt Marsh Edges on the Eastern Shore of Virginia. Master's Thesis. University of Virginia, Charlottesville, VA.
- McLoughlin, S.M., K. McGlathery, and P.L. Wiberg. 2011. Quantifying Changes along Mainland Marshes in the Virginia Coast Reserve. Report for The Nature Conservancy of Virginia. July 15, 2011.
- Merriam-Webster Dictionary. "Cultch" Online edition. <http://www.merriam-webster.com/dictionary/cultch>. Accessed Feb 10, 2012.
- Meyer, D. L., E. C. Townsend, and G. W. Thayer. 1997. Stabilization and erosion control value of oyster cultch for intertidal marsh. *Restoration Ecology* 5, 1:93-99.
- Möller, I., T. Spencer, J. R. French, D. J. Leggett, and M. Dixon. 1999. Wave transformation over salt marshes: A field and numerical modeling study from North Norfolk, England. *Estuarine, Coastal and Shelf Science* 49:411-426.
- Moore, L.J. 2000. Shoreline mapping techniques. *Journal of Coastal Research* 16:111-124.
- Moreira, M. E. S. D. A. 1992. Recent saltmarsh changes and sedimentation rates in the Sado Estuary, Portugal. *Journal of Coastal Research* 8:631-640.
- The Nature Conservancy. 2011. Florida Department of Environmental Protection. Deepwater Horizon oil spill response & restoration. <http://www.dep.state.fl.us/deepwaterhorizon>. Accessed Mar 12, 2013.
- The Nature Conservancy. Alabama – Mobile Bay Restoration Project. Aug 20, 2012. <http://www.nature.org/ourinitiatives/regions/northamerica/unitedstates/alabama/explore/main-page-mobile-bay-restoration.xml>. Accessed Mar 12, 2013.
- National Oceanic and Atmospheric Administration (NOAA). 2003. Over half of the American population lives within 50 miles of the coast. *National Ocean Service – Ocean Facts*. <http://oceanservice.noaa.gov/facts/population.html>. Accessed Feb 8, 2012.
- National Oceanic and Atmospheric Administration. 2011. Historical Hurricane Tracks <http://csc.noaa.gov/hurricanes/#>. Accessed March 15, 2011.
- National Oceanic and Atmospheric Administration. 2012. Sea level trends. <http://tidesandcurrents.noaa.gov/sltrends>. Accessed Feb 8, 2012.

- National Oceanic and Atmospheric Administration. 2013. Living shoreline planning and implementation. *Habitat Conservation, National Marine Fisheries Service - Restoration Center*.
<http://www.habitat.noaa.gov/restoration/techniques/limplementation.html>.
 Accessed Jan 8, 2013.
- National Oceanic and Atmospheric Association . 2013. Wachapreague, VA buoy datums.
<http://tidesandcurrents.noaa.gov>. Accessed Jan 8, 2013.
- Nittrouer, C. A., R. W. Sternberg, R. Carpenter, J. T. Bennett. 1979. The use of Pb-210 geochronology as a sedimentological tool: Application to the Washington continental shelf. *Marine Geology* 31:297-316.
- Oertel, G. F. (2001), Hypsographic, hydro-hypsographic and hydrological analysis of coastal bay environments, Great Machipongo Bay, Virginia, *Journal of Coastal Research* 17, 4:775–783.
- Oyster Restoration Project. “What is oyster cultch?” Frequently Asked Questions.
<http://www.oysterrestoration.com/faq.html#7>. Accessed Feb 10, 2012.
- Pestrong, R. 1969. The shear stress of tidal marsh sediments. *Journal of Sedimentary Petrology* 39:322-326
- Pethick, J. S. 1992. Saltmarsh geomorphology in Saltmarshes: morphodynamics, conservation, and engineering significance. In *Saltmarshes, Morphodynamics, Conservation, and Engineering Significance* (Allen, J.R.L., and K. Pye, eds). Cambridge University Press, Cambridge, UK, pp. 41-62.
- Phillips, J.D. 1985. A spatial analysis of shoreline erosion, Delaware Bay, New Jersey. Ph.D. dissertation, Rutgers University, New Brunswick, p. 194.
- Phillips, J.D. 1986. Coastal submergence and marsh fringe erosion. *Journal of Coastal Research* 2:427-436.
- Piazza, B. P., P. D. Banks, and M. K. La Peyre. 2005. The potential for created oyster shell reefs as a sustainable shoreline protection strategy in Louisiana. *Restoration Ecology* 13, 3:499-506.
- Pilkey, O.H., N. Longo, R. Young, A. Coburn. 2012. Rethinking Living Shorelines. Program for the Study of Developed Shorelines, Western Carolina University March 1, 2012.
http://www.wcu.edu/WebFiles/PDFs/PSDS_Living_Shorelines_White_Paper.pdf.
 Accessed Mar 12, 2013.

- Ramsey, K.W., D.J. Leathers, D.V. Wells, and J.H. Talley. 1998. A summary report of the coastal storms of January 27-29 and February 4-6, 1998, Delaware and Maryland. Delaware Geological Survey, Open File Report No. 40:43.
- Rosen, P. S. 1980. Erosion susceptibility of the Virginia Chesapeake Bay shoreline. *Marine Geology* 34:45-59.
- Schwimmer, R. A. 2001. Rates and processes of marsh shoreline erosion in Rehoboth Bay, Delaware, U.S.A. *Journal of Coastal Research* 17:672-683.
- Scyphers, S.B., S.P. Powers, K.L. Heck Jr., D. Byron. 2011. Oyster Reefs as Natural Breakwaters Mitigate Shoreline Loss and Facilitate Fisheries. *PLoS ONE* 6(8):e22396. doi:10.1371/journal.pone.0022396.
- Silberhorn, G. M., illu. M. Warriner. 1976. Tidal Wetland Plants of Virginia. *Educational Series of the Virginia Institute of Marine Science* 19:12-13, 20-21.
- Silliman, B. R. and M. D. Bertness. 2002. A trophic cascade regulates salt marsh primary productivity. *Proceedings of the National Academy of Sciences* 99:10500-10505.
- Stricklin, A. G., M. S. Peterson, J. D. Lopez, C. A. May, C. F. Mohrann, and M. S. Woodrey. 2009. Do small, patchy, constructed intertidal oyster reefs reduce salt marsh erosion as well as natural reefs? *Gulf and Caribbean Research* 22:21-27.
- Swift, D. J. P, B. S. Parsons, A. Foyle, and G. F. Oertel. 2003. Between beds and sequences: stratigraphic organization at the intermediate scales in the Quaternary of the Virginia coast, USA. *Sedimentology* 50:81-111.
- Swisher, M. 1982. The rates and causes of coastal erosion around a transgressive coastal lagoon, Rehoboth Bay, Delaware. M.S. thesis, University of Delaware, Newark, p. 210.
- Teal, J. M. 1958. Distribution of fiddler crabs in Georgia salt marshes. *Ecology* 39:185-193.
- Thieler, E. R., E. A Himmelstoss, J. L. Zichichi, and A. Ergul. 2009. Digital Shoreline Analysis System (DSAS) version 4.0 – An ArcGIS extension for calculating shoreline change. U.S. Geological Survey Open-File Report 2008-1278.
- Titus, J. G., D. E. Hudgens, D. L. Trescott, M. Graghan, W. H. Nuckols, C. H. Hershner, J. M. Kassakian, C. J. Linn, P. G. Merritt, T. M. McCue, J. F. O'Connell, J. Tanski, and J. Wang. 2009. State and local governments plan for development of

most land vulnerable to rising sea level along the US Atlantic coast.
Environmental Research Letters 4:7pp doi:10.1088/1748-9326/4/4/044008.

Truitt, Barry. Personal communication. Feb 5, 2012.

United States Geological Survey (USGS). 2012. *Crassostrea virginica*. USGS Nonindigenous Aquatic Species Database, Gainesville, FL.
<http://nas.er.usgs.gov/queries/factsheet.aspx?SpeciesID=115> Revision Date: 12/8/2004.

van der Wal, D. and K. Pye. 2004. Patterns, rates and possible causes of saltmarsh erosion in the Greater Thames area (UK). *Geomorphology* 61:367-373.

van Eerdt, M. M. 1985. The influence of vegetation on erosion and accretion in salt marshes of the Oosterschelde, The Netherlands. *Vegetatio* 62:367-373.

Wheatcroft, R.A., R.D. Sanders, and B.A. Law. 2012. Seasonal variation in physical and biological factors that influence sediment porosity on a temperate mudflat: Willapa Bay, Washington, USA. *Continental Shelf Research* in press.
<http://dx.doi.org/10.1016/j.csr.2012.07.022>.

Wiberg, P.L and C.R. Sherwood. 2008. Calculating wave-generated bottom orbital velocities from surface-wave parameters. *Computers & Geosciences* 34:1243-1262.

Wilson, C. A. and M. A. Allison. 2008. An equilibrium profile model for retreating marsh shorelines in southeast Louisiana. *Estuarine, Coastal and Shelf Science* 80:483-494.

Whitman, E.R. and M.A. Reidenbach. 2012. Benthic flow environments affect recruitment of *Crassostrea virginica* larvae to an intertidal oyster reef. *Marine Ecology Progress Series* 463:117-191.

Woodhouse, W. E. Jr. and P. L. Knutson. 1982. Atlantic coastal marshes. Pp. 45-109, in , R. R. Lewis, III (ed.), *Creation and restoration of coastal plant communities*. CRC Press, Inc., Boca Raton, FL. 219 p.

Wray, R. D., S. P. Leatherman, and R. J. Nicholls. 1995. Historic and future land loss for upland and marsh islands in the Chesapeake Bay, Maryland, U.S.A. *Journal of Coastal Research* 11:1195-1203.

Young, I. R. and L. A. Verhagen. 1996. The growth of fetch limited waves in water of finite depth. 1. Total energy and peak frequency. *Coastal Engineering* 29(1-2):47-78. doi: 10.1016/S0378-3839(96)00006-3.

Young, I. R. and L. A. Verhagen. 1996. The growth of fetch limited waves in water of finite depth. 2. Spectral evolution. *Coastal Engineering* 29(1-2):79-99. doi:10.1016/S0378-3839(96)00007-5.

Appendix I – additional methods

In studies of coral reef wave dissipation, wave spectra were used to quantify changes in the energy from all wave frequencies. In this case, power spectral density plots (PSD) were used to visualize the amount of energy contributed by each frequency. Wave spectra for the records of interest were analyzed in MATLAB to determine changes in the spectra associated with ΔH_s across the reefs. The spectra fell into a number of categories in terms of their shape (peaks or plateaus, multiple or single peaks, symmetrical or asymmetrical, etc.) and relationship to each other (same or different shapes, vertical or horizontal shift, nested or stacked on each other, etc.). The most important of these aspects were the change in peak spectral density and shift in frequency. In order to account for these as well as the change in shape, a rectangle was calculated for each spectrum such that the area of the rectangle was equal to the area under the curve of the spectrum where the height was determined by the maximum spectral density (Figure 54). The width was equal to the integration of the spectral density (area) divided by the maximum spectral density (height) and was centered over the median frequency (f_{50}) for the spectrum. This approximation captured change in area under the curve (analogous to ΔH_s), vertical change (spectral density), and horizontal change (frequency) between each pair of records.

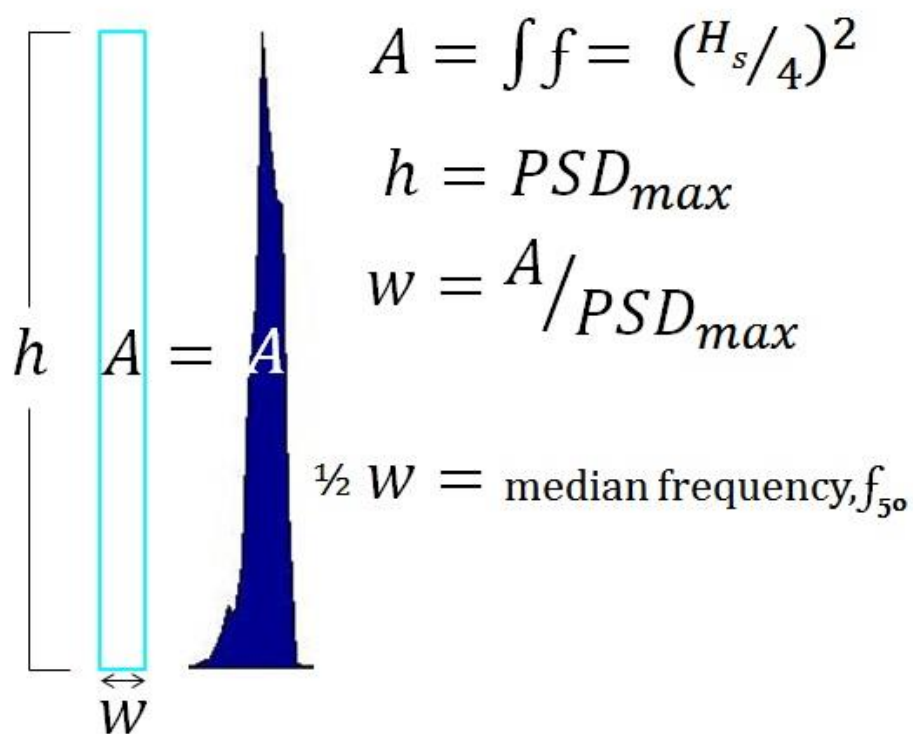
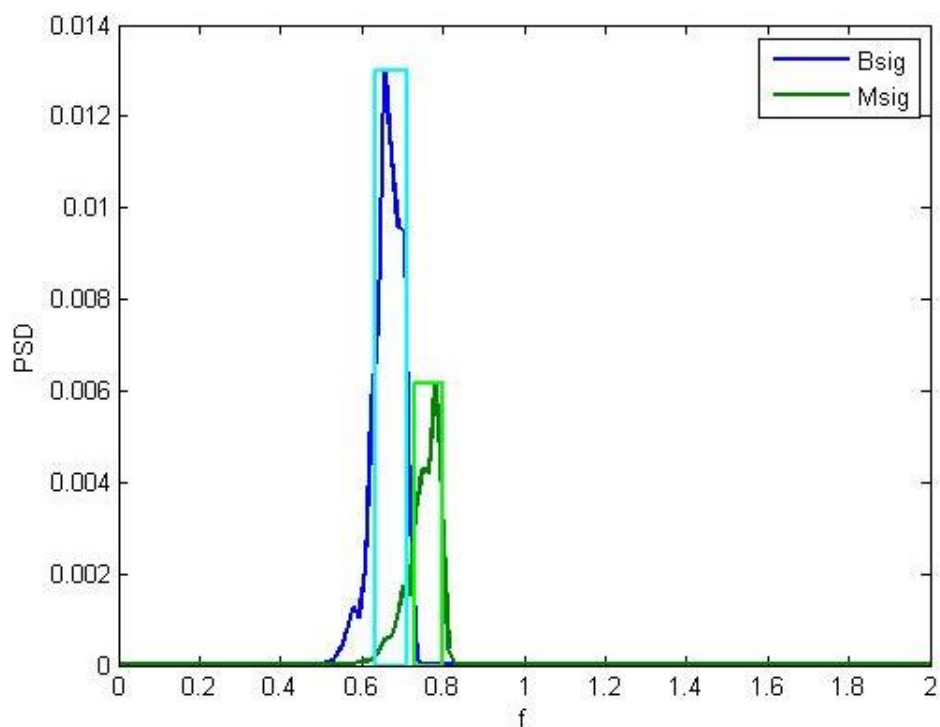


Figure 54: Power spectral density plot with rectangles where height = maximum spectral density, area = integration under the spectral curve, and width is a floating variable centered over the spectrum's median frequency. These rectangles were used to represent the key aspects of the wave spectra.

Appendix II – additional data

Table 16: ANOVA results of tidal speeds (square root). Significance at $p = 0.025$.

Tidal speeds ^{sr}			
	df	F	p
All sites	3	809.05	<0.0001
CRM4 BT5 BT6	2	2.56	0.078

Table 17: Statistical results testing for differences in wind speed and wind direction during the sampling periods and year. Wind speed was tested with a Welch ANOVA for difference of means using the square root of the data, and wind direction was run with a Bartlett test for homogeneity of distribution. Significance at $p = 0.0125$ from Bonferroni correction factor. Wind speeds were significantly different during the Northern sampling, as was wind direction from the annual average.

Wind speed ^{sr}	df	F	p
All periods	2	32.45	<0.0001
Year · Northern	1	38.40	<0.0001
Year · Box Tree	1	0.24	0.64
Northern · Box Tree	1	39.55	<0.0001
Wind direction			
All periods	2	256.0	<0.0001
Year · Northern	1	30.6	<0.0001
Year · Box Tree	1	4.6	0.03
Northern · Box Tree	1	1.3	0.26

Table 18: Statistical results for ANOVA tests of physical properties. Significance at $p = 0.05$ for biomass and burrows, $p = 0.0125$ for d_{50} and percent organic material.

	df	F	p
Biomass (study sites)			
Aboveground	3	0.86	0.48
Belowground	3	1.99	0.15
Total	3	2.03	0.15
Crab burrows (study sites)			
< 2 mm	2	2.17	0.14
2-8 mm	3	0.89	0.46
8-14 mm	3	0.57	0.64
Percent area	3	0.50	0.69
d_{50}			
All sites	6	16.50	< 0.0001

Study sites	3	26.69	< 0.0001
N vs. S	1	57.27	< 0.0001
SEB3 CRM4	1	14.78	0.0016
BT5 BT6	1	0.14	0.71
Percent organic material			
All sites	6	11.29	< 0.0001
Study sites	3	14.94	< 0.0001
SEB3 CRM4	1	13.57	0.0012
BT5 BT6	1	4.00	0.06

Table 19: Grain size and organic attributes of sediment samples. Box Tree sites were highly similar in sediment properties, though SEB3 and CRM4 differed significantly. Elk was the only control site that exhibited characteristics like those at CRM4 (small grain size and low organic content) while the others were more like Box Tree.

averages	SEB3	CRM4	BT5	BT6	UN	nFP	I-I	Elk
Mean grain size (μm)	229	38	622	577	-	358	380	38
Median grain size/ d_{50} (μm)	200	22	503	499	-	327	277	21
Mean/median ratio	1.14	1.76	1.24	1.16	-	1.09	1.37	1.82
Standard deviation (μm)	254	41	426	419	-	269	397	43
Percent sand	66.9%	20.7%	93.4%	86.8%	-	86.9%	71.9%	18.6%
Percent organic matter	2.0%	4.6%	1.0%	1.7%	-	0.7%	2.4%	5.3%

Table 20: Aerial image georectification error and ground resolution. Images from 2002-2009 were georectified by VBMP. *RMS is high because of few ground control points available on eastern side of image.

Year	RMS	Ground Resolution (m)
1957	< 0.1	0.25
1966		
Northern*	1.97	0.25
Southern	< 0.1	0.25
1994	< 0.1	0.99
2002	-	0.60
2007	-	0.34
2009	-	0.07-0.30

Table 21: Fetch area estimates.

Fetch Area Estimates (km^2)

	< 2 km	2-4 km	4-6 km	6-8 km	8-10 km	>10 km	Total
SEB3	0%	0%	0%	37%	27%	37%	54.5
CRM4	0%	0%	8%	51%	18%	23%	50.0
BT5	9%	11%	14%	34%	32%	0%	22.0
BT6	4%	7%	52%	7%	30%	0%	23.0
nFP	0%	0%	0%	34%	36%	30%	56.0
UN	8%	0%	6%	24%	0%	61%	49.0
ii	14%	14%	29%	43%	0%	0%	14.0
Elk	0%	30%	15%	0%	0%	55%	20.0

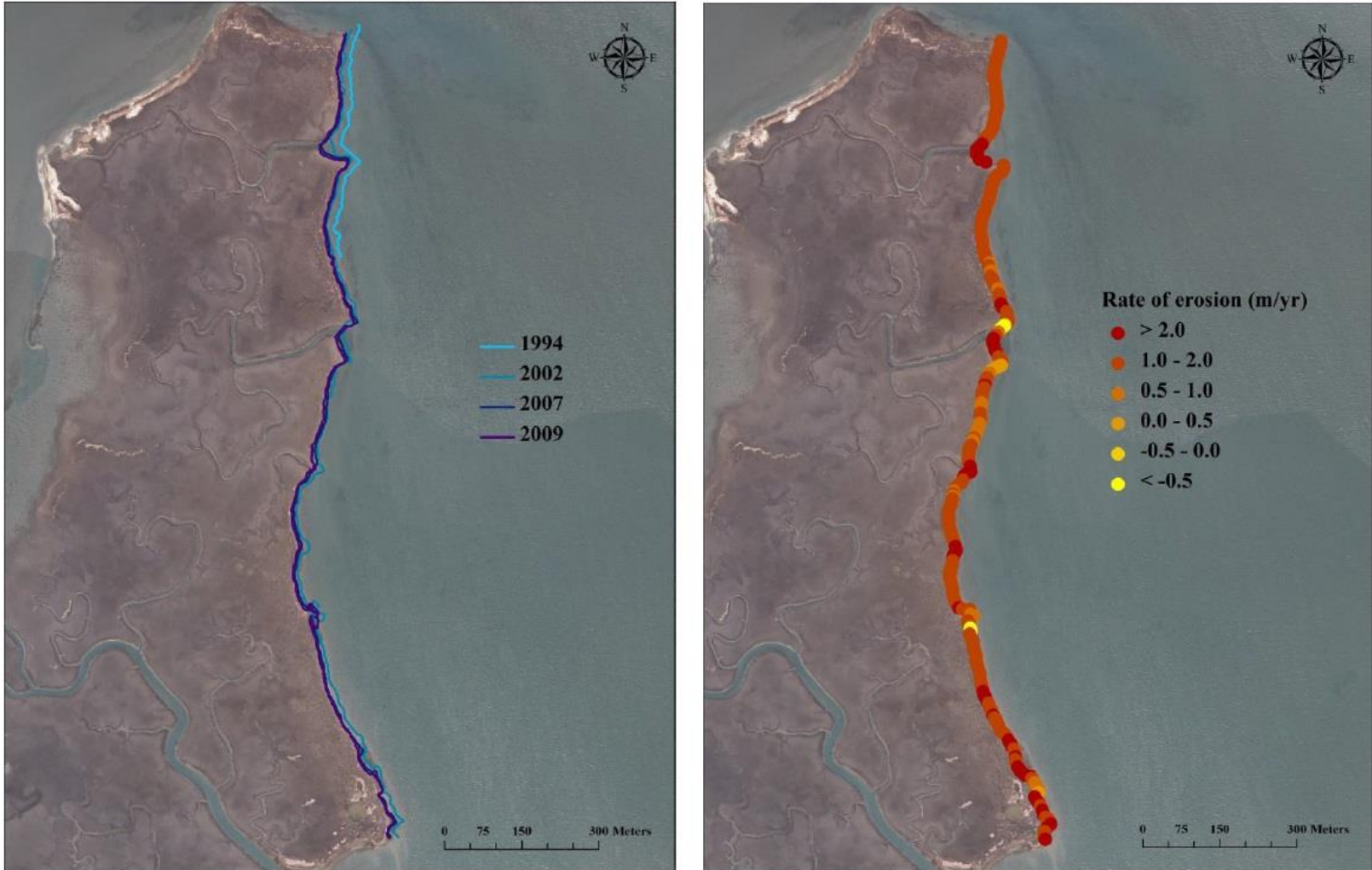


Figure 55: Elkins Island shorelines and rate of erosion.

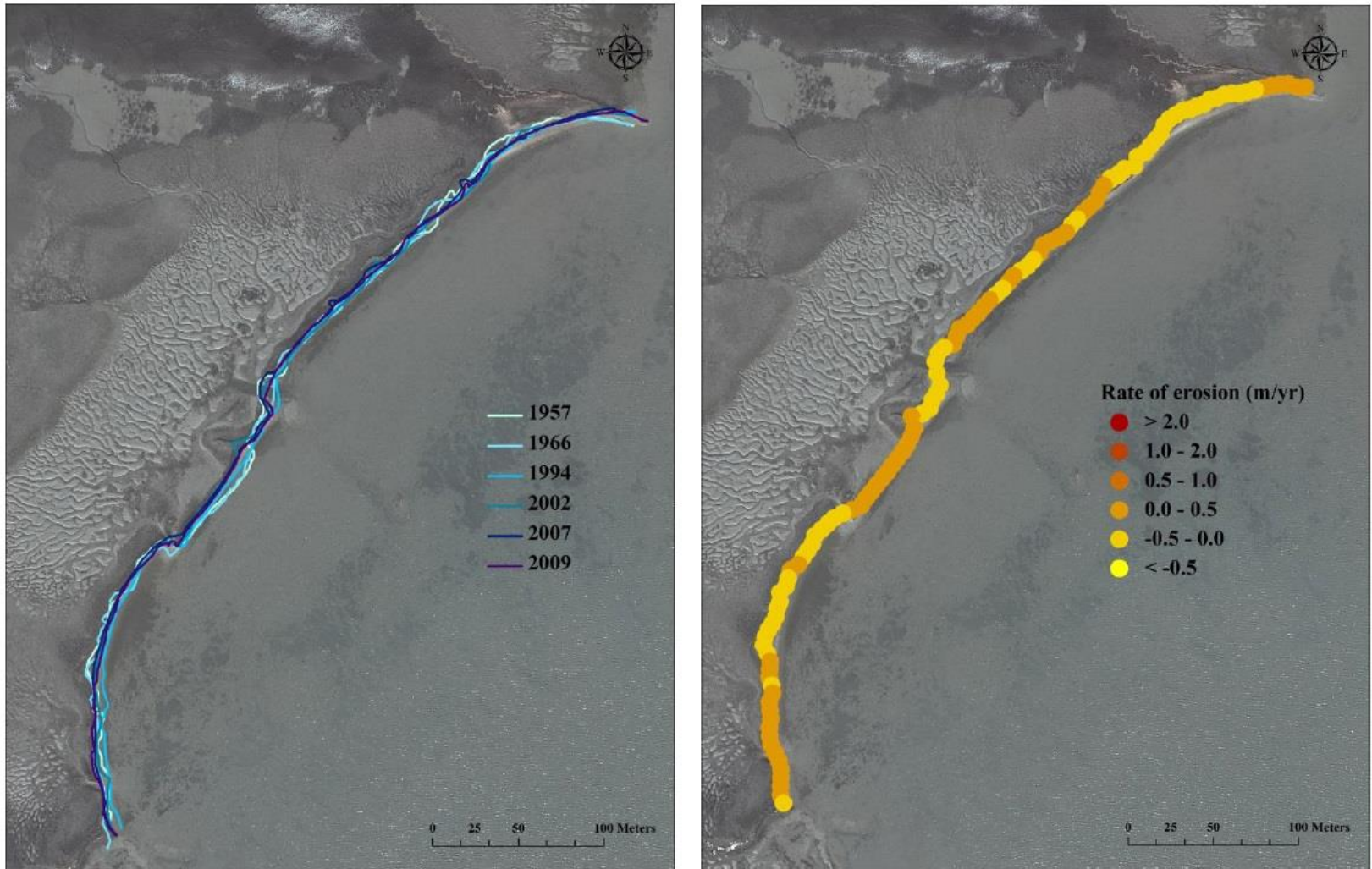


Figure 56: Inter-island shorelines and rates of erosion.

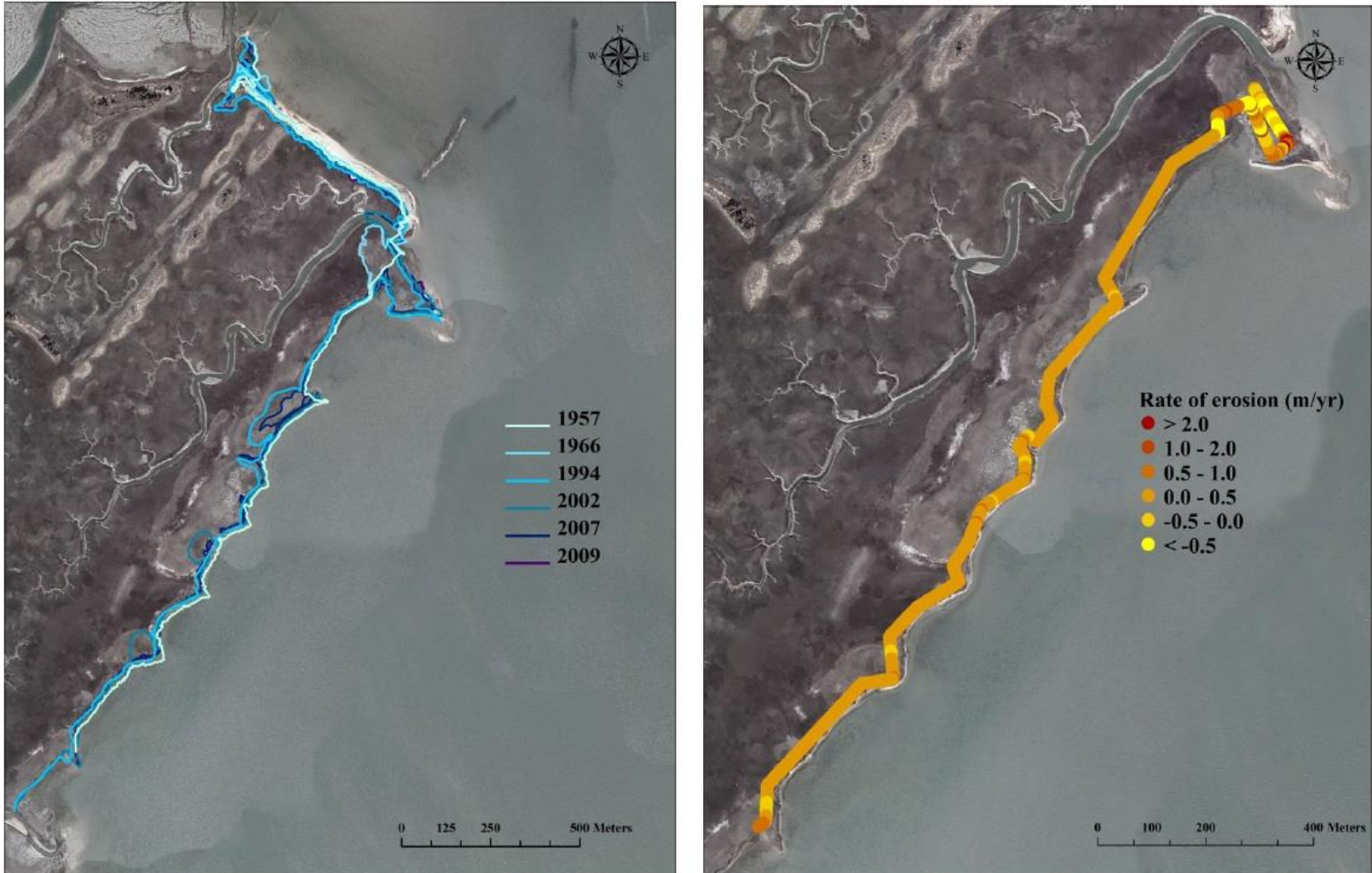


Figure 57: northern Fowling Point shorelines and rates of erosion.

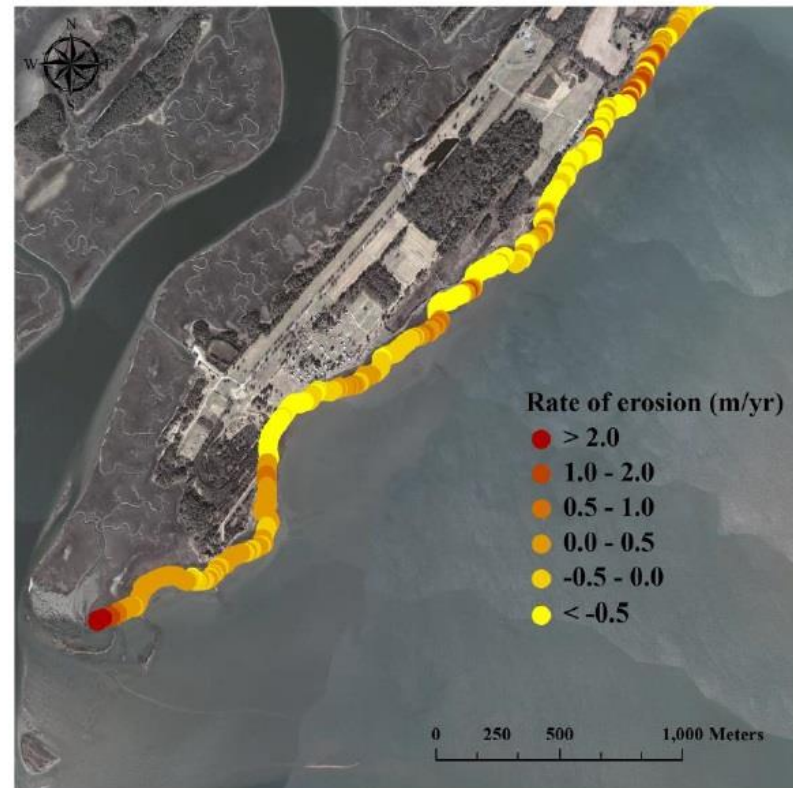


Figure 58: Upshur Neck shorelines and rates of erosion.

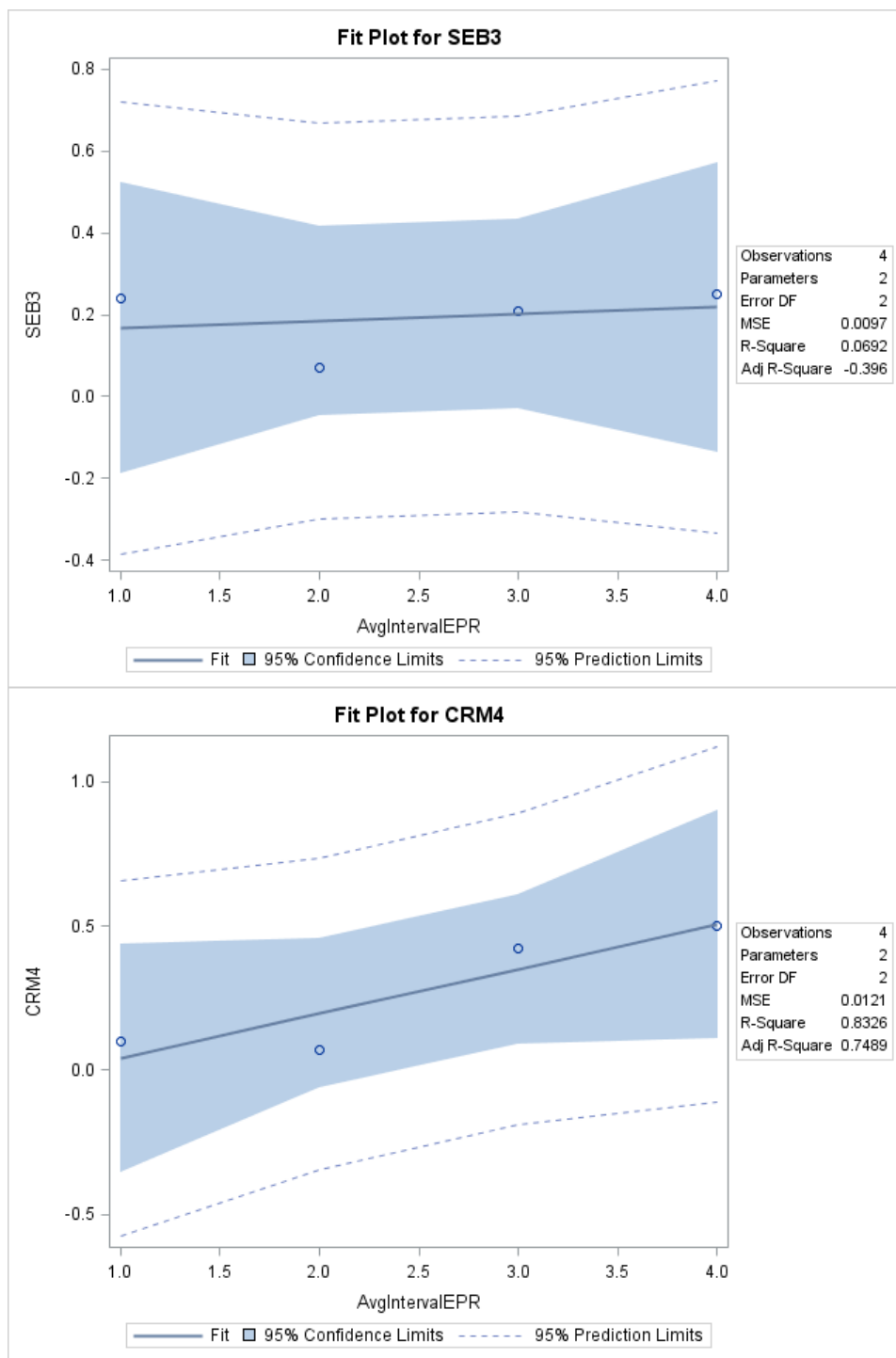


Figure 59: SEB3 (upper) and CRM4 (lower) fit plots for increasing erosion rates over time. SEB3 had no significant relationship but the trend was significant at CRM4.

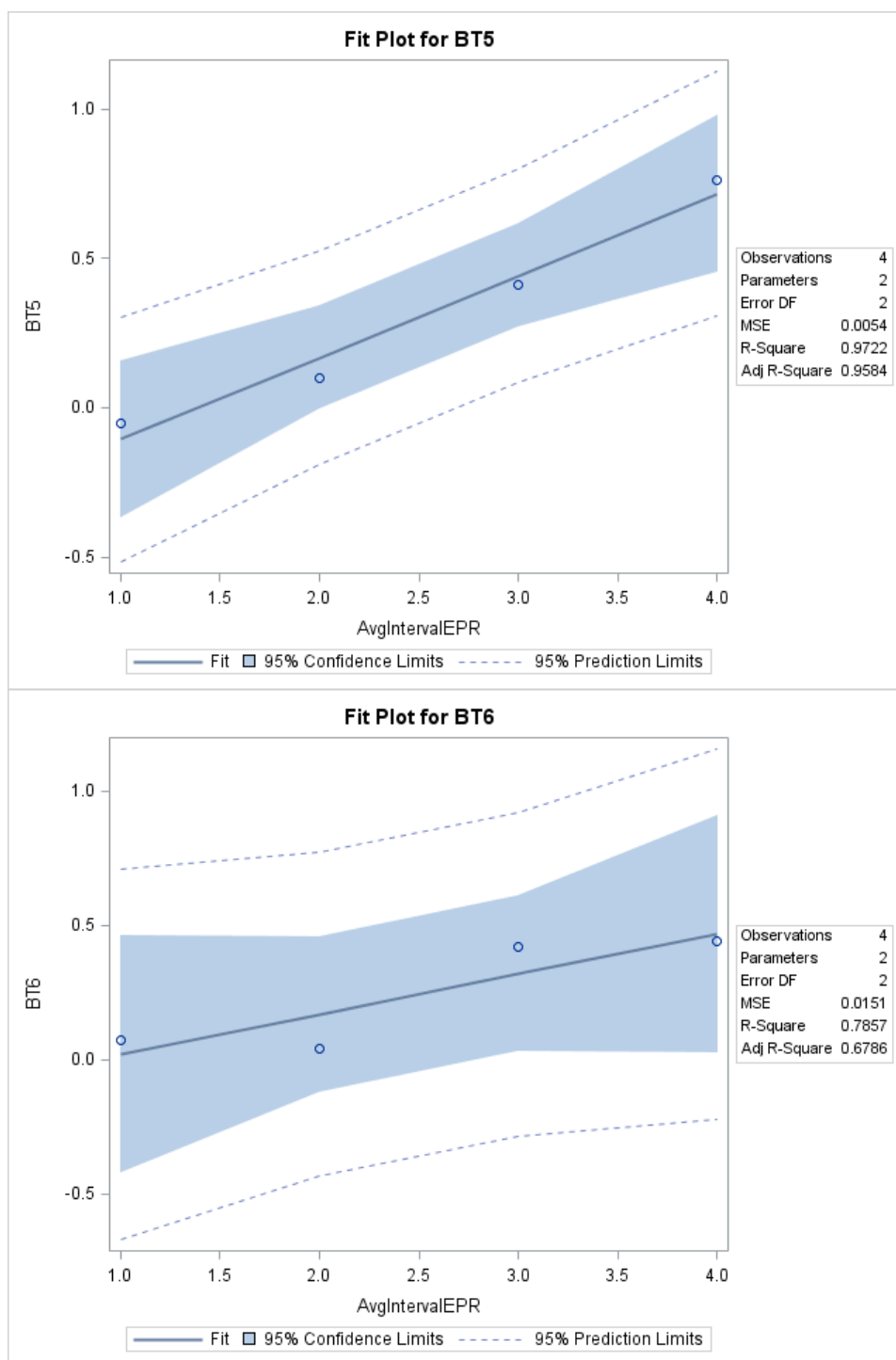


Figure 60: BT5 (upper) and BT6 (lower) fit plots for increasing erosion rates over time. Both sites had a significant upward trend which was particularly strong at BT5.

Table 22: Linear regression results for erosion rates and physical properties. Significance at $p = 0.05$. No physical traits had a significant relationship to erosion rates which suggests that none of these sites were predisposed to erosion over the others.

1957-2009	r^2	P	n
Percent sand	0.20	0.558	4
Mean organic content	0.16	0.600	4
Total biomass	0.01	0.897	4
Belowground biomass	0.02	0.867	4
Burrow area	0.03	0.867	4
Reef length	0.06	0.761	4
Reef area	0.05	0.776	4
Reef density	0.03	0.828	4
Oyster population estimate	0.52	0.783	4
Mean tidal range	0.002	0.952	4
Fetch area estimate	0.02	0.875	4
<hr/>			
2002-2009			
Percent sand	0.08	0.725	4
Mean organic content	0.05	0.773	4
Total biomass	0.60	0.223	4
Belowground biomass	0.06	0.207	4
Burrow area	0.24	0.505	4
Reef length	0.31	0.447	4
Reef area	0.63	0.206	4
Reef density	0.61	0.217	4
Oyster population estimate	0.63	0.205	4
Mean tidal range	0.14	0.632	4
Fetch area estimate	0.46	0.321	4

Table 23: Hurricanes and tropical storms within 100 km of the VCR during erosion rate study periods. H3 and higher storms are considered to be “major” events.

Period	Year	Duration	Name	Intensity
1957-1966				
	1959	7/5-7/12	Cindy	H1
	1960	8/29-9/14	Donna	H5
	1961	9/12-9/15	-	TS
1966-1994				
	1967	9/8-9/21	Doria	H1
	1969	8/14-8/22	Camille	H5
	1970	5/17-5/27	Alma	H1
	1971	8/20-8/29	Doria	TS
	1971	9/6-10/5	Ginger	H2
	1979	7/9-7/16	Bob	H1
	1981	6/29-7/1	Bret	TS
	1983	8/26-8/30	Dean	TS
	1985	8/12-8/20	Danny	H1
	1985	9/16-10/2	Gloria	H4
	1986	8/13-8/30	Charley	H1
	1992	9/22-9/26	Danielle	H2
1994-2002				
	1996	7/5-7/17	Bertha	H3
	1997	7/16-7/27	Danny	H1
	1999	9/7-9/19	Floyd	H5
	2000	9/15-9/25	Helene	TS
	2001	6/5-6/19	Allison	TS
2002-2009				
	2004	8/3-8/14	Bonnie	TS
	2004	8/9-8/15	Charley	H4
	2004	8/27-9/1	Gaston	H1
	2004	9/2-9/24	Ivan	H5
	2008	9/7	Hanna	H1

Table 24: Statistical analysis of major hurricane events with respect to average erosion rate. The correlation between storm frequency and erosion rates, as well as impact value and erosion rates, increased from analysis using all storm events. This suggests that major hurricanes were more influential than smaller-scale storms.

Years	Frequency (events per year)	Mean intensity	Impact value	Mean erosion rate (m·yr ⁻¹)
				Study sites
1957-1966	0.11	5.0	0.56	0.09
1966-1994	0.11	4.5	0.50	0.07
1994-2002	0.25	4	1.00	0.37
2002-2009	0.29	4.5	1.29	0.49

	r ²	p	n
Frequency	0.99	0.003	4
Mean intensity	0.30	0.451	4
Impact value	0.99	0.004	4

Table 25: Linear regression results for the relationship between significant wave height and hydrodynamic setting variables. Square root of wind speed was used. Results significant at $p = 0.05$. Wave heights measured at all sites had a significant positive relationship to wind speed and water depth above the reef. These trends were the strongest at BT5 and weakest at CRM4.

BT5		
<i>Bsig</i>	r^2	p
Wind speed	0.430	< 0.0001
Wind direction	0.122	0.0007
Depth to reef	0.253	< 0.0001
<i>Msig</i>		
Wind speed	0.430	< 0.0001
Wind direction	0.112	0.0007
Depth to reef	0.253	< 0.0001
n = 91		

BT6		
<i>Bsig</i>	r^2	p
Wind speed	0.244	< 0.0001
Wind direction	0.080	0.0083
Depth to reef	0.150	0.0003
<i>Msig</i>		
Wind speed	0.255	< 0.0001
Wind direction	0.101	0.0029
Depth to reef	0.068	0.0154
n = 94		

CRM4		
<i>Bsig</i>	r^2	p
Wind speed	0.148	0.0004
Wind direction	0.091	0.0063
Depth to reef	0.061	0.0257
<i>Msig</i>		
Wind speed	0.390	< 0.0001
Wind direction	0.216	< 0.0001
Depth to reef	0.046	0.0553
n = 81		

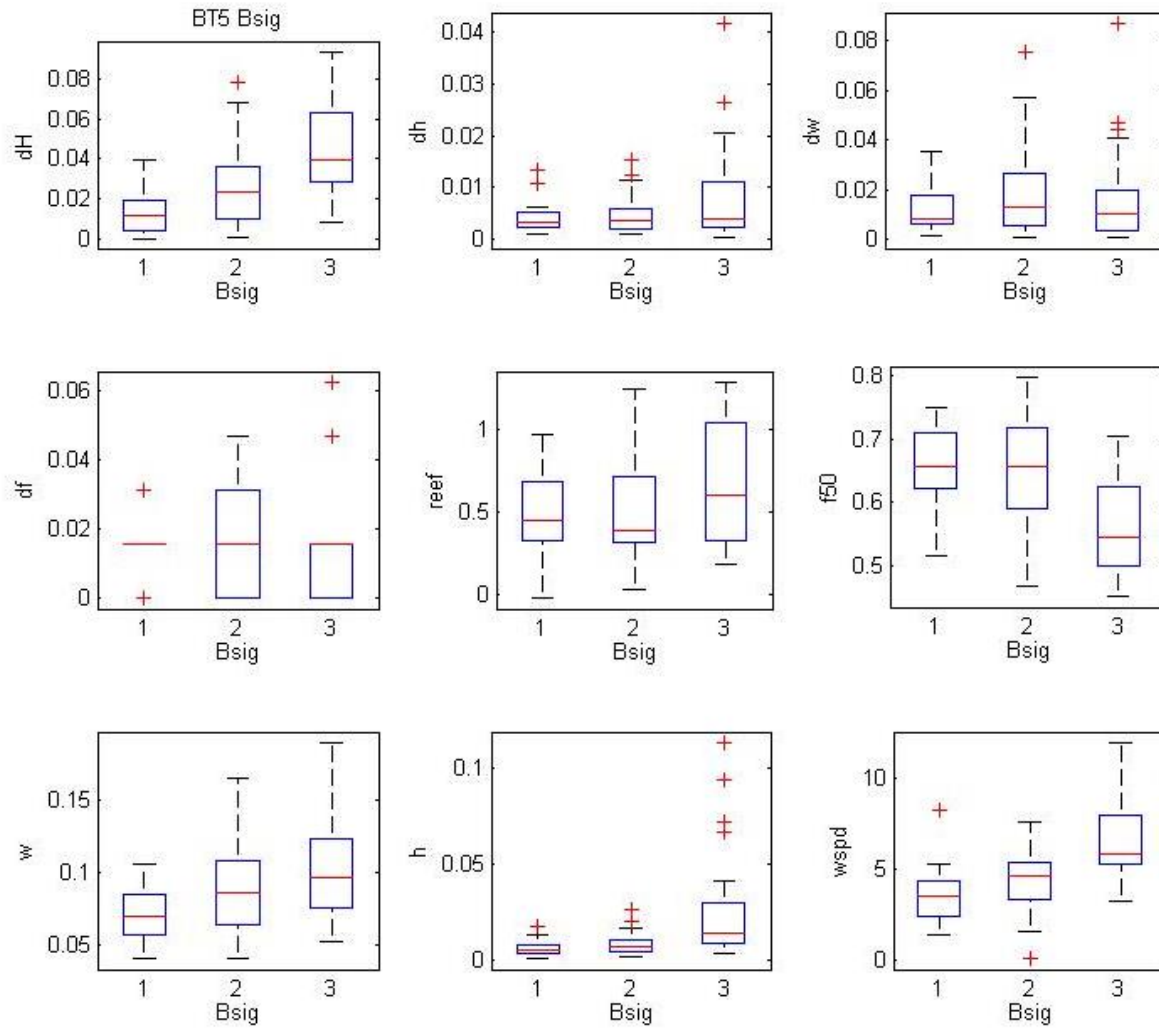
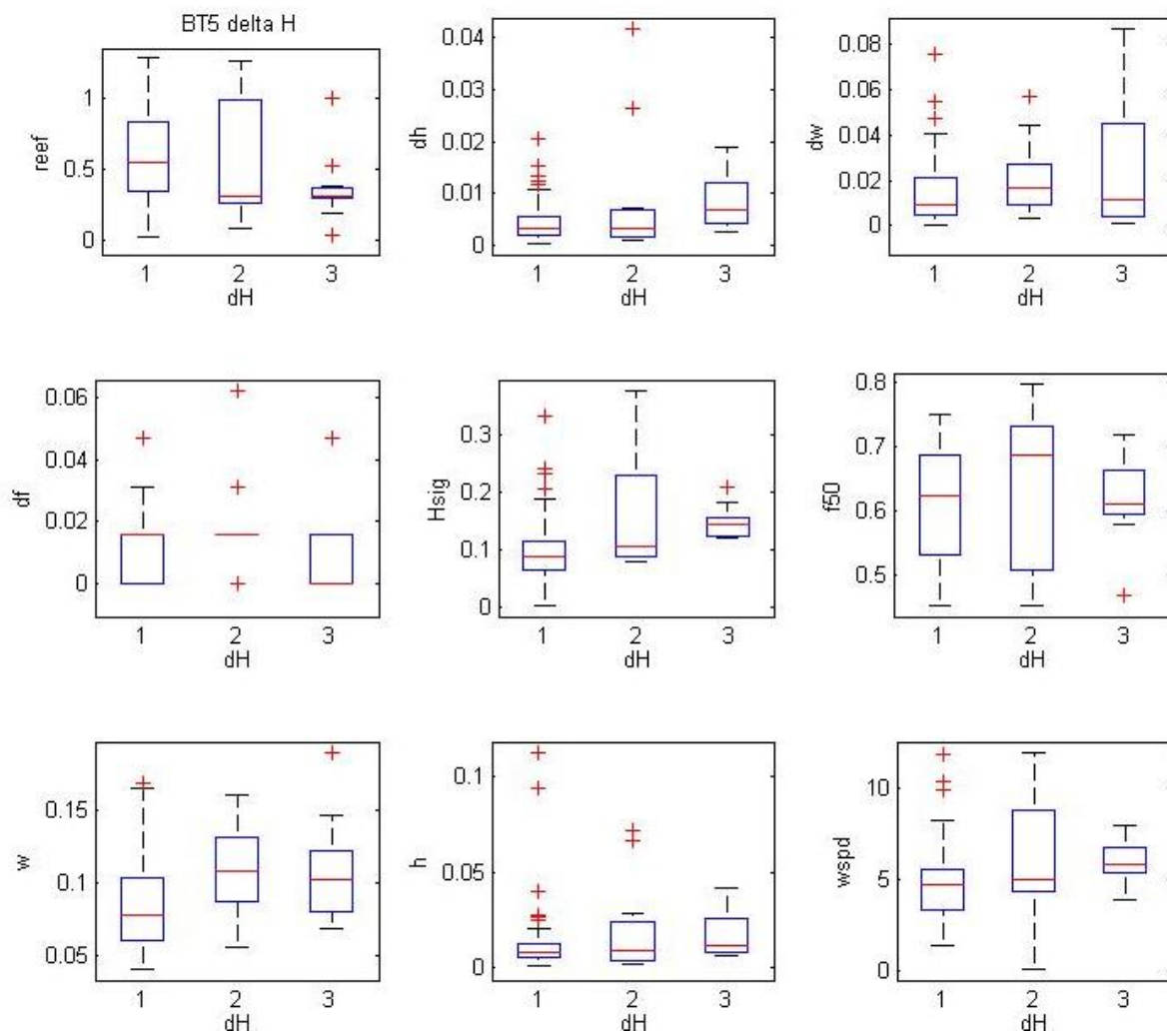
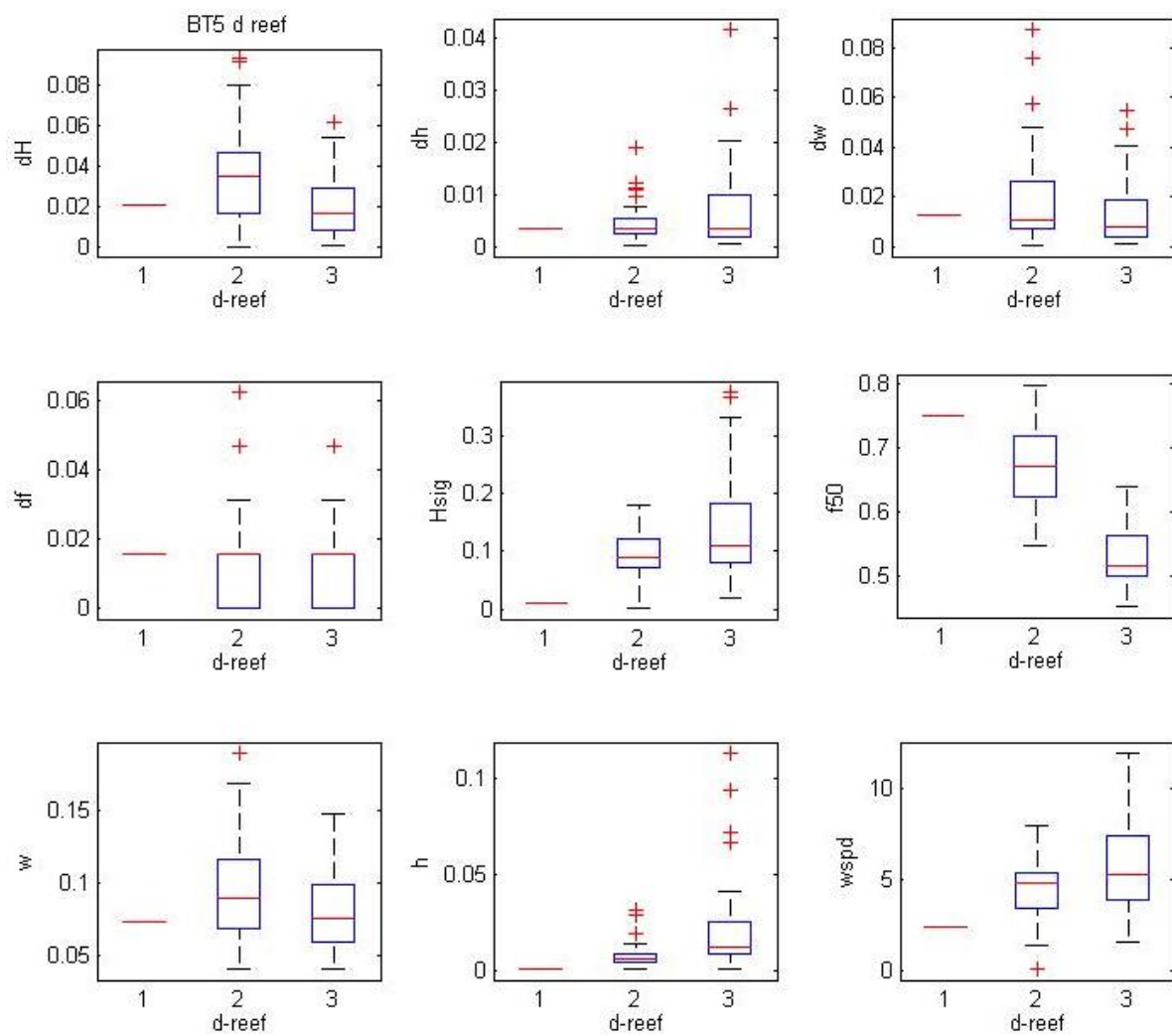
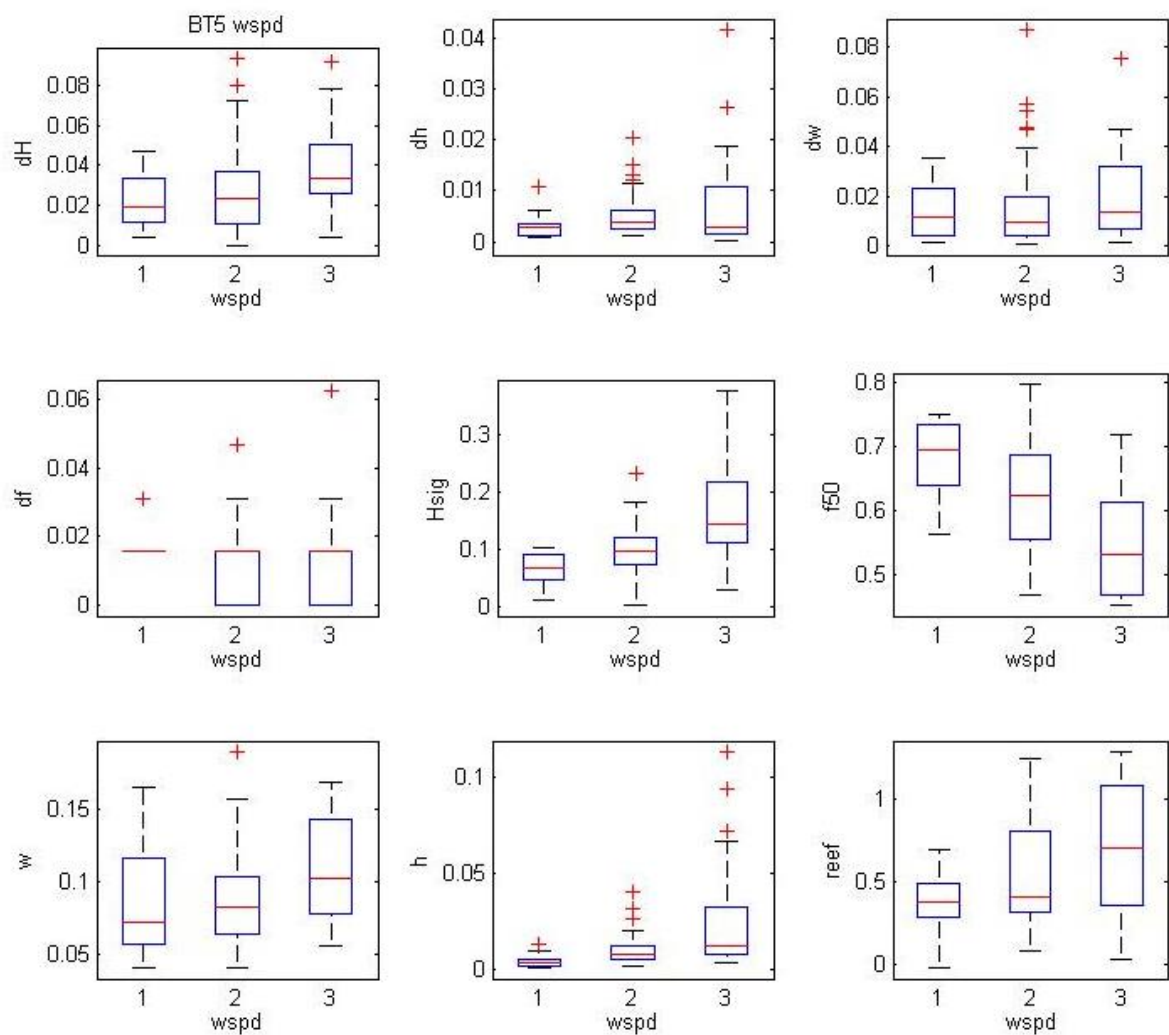


Figure 61: A series of box plots from BT5 used for analysis in the relationship of significant wave height to other measured variables.







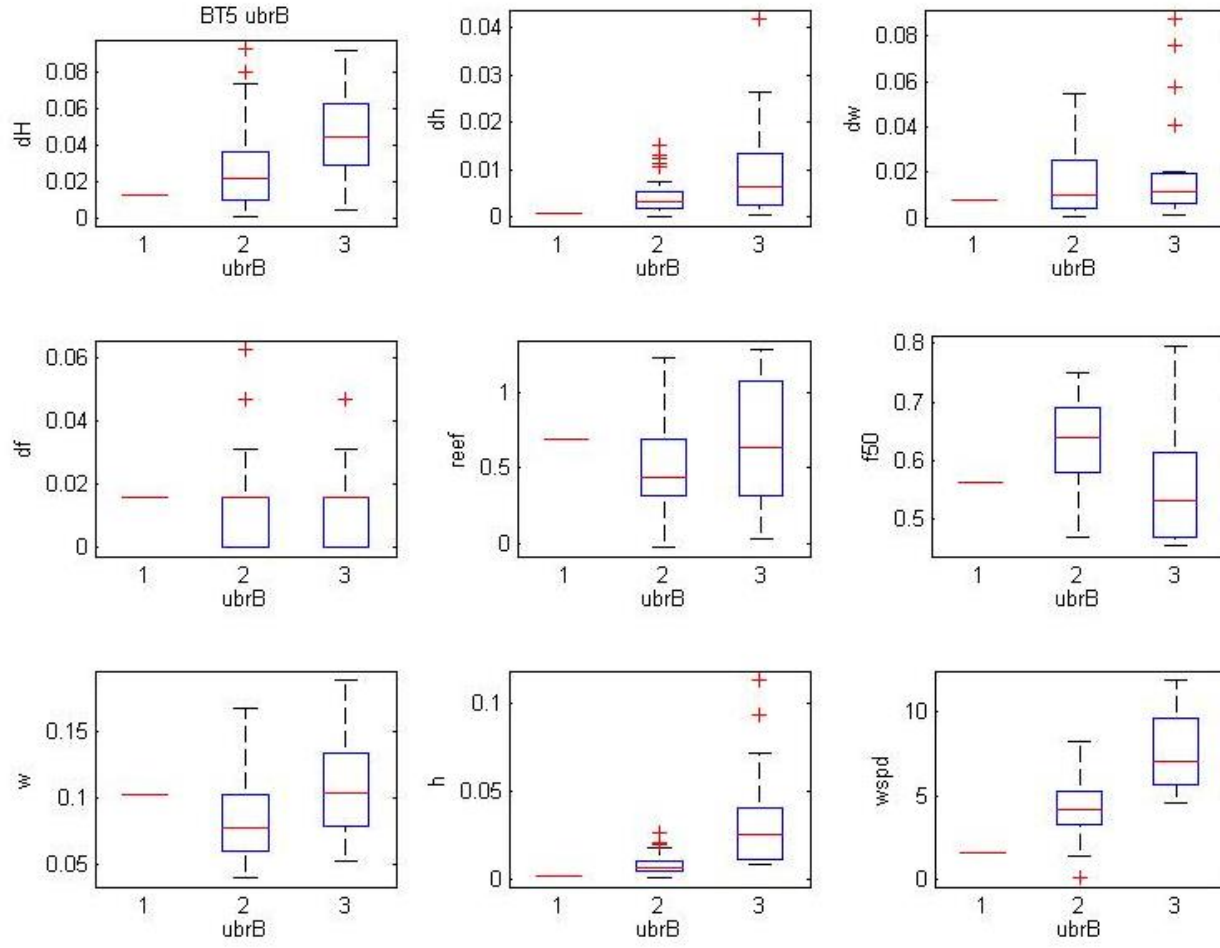


Table 26: ANOVA results for change in significant wave height. f_{50} was omitted because of weak correlation. Significance at $p = 0.05$. Initial wave height and water depth had the greatest impact on change in significant wave height. Dissipation was mostly a function of change in h and had no relationship to changes in w .

BT5			BT6			CRM4		
	r^2	p		r^2	p		r^2	p
Wind speed	0.026	0.127	Wind speed	0.044	0.05	Wind speed	0.366	<0.0001
Depth to reef	0.132	0.000	Depth to reef	0.172	<0.0001	Depth to reef	0.024	0.171
Bayside			Bayside			Bayside		
<i>Bsig</i>	0.088	0.004	<i>Bsig</i>	0.733	<0.0001	<i>Bsig</i>	0.012	0.325
<i>h</i>	0.010	0.342	<i>h</i>	0.287	<0.0001	<i>h</i>	0.190	0.220
<i>w</i>	0.050	0.035	<i>w</i>	0.034	0.090	<i>w</i>	0.002	0.719
<i>u_{br}</i>	0.105	0.002	<i>f₅₀</i>	0.177	<0.0001	<i>u_{br}</i>	0.007	0.452
Marshside			Marshside			Marshside		
<i>Msig</i>	0.005	0.511	<i>Msig</i>	0.273	<0.0001	<i>Msig</i>	0.553	<0.0001
<i>h</i>	0.000	0.935	<i>h</i>	0.055	0.03	<i>h</i>	0.400	<0.0001
<i>w</i>	0.056	0.023	<i>w</i>	0.045	0.050	<i>w</i>	0.018	0.229
<i>u_{br}</i>	0.000	0.861	<i>f₅₀</i>	0.130	0.001	<i>u_{br}</i>	0.585	<0.0001
change			change			change		
<i>h</i>	0.050	0.034	<i>u_{br}</i>	0.007	0.458	<i>h</i>	0.634	<0.0001
<i>w</i>	0.000	0.874	<i>change</i>			<i>w</i>	0.051	0.042
			<i>h</i>	0.070	0.014			
			<i>w</i>	0.005	0.533			

Table 27: Grain size distributions.

Grain diameter (μm)	SEB3	CRM4	BT5	BT6	nFP	ii	Elk
0.375	0.0587	0.1220	0.0136	0.0216	0.0166	0.0617	0.1246
0.412	0.1046	0.2166	0.0248	0.0388	0.0295	0.1096	0.2213
0.452	0.1546	0.3182	0.0387	0.0584	0.0436	0.1609	0.3249
0.496	0.2195	0.4518	0.0540	0.0826	0.0623	0.2281	0.4608
0.545	0.2728	0.5604	0.0673	0.1036	0.0801	0.2823	0.5705
0.598	0.3185	0.6524	0.0793	0.1228	0.0989	0.3278	0.6627
0.657	0.3587	0.7326	0.0897	0.1400	0.1163	0.3668	0.7421
0.721	0.3965	0.8072	0.0988	0.1561	0.1327	0.4027	0.8151
0.791	0.4266	0.8657	0.1063	0.1697	0.1465	0.4298	0.8707
0.869	0.4478	0.9052	0.1118	0.1802	0.1573	0.4468	0.9060
0.954	0.4615	0.9288	0.1153	0.1882	0.1655	0.4553	0.9243
1.047	0.4695	0.9405	0.1170	0.1942	0.1714	0.4573	0.9299
1.149	0.4736	0.9450	0.1174	0.1991	0.1756	0.4554	0.9278
1.261	0.4728	0.9397	0.1165	0.2027	0.1777	0.4483	0.9156
1.385	0.4688	0.9288	0.1147	0.2054	0.1784	0.4382	0.8981
1.520	0.4634	0.9156	0.1124	0.2079	0.1783	0.4270	0.8791
1.669	0.4599	0.9077	0.1102	0.2113	0.1783	0.4185	0.8667
1.832	0.4584	0.9054	0.1085	0.2156	0.1787	0.4129	0.8614
2.011	0.4599	0.9103	0.1074	0.2212	0.1796	0.4111	0.8654
2.208	0.4651	0.9237	0.1073	0.2282	0.1815	0.4136	0.8801
2.423	0.4755	0.9486	0.1085	0.2370	0.1849	0.4220	0.9089
2.660	0.4920	0.9868	0.1113	0.2480	0.1899	0.4368	0.9533
2.920	0.5142	1.0379	0.1157	0.2611	0.1964	0.4577	1.0126
3.206	0.5418	1.1006	0.1218	0.2759	0.2042	0.4841	1.0854
3.519	0.5734	1.1718	0.1290	0.2916	0.2130	0.5142	1.1685
3.863	0.6080	1.2495	0.1369	0.3072	0.2225	0.5469	1.2593
4.241	0.6438	1.3296	0.1448	0.3217	0.2321	0.5802	1.3533
4.656	0.6788	1.4082	0.1518	0.3335	0.2413	0.6120	1.4461
5.111	0.7105	1.4792	0.1570	0.3414	0.2493	0.6398	1.5318
5.611	0.7375	1.5387	0.1600	0.3444	0.2560	0.6618	1.6065
6.159	0.7589	1.5845	0.1606	0.3424	0.2609	0.6773	1.6680
6.761	0.7750	1.6175	0.1591	0.3360	0.2641	0.6866	1.7159
7.422	0.7866	1.6406	0.1559	0.3262	0.2657	0.6906	1.7513
8.148	0.7944	1.6554	0.1517	0.3139	0.2656	0.6901	1.7747
8.944	0.7991	1.6624	0.1469	0.2998	0.2644	0.6854	1.7863

9.819	0.8011	1.6616	0.1418	0.2843	0.2621	0.6767	1.7860
10.78	0.8018	1.6576	0.1368	0.2687	0.2594	0.6658	1.7771
11.83	0.8037	1.6594	0.1327	0.2550	0.2572	0.6556	1.7661
12.99	0.8101	1.6782	0.1306	0.2456	0.2568	0.6500	1.7622
14.26	0.8228	1.7190	0.1309	0.2419	0.2592	0.6504	1.7719
15.65	0.8399	1.7750	0.1331	0.2429	0.2647	0.6544	1.7953
17.18	0.8558	1.8284	0.1355	0.2454	0.2725	0.6567	1.8270
18.86	0.8633	1.8614	0.1358	0.2454	0.2815	0.6518	1.8602
20.71	0.8582	1.8718	0.1331	0.2415	0.2912	0.6384	1.8950
22.73	0.8414	1.8743	0.1284	0.2352	0.3021	0.6196	1.9387
24.95	0.8185	1.8933	0.1240	0.2307	0.3154	0.6012	2.0034
27.39	0.7963	1.9474	0.1224	0.2318	0.3314	0.5872	2.0975
30.07	0.7783	2.0413	0.1244	0.2400	0.3494	0.5765	2.2190
33.01	0.7636	2.1638	0.1287	0.2536	0.3668	0.5645	2.3561
36.24	0.7466	2.2916	0.1319	0.2680	0.3806	0.5455	2.4917
39.78	0.7215	2.4059	0.1308	0.2783	0.3892	0.5174	2.6118
43.67	0.6843	2.5066	0.1242	0.2820	0.3939	0.4840	2.7087
47.94	0.6361	2.6094	0.1141	0.2805	0.3984	0.4530	2.7782
52.63	0.5820	2.7302	0.1050	0.2779	0.4070	0.4315	2.8128
57.77	0.5291	2.8664	0.1007	0.2775	0.4215	0.4212	2.7969
63.42	0.4865	2.9913	0.0998	0.2770	0.4387	0.4185	2.7104
69.62	0.4620	3.0568	0.0961	0.2683	0.4516	0.4163	2.5416
76.43	0.4651	3.0103	0.0876	0.2474	0.4526	0.4101	2.3001
83.90	0.5103	2.8267	0.0806	0.2209	0.4396	0.4039	2.0287
92.10	0.6162	2.5292	0.0808	0.1975	0.4175	0.4119	1.7921
101.10	0.7974	2.2016	0.0895	0.1833	0.3965	0.4542	1.6436
110.99	1.0578	1.9018	0.1092	0.1841	0.3893	0.5507	1.5956
121.84	1.3928	1.6187	0.1490	0.2062	0.4130	0.7200	1.5988
133.75	1.7984	1.3155	0.2246	0.2579	0.4968	0.9778	1.5604
146.82	2.2751	0.9840	0.3598	0.3539	0.6890	1.3299	1.3920
161.18	2.8211	0.6461	0.5883	0.4852	1.0583	1.7639	1.0710
176.93	3.4188	0.3612	0.9504	0.6644	1.6782	2.2472	0.6549
194.23	4.0280	0.1607	1.4768	0.9394	2.5891	2.7297	0.2913
213.22	4.5860	0.0540	2.1618	1.3448	3.7621	3.1558	0.0821
234.07	5.0180	0.0099	2.9462	1.8941	5.0857	3.4813	0.0123
256.95	5.2578	0.0008	3.7282	2.5573	6.3839	3.6851	0.0008
282.07	5.2644	0.0000	4.3958	3.2563	7.4558	3.7720	0.0000
309.64	5.0314	0.0000	4.8641	3.8998	8.1241	3.7638	0.0000
339.92	4.5847	0.0000	5.1039	4.4110	8.2772	3.6855	0.0000
373.15	3.9736	0.0000	5.1451	4.7562	7.8929	3.5599	0.0000

409.63	3.2595	0.0000	5.0506	4.9458	7.0401	3.4004	0.0000
449.67	2.5096	0.0000	4.8834	5.0179	5.8602	3.2136	0.0000
493.63	1.7871	0.0000	4.6851	5.0142	4.5341	3.0146	0.0000
541.89	1.1625	0.0000	4.4734	4.9625	3.2510	2.8216	0.0000
594.87	0.7043	0.0000	4.2613	4.8691	2.1635	2.6499	0.0000
653.02	0.4346	0.0000	4.0765	4.7361	1.3717	2.5092	0.0000
716.87	0.3211	0.0000	3.9672	4.5735	0.8975	2.3984	0.0000
786.95	0.3198	0.0000	3.9728	4.4017	0.6924	2.3080	0.0000
863.88	0.3932	0.0000	4.0510	4.1978	0.6689	2.2086	0.0000
948.34	0.4725	0.0000	4.0667	3.8899	0.7168	2.0638	0.0000
1041.0	0.4829	0.0000	3.8900	3.4305	0.7523	1.8345	0.0000
1142.8	0.4095	0.0000	3.5144	2.8807	0.7496	1.5411	0.0000
1254.6	0.2972	0.0000	2.9929	2.3115	0.5302	1.2229	0.0000
1377.2	0.2205	0.0000	2.3897	1.7897	0.3085	0.9569	0.0000
1511.8	0.2128	0.0000	1.8804	1.4009	0.2852	0.7896	0.0000
1659.6	0.2322	0.0000	1.4769	1.1401	0.3023	0.7118	0.0000
1821.9	0.2802	0.0000	1.1629	0.9794	0.3642	0.7766	0.0000
2000							

Table 28: Carbon and nitrogen content in sediment samples.

Study sites				Comparison sites			
Sample	Weight (g)	Percent N	Percent C	Sample	Weight (g)	Percent N	Percent C
seb 3 1	30.134	0.045	0.614	ii 1 1	28.431	0.021	0.446
seb 3 1	30.007	0.043	0.561	ii 1 2	22.117	0.020	0.467
seb 3 2	21.491	0.014	0.257	ii 2 1	21.575	0.087	1.125
seb 3 2	21.269	0.011	0.224	ii 2 2	22.743	0.086	1.140
seb 3 3	22.264	0.015	0.249	ii 3 1	25.364	0.085	1.113
seb 3 3	21.463	0.014	0.241	ii 3 2	20.412	0.083	1.100
seb 3 4	25.893	0.013	0.157	ii 4 1	27.379	0.024	0.401
seb 3 4	28.671	0.013	0.172	ii 4 2	23.726	0.030	0.459
seb 3 5	27.770	0.022	0.341	ii 5 1	27.819	0.060	0.753
seb 3 5	29.472	0.018	0.310	ii 5 2	24.904	0.054	0.705
seb 3 6	22.496	0.016	0.288	ii 6 1	24.929	0.082	1.691
seb 3 6	23.989	0.017	0.312	ii 6 2	28.018	0.085	1.660
seb 3 7	24.873	0.011	0.203	ii 7 1	25.771	0.027	0.372
seb 3 7	29.563	0.015	0.221	ii 7 2	25.097	0.025	0.439
seb 3 8	26.847	0.083	1.378	ii 8 1	26.996	0.019	0.241
seb 3 8	28.496	0.084	1.408	ii 8 2	25.620	0.020	0.254
seb 3 9	28.966	0.045	0.706	ii 9 1	25.215	0.011	0.220
seb 3 9	28.103	0.044	0.686	ii 9 2	27.843	0.010	0.201
seb 3 10	20.511	0.110	1.886	ii 10 1	27.504	0.039	0.827
seb 3 10	29.786	0.113	1.780	ii 10 2	22.786	0.037	0.753
seb 3 11	25.536	0.042	0.660	elk 1 1	27.624	0.088	1.283
seb 3 11	20.670	0.039	0.625	elk 1 2	29.070	0.095	1.309
seb 3 12	20.284	0.022	0.401	elk 2 1	26.827	0.076	1.098
seb 3 12	22.619	0.015	0.478	elk 2 2	23.859	0.074	1.049
seb 3 13	26.471	0.012	0.244	elk 3 1	24.580	0.119	1.918
seb 3 13	25.476	0.012	0.239	elk 3 2	20.418	0.108	1.748
crm 4 1	22.953	0.063	1.035	elk 4 1	26.576	0.104	1.742
crm 4 1	20.279	0.061	1.064	elk 4 2	27.404	0.106	1.767
crm 4 2	24.529	0.076	1.187	elk 5 1	27.158	0.076	1.229
crm 4 2	21.346	0.072	1.013	elk 5 2	22.352	0.078	1.274
crm 4 3	29.286	0.123	2.000	elk 6 1	22.245	0.101	1.794
crm 4 3	25.756	0.128	2.118	elk 6 2	29.329	0.102	1.742
crm 4 4	22.498	0.136	2.247	elk 7 1	25.464	0.071	1.207
crm 4 4	28.302	0.139	2.232	elk 7 2	28.533	0.067	1.147
crm 4 5	24.578	0.341	5.938	elk 8 1	29.370	0.113	1.787
crm 4 5	26.101	0.339	5.922	elk 8 2	21.572	0.110	1.867
crm 4 6	25.409	0.167	2.213	elk 9 1	27.344	0.179	2.549
crm 4 6	20.762	0.168	2.237	elk 9 2	27.412	0.173	2.523
crm 4 7	21.394	0.175	2.453	elk 10 1	22.248	0.096	1.378
crm 4 7	24.320	0.181	2.614	elk 10 2	27.282	0.094	1.394
crm 4 8	27.745	0.139	2.206	nfp 1 1	21.815	0.000	0.096
crm 4 8	26.465	0.139	2.145	nfp 1 2	26.931	0.000	0.085

crm 4 9	27.551	0.161	2.366
crm 4 9	24.484	0.175	2.659
crm 4 10	21.148	0.134	3.037
crm 4 10	17.487	0.216	3.165
crm 4 11	25.150	0.128	1.927
crm 4 11	28.382	0.136	2.040
crm 4 12	27.034	0.068	1.065
crm 4 12	26.124	0.070	1.035
crm 4 13	27.401	0.071	1.071
crm 4 13	26.459	0.077	1.183
bt 5 1	21.756	0.049	0.683
bt 5 1	28.809	0.055	0.692
bt 5 2	23.509	0.000	0.051
bt 5 2	29.380	0.002	0.064
bt 5 3	26.436	0.016	0.251
bt 5 3	28.518	0.021	0.290
bt 5 4	22.513	0.005	0.090
bt 5 4	23.650	0.003	0.089
bt 5 5	24.270	0.038	0.402
bt 5 5	23.132	0.027	0.371
bt 5 6	27.476	0.008	0.171
bt 5 6	22.062	0.003	0.123
bt 5 7	29.304	0.069	0.880
bt 5 7	21.418	0.072	0.938
bt 5 8	26.637	0.028	0.343
bt 5 8	25.565	0.025	0.317
bt 5 9	29.993	0.047	0.662
bt 5 9	20.910	0.047	0.695
bt 5 10	21.772	0.058	0.773
bt 5 10	26.774	0.048	0.659
bt 5 11	21.180	0.027	0.346
bt 5 11	23.756	0.029	0.355
bt 6 1	21.616	0.027	0.342
bt 6 1	20.075	0.025	0.363
bt 6 2	22.022	0.026	0.365
bt 6 2	29.389	0.004	0.354
bt 6 3	22.581	0.067	1.140
bt 6 3	24.226	0.062	1.006
bt 6 4	25.324	0.005	0.121
bt 6 4	25.334	0.003	0.104
bt 6 5	22.380	0.036	0.604
bt 6 5	22.315	0.031	0.540
bt 6 6	20.269	0.088	1.458
bt 6 6	24.684	0.101	1.630
bt 6 7	29.118	0.079	1.400
bt 6 7	25.765	0.094	1.608

nfp 2 1	20.766	0.013	0.270
nfp 2 2	27.027	0.011	0.219
nfp 3 1	28.612	0.021	0.338
nfp 3 2	26.163	0.024	0.390
nfp 4 1	20.495	0.010	0.221
nfp 4 2	24.623	0.010	0.205
nfp 5 1	21.204	0.013	0.268
nfp 5 2	23.725	0.014	0.241
nfp 5.5 1	20.754	0.010	0.247
nfp 5.5 2	28.098	0.009	0.201
nfp 5.55 1	20.810	0.000	0.033
nfp 5.55 2	27.247	0.000	0.027
nfp 6 1	29.558	0.006	0.156
nfp 6 2	27.342	0.002	0.148
nfp 7 1	25.041	0.000	0.087
nfp 7 2	28.927	0.000	0.078
nfp 8 1	21.520	0.006	0.201
nfp 8 2	22.597	0.011	0.264
nfp 9 1	23.052	0.039	0.779
nfp 9 2	23.050	0.048	0.820
nfp 10 1	20.133	0.000	0.057
nfp 10 2	22.048	0.000	0.068

bt 6 8	28.918	0.005	0.088
bt 6 8	24.756	0.005	0.095
bt 6 9	24.219	0.059	0.844
bt 6 9	21.106	0.052	0.774
bt 6 10	21.300	0.044	0.611
bt 6 10	25.555	0.037	0.620
bt 6 11	25.290	0.000	0.064
bt 6 11	23.733	0.000	0.058